

https://dspace.org/

# Investigating the influence of burden response on fragmentation at Sishen Mine

**Moabelo, Matshidiso Tlou**

**2024**

University of the Witwatersrand, Johannesburg

https://hdl.handle.net/10539/45884

Moabelo, Matshidiso Tlou. (2024). Investigating the influence of burden response on fragmentation at Sishen Mine [Master`s dissertation, University of the Witwatersrand, Johannesburg]. WIReDSpace. https://hdl.handle.net/10539/45884

Downloaded from a DSpace repository. https://dspace.org/

School of Mining Engineering



UNIVERSITY OF THE
WITWATERSRAND,
JOHANNESBURG

# INVESTIGATING THE INFLUENCE OF BURDEN RESPONSE ON FRAGMENTATION AT SISHEN MINE

Matshidiso Tlou Moabelo

A research report submitted to the Faculty of Engineering and the Built Environment, University of the Witwatersrand, Johannesburg, in partial fulfilment of the requirements for the degree of Master of Science in Engineering.

Johannesburg, 2024

## DECLARATION

I have familiarised myself with the University of the Witwatersrand Student Academic Misconduct Policy (SAMP). I hereby declare that the work I am submitting for assessment is my original work. I affirm that I have not plagiarised, misrepresented, or colluded with any other person or source. I have properly acknowledged, cited, and referenced all the sources that I have used in my work. I also declare that I have used artificial intelligence (AI) tools only as a means of guidance. The ideas and arguments presented in my work are my original thoughts and interpretations. I acknowledge that any academic misconduct, such as plagiarism or collusion will result in serious consequences. These consequences may include a reduced grade, a fail mark, or disciplinary action according to the SAMP. The School of Mining Engineering has my consent to investigate any potential academic misconduct in my work. This investigation may include the use of similarity and AI detection software to check the originality of my work. I undertake to abide by the decision of any such investigation.



13/08/2024

Signature of Candidate Date

*“Education is not the filling of a pail, but the lighting to a fire.”*

William Butler Yeats

## ABSTRACT

Sishen Mine is an iron ore mine based in the Northern Cape, 280 km north-west of Kimberley. The iron ore is extracted through means of drilling and blasting which utilises explosives to fragment the rock. This method of rock breakage requires blastholes to be assigned a delay timing. At Sishen Mine this is done through burden response. The mine has a set of timing guidelines that indicate the burden response range for each geological domain. The main focus of the study was on the waste and ore domains, which are blasted using the same burden response of between 12 ms/m to 18 ms/m.

The aim of the study was to investigate the relationship between burden response and fragmentation and whether these timing guidelines for the ore domain result in the mine's preferred fragmentation size of between 230 mm and 1400 mm where $X_{80}$ is 600 mm. The study also aimed to investigate the impacts of fragmentation on loading rates and to measure the DMS ROM lump to fine ratio during and after determining the optimal burden response for the ore domain. The investigation was done from March 2022 to December 2023. It was carried out on 18 blocks in the North and South Mine pits.

The research found that in the ore domain, fragmentation sizes increase with faster burden response. The fastest burden response used in the study was 14 ms/m and yielded $X_{80}$ of 354.63 mm. Furthermore, Powergel Eco 35 explosive product resulted in coarser fragmentation in the ore domain compared to Innovex EGA. It was also found that loading rates reduced with increasing fragmentation size. The DMS ROM lump to fine ratio improved during the duration of the investigation. In 2021, the average lump to fine ratio was 77.74% which increased by 1.69% to 79.43% in 2022 and by 3.76% to 81.50% in 2023 indicating that a faster burden response improved lump to fine ratio. Ore blocks should be blasted with a burden response faster than 14 ms/m and waste blocks with a burden response range of 16

ms/m to 18 ms/m. However, more studies should be conducted on burden responses faster than 14 ms/m. Powergel Eco 35 should be used to charge ore blocks over Innovex EGA. Sishen Mine should consider including inter-hole delay timing on the timing guidelines.

## ACKNOWLEDGMENTS

I would like to thank God, the following company and people:

- Anglo American Kumba Iron Ore: Sishen Mine for granting me permission to conduct this research
- My supervisors Ms Matsobane Nong and Dr Tinashe Tholana for their continued guidance and patience.
- My colleagues at Anglo American Kumba Iron Ore: Sishen Mine for assisting me with data gathering and being available to assist with study blocks when I was off shift. Thank you to my colleagues at Bulk Mining Explosives for assisting with the investigation as well.
- My parents Semetja Moabelo and Frans Moabelo for their support, love and words of encouragement.
- My husband, Peter Phahlane for his patience, love and understanding throughout this journey. Thank you for holding my hand through it all.
- This is dedicated to my son Tumishang Lenex Moabelo, the one who kept me motivated through this journey. Thank you for making me want to work harder than I have ever worked in my life.

# TABLE OF CONTENTS

DECLARATION ..... i

ABSTRACT ..... iii

ACKNOWLEDGMENTS ..... v

LIST OF FIGURES ..... ix

LIST OF TABLES ..... xi

LIST OF ABBREVIATIONS AND ACRONYMS ..... xii

1 INTRODUCTION ..... 1

1.1 Overview of Chapter 1 ..... 1

1.2 Research background and context ..... 1

1.3 Problem statement ..... 7

1.4 Justification and significance of the research ..... 8

1.5 Research aim and objectives ..... 9

1.6 Research scope ..... 9

1.7 Summary of Chapter 1 and structure of the research report ..... 10

2 LITERATURE REVIEW ..... 12

2.1 Overview of Chapter 2 ..... 12

2.2 Mechanism of rock breaking with explosives ..... 12

2.3 Influence of fragmentation on downstream processes ..... 15

2.4 Factors influencing fragmentation ..... 17

2.4.1 Uncontrollable factors ..... 18

2.4.2 Controllable factors ..... 20

2.5 Fragmentation analysis ..... 36

2.6 Chapter summary ..... 38

3 RESEARCH METHODOLOGY ..... 40

3.1 Overview of chapter 3 ..... 40

3.2 Research design ..... 40

3.3 Data collected and the collection process ..... 42

3.3.1 Pre-blast data ..... 43

3.3.2 Post-blast data ..... 48

3.3.3 Application of Split-Desktop for fragmentation analysis ..... 48

Stage 1: Capturing and scaling images ..... 48

Stage 3: Delineation of fragmentation images ..... 49

Stage 4: Calculation of results ..... 50

Stage 5: Fragmentation size distribution curve ..... 51

3.4 Data validation process ..... 52

3.5 Data analysis approach ..... 52

3.6 Chapter summary ..... 53

4 RESULTS AND ANALYSIS OF RESULTS ..... 54

4.1 Overview of chapter 4 ..... 54

4.2 Ore domain results ..... 54

4.3 Waste domain results ..... 63

4.4 Ore and waste comparison ..... 67

4.5 The influence of fragmentation on loading rates ..... 69

4.6 DMS ROM lump to fine results ..... 72

4.7 Chapter summary ..... 73

5 CONCLUSIONS AND RECOMMENDATIONS ..... 74

5.1 Overview of chapter 5 ..... 74
5.2 Summary of the research ..... 74
5.3 Research conclusions ..... 78
5.4 Research limitations ..... 79
5.5 Recommendations ..... 80
References ..... 82
Appendix A: Sishen Mine geology ..... 93
Appendix B: Sishen Mine ore/waste classifications ..... 94
Appendix C: UCS and hardness rating for each rock type ..... 95
Appendix D: Ore blocks geology ..... 96
Appendix E: Ore blocks timing plans ..... 99
Appendix F: Waste blocks geology ..... 105
Appendix G: Waste blocks timing plans ..... 107
Appendix H: Ore blocks fragmentation results ..... 111
Appendix I: Waste blocks fragmentation results ..... 116

## LIST OF FIGURES

Figure 1.1: Plan view illustration of a block containing various rock types ..... 2
Figure 1.2: Plan view of a block classified as a waste block ..... 4
Figure 1.3: Plan view of a block classified as an ore block ..... 4
Figure 1.4: Crusher feed particle size distribution guideline ..... 6
Figure 1.5: Dense Medium Separation Run of Mine lump to fine ratio ..... 7
Figure 2.1: Section view illustration of a charged blasthole ..... 13
Figure 2.2: Gas expansion theory ..... 14
Figure 2.3: Reflection theory ..... 15
Figure 2.4: Relationship between fragmentation size and mining operational costs ..... 16
Figure 2.5: Factors that have an influence on fragmentation ..... 18
Figure 2.6: Illustration of stemming relative to an explosive column and blasthole length ..... 24
Figure 2.7: Relationship between rock fragment sizes and powder factor for a mine in India ..... 29
Figure 2.8: Relationship between rock fragment sizes and powder factor for a limestone quarry ..... 30
Figure 2.9: Inter-hole delay timing and inter-row delay timing ..... 31
Figure 2.10: Detonation sequence showing Chapman-Jouguet Plane .... 35
Figure 3.1: Spectrum for interpreting correlation coefficients ..... 41
Figure 3.2: Captured image for fragmentation analysis ..... 49
Figure 3.3: A delineated fragmentation analysis image ..... 50
Figure 3.4: Fragmentation size distribution curve for block 241127 ..... 51
Figure 4.1: Crusher feed PSD guidelines and ore blocks fragmentation results for ore blocks charged using Powergel Eco 35 ..... 56
Figure 4.2: Crusher feed PSD guidelines and ore blocks fragmentation results for ore blocks charged using Innovex EGA ..... 58
Figure 4.3: Crusher feed PSD guideline and fragmentation results for block 241129 ..... 59

Figure 4.4: Crusher feed PSD guideline and fragmentation results for blocks 4311336 and 4311337 ..... 60
Figure 4.5: Burden response versus $X_{80}$ for ore blocks charged using Powergel Eco 35 ..... 61
Figure 4.6: Burden response versus $X_{80}$ for ore blocks charged with Innovex EGA ..... 62
Figure 4.7: Burden response versus $X_{80}$ for all ore blocks ..... 63
Figure 4.8: Burden response versus $X_{80}$ for waste blocks charged using Powergel Eco 35 ..... 65
Figure 4.9: Burden response versus $X_{80}$ for waste blocks charged using Innovex EGA ..... 66
Figure 4.10: A comparison of burden response versus $X_{80}$ for ore and waste blocks charged with Powergel Eco 35 ..... 68
Figure 4.11: A comparison of burden response versus $X_{80}$ for ore and waste blocks charged using Innovex EGA ..... 69
Figure 4.12: $X_{80}$ versus loading rates for ore and waste blocks charged using Powergel Eco 35 ..... 70
Figure 4.13: $X_{80}$ versus loading rates for ore and waste blocks charged using Innovex EGA ..... 71
Figure 4.14: DMS ROM lump to fine 2021 to 2023 ..... 72

## LIST OF TABLES

Table 2.1: Stemming length rules of thumb ..... 25
Table 2.2: Rock types and their technical powder factors..... 28
Table 3.1: Type of data collected and data source ..... 43
Table 3.2: Blast design parameters ..... 44
Table 3.3: Explosive properties..... 45
Table 3.4: Ore domain pre-blast data for blocks charged using Powergel Eco 35..... 46
Table 3.5: Ore domain pre-blast data for blocks charged with Innovex EGA ..... 46
Table 3.6: Waste domain pre-blast data for blocks charged using Powergel Eco 35..... 47
Table 3.7: Waste domain pre-blast data for blocks charged with Innovex EGA..... 47
Table 4.1: Ore domain post-blast results for blocks charged using Powergel Eco 35..... 55
Table 4.2: Ore domain post-blast results for blocks charged using Innovex EGA..... 57
Table 4.3: Waste domain post-blast results for blocks charged using Powergel Eco 35..... 64
Table 4.4: Waste domain post-blast results for blocks charged using Innovex EGA..... 66

## LIST OF ABBREVIATIONS AND ACRONYMS

| Abbreviation | Description |
|---|---|
| ANFO | Ammonium Nitrate Fuel Oil |
| BIF | Banded Iron Formation |
| CGB | Conglomerate BIF |
| DMS | Dense Medium Separation |
| EDD | Electronic Delay Detonator |
| Fe | Iron |
| $K_2O$ | Potassium oxide |
| KPI | Key Performance Indicator |
| ROM | Run of Mine |
| m/s | Metre per second |
| ms/m | Millisecond per metre |
| PSD | Particle Size Distribution |
| ToR | Terms of Reference |
| UCS | Uniaxial Compressive Strength |
| VOD | Velocity of Detonation |
| $X_{50}$ | Mean Fragmentation Size |
| $X_{80}$ | Fragmentation size at 80% passing |

# 1 INTRODUCTION

## 1.1 Overview of Chapter 1

This chapter introduces the background and context of the research. The problem statement and the justification of the research are also discussed. The chapter also provides the research aims, objectives and further describes the structure of the report.

## 1.2 Research background and context

Sishen Mine is a surface mine located close to a town called Kathu 280 km north-west of Kimberly in the Northern Cape province. It is a wholly owned subsidiary of Kumba Iron Ore which is managed by Anglo American PLC. It is a well-established open pit operation and accounts for the majority of Kumba Iron Ore's production. High-grade hematite ore is mined from stratigraphic units that belong to the Palaeo-Proterozoic, Transvaal and Olifantshoek Supergroups. The bulk of the iron ore mined and processed is exported to international markets (Shangoni Management Services, 2017). Export customers include China, South Korea, India, Japan and countries in Europe. Locally, the iron ore is sold to ArcelorMittal South Africa for steel manufacturing (Anglo American, 2023a).

The mine has three pits namely North Mine, South Mine and Lyleveld Pit. Each pit is divided into five stratified geological domains namely:

- Clay.
- Calcrete.
- A combination of clay and calcrete.
- Waste.
- Ore.

The clay domain is mined prior to the calcrete followed by the combination of clay and calcrete, and lastly waste and ore domains. Sishen Mine's geology comprises of the rock types that are indicated in Appendix A. The predominant rock types are Banded Iron Formation (BIF), conglomerate BIF (CGB), chert, chert breccia, shale, quartzite and hematite (conglomeratic, laminated and brecciated). There are areas where these rock types can be found on the same block as illustrated in Figure 1.1.

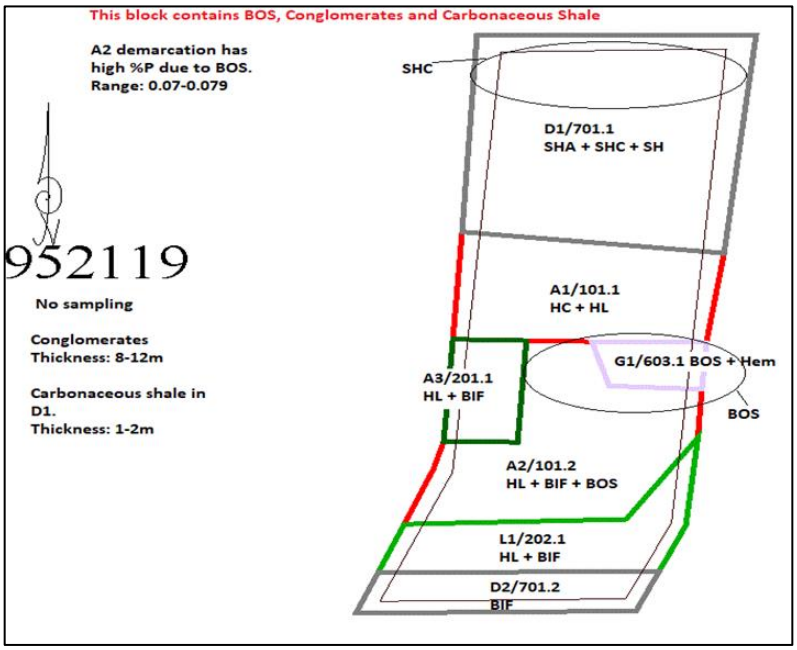



***Figure 1.1: Plan view illustration of a block containing various rock types***

(Source: Anglo American, 2023b)

Figure 1.1 shows a block containing the rock types indicated in Appendix A which can be classified as either ore or waste depending on the percentage of iron (Fe) and flagstone contained in the block. Fe classifications are illustrated in Appendix B. Rock types where the composition of Fe is equal to or more than 58.5% are considered as ore. Low grade ore consists of rock types where the composition of Fe is between 40% and 58.5% and flagstone of less than 25%. Waste is made up of rock types where the composition of Fe is less than 40% and flagstone of more than 25%.

The rock types are further divided into mining classes. The mining classes are also referred to as material types. DMS grade ore is A type material, jig grade ore is B and L type material. The jig grade ore is L type material if it contains high density BIF and CGB that is more than 50% of the total waste and considered as B type material if the total waste is less than 50%. Both DMS and jig grade ore can be K type material if the material contains potassium oxide ($K_2O$) of more than 0.6%. The low-grade ore material can be classified as C or G type material. It is C type material if the Fe is between 58.5% and 43% and G type material if the Fe is less than 43%. Waste is classified as either D or E type material. It is D type material if it is sterile waste and/or is dominated by flagstone and E type material if it is clay rich material.

A block is defined as an ore block if majority of the block contains A, K, L, B, C and G material types. The study focused on these ore blocks. Blocks with majority of D and E type materials are classified as waste. Figures 1.2 and 1.3 show examples of blocks which are classified as waste and ore, respectively. The A, K, L, B, C and G material types are the end product that, post processing are sold to the mine's customers.

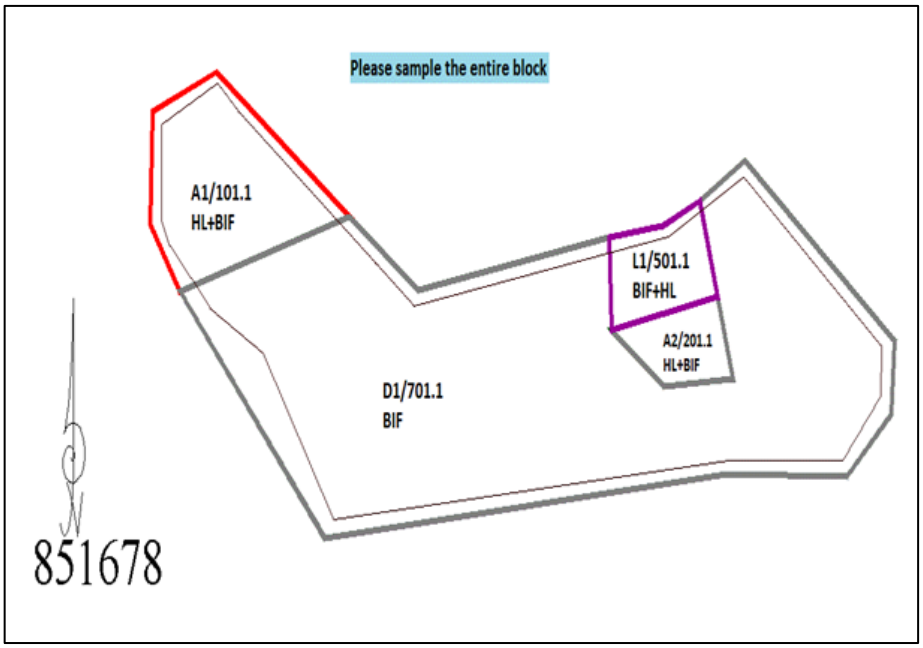



***Figure 1.2: Plan view of a block classified as a waste block***

(Source: Anglo American, 2023b)




***Figure 1.3: Plan view of a block classified as an ore block***

(Source: Anglo American, 2023b)

The iron ore is extracted by drilling and blasting using explosives. The blasting process requires that blastholes be assigned a delay timing, which at Sishen Mine is guided by burden response which is also known as burden relief. Burden response is the amount of time it takes to move a burden of rock. It is measured in milliseconds per meter of the effective burden (ms/m). According to Onederra and Esen (2003), the concept of burden relief considers $T_{min}$ and delay scatter. $T_{min}$ is the minimum time that the first row of blastholes begin to move after initiation while delay scatter considers accuracy of timing devices. The concept is important because for an explosives deck to successfully fragment and displace rock, a free face must be available for blasted material to move into. This is enabled by $T_{min}$ and determined by the accuracy of the timing devices. The free face is created when preceding blastholes detonate within the set time to enable rock fragmentation and movement. This ensures that there is sufficient burden relief (Onederra & Esen, 2003).

Timing guidelines used at Sishen Mine state that waste blocks should be blasted using a burden response of between 12 ms/m and 18 ms/m in all pits, which is similar to the burden response used to blast ore blocks. This is because the blocks in both the waste and ore domains contain similar rock types and only differentiated by the amount of Fe and flagstone present in the blocks. However, the higher-grade ore bearing rock types have a higher density as compared to lower grade ore bearing rock types, and an even higher density compared to rock types with a higher flagstone content of more than 25%. The difference in density was not taken into consideration when developing these timing guidelines.

Clay blocks are blasted using a burden response between 15 ms/m and 24 ms/m. The combination of clay and calcrete blocks are blasted using a burden response between 12 ms/m and 20 ms/m in all pits. Calcrete blocks are blasted using a burden response between 8 ms/m and 15 ms/m in the North Mine and between 15 ms/m and 20 ms/m in the South Mine pit. This is because the calcrete in the North Mine is harder than the calcrete in the

South Mine. For all these domains, the burden response is increased for smaller blocks (Olivier, 2022). These guidelines were developed from historic data based on previous timing designs, analysis of blast videos and the geology of the blocks by the Sishen Mine Drill and Blast Technical team. Since waste and ore blocks are blasted using similar burden response without taking into consideration density differences, the blasting output at the mine may be affected.

It is known and accepted that fragmentation from a blast must be of a size that is appropriate for downstream processes such as loading, hauling, and crushing (Balasubramanian, 2017). This is because fragmentation size has a direct impact on the cost and efficiency of all downstream mining processes (Rout & Parida, 2007). Therefore, when looking into ways of optimising fragmentation, it is imperative to take the fragmentation requirements of downstream processes into consideration. Figure 1.4 shows the crusher feed particle size distribution (PSD) guideline which illustrates the mine's plant fragmentation requirements.

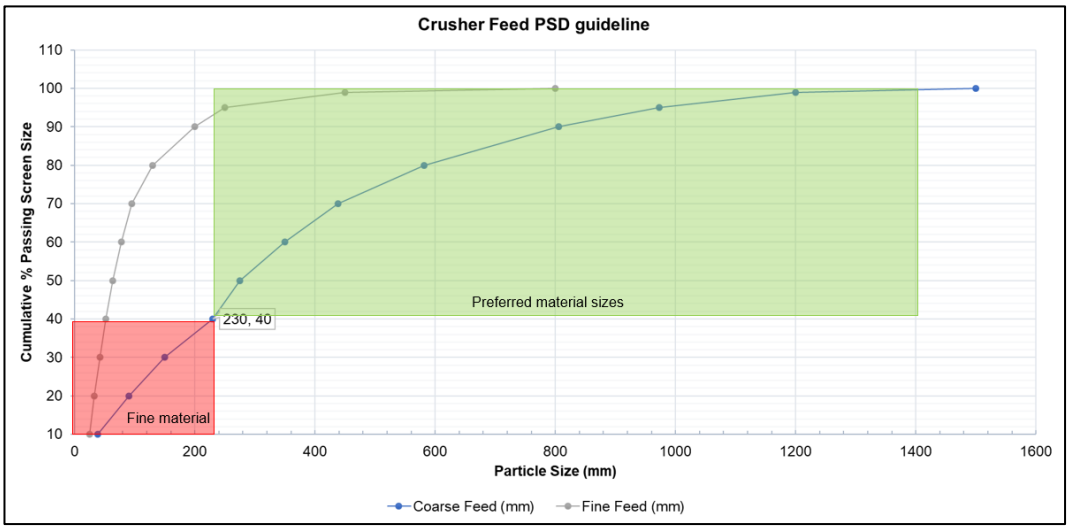



***Figure 1.4: Crusher feed particle size distribution guideline***

(Source: Anglo America, n.d.)

The mine's preferred fragmentation size range is 230 mm to 1400 mm. Ore fragmentation sizes below 230 mm are considered as fine feed and are thus

undesirable. Further fragment sizes larger than 1400 mm are also undesirable because they tend to block the crusher. As a result the boulders require secondary blasting (Anglo American, n.d.).

## 1.3 Problem statement

Sishen Mine's processing plant measures fragmentation sizes using lump to fine ratio. This is one of the mine's Key Performance Indicators (KPI). Lump to fine ratio refers to the amount of ore bearing lumps compared to ore bearing fines. The aim is to ensure that the end product from the plant has more lumps than fines as there is a premium on the lumps meaning added financial gains. For example, the steel making industry highly values lumps as they eliminate the need to sinter or pelletize (Skosana, 2023) and thus are willing to pay more. The Run of Mine (ROM) lump to fine feed into the Dense Medium Separator (DMS) crusher target is 79:21 or 79% lumps and the post processing ratio target is 70:30 or 70% lumps. Figure 1.5 indicates the DMS ROM lump to fine for 2021.

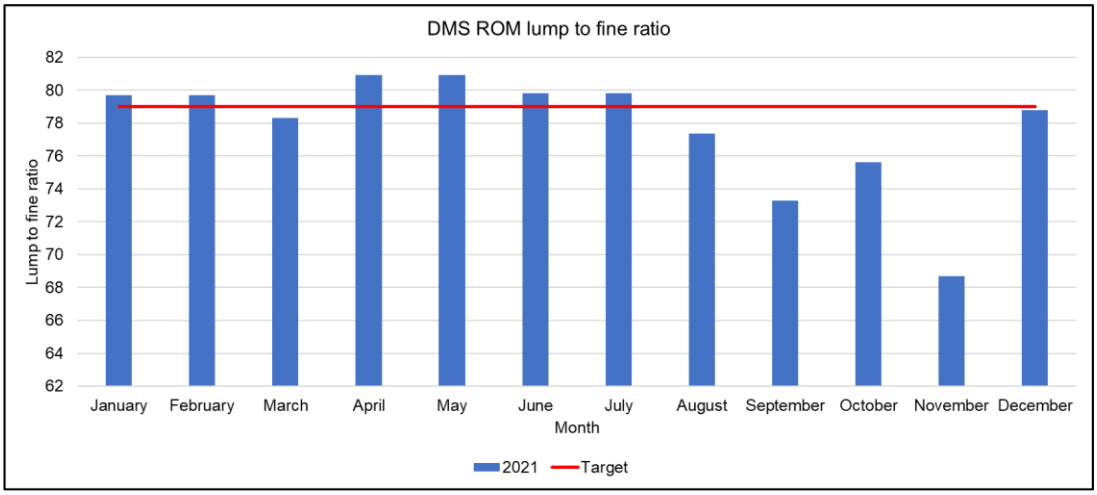



***Figure 1.5: Dense Medium Separation Run of Mine lump to fine ratio***

(Source: Kename, 2024)

The average lump to fine for 2021 was 77.74% which was below the 79% target. During that year, there were months where the target was reached

by not more than 2% above the target. This was only achieved in January, February, April, May, June and July with lump to fine ratios of 79.70%, 79.70%, 80.90%, 80.90%, 79.80% and 79.80%, respectively. For the six months more lumps than fines were received. However, the overall lump to fine ratio for the 12 months was below target. This led to the metallurgy team having concerns regarding fragmentation sizes received at the plant which was highlighted in 2022. The ore which was sent to the plant yielded more fines than lumps thus reducing the product lump to fine ratio. This resulted in less revenue.

A significant drop was experienced between July 2021 and November 2021. This brought forth the need to review the drill and blast Terms of Reference (ToR) which encompasses delay timing guidelines to optimise fragmentation within the ore domain. According to Rout and Parida (2007), optimisation of drilling and blasting within the mining cycle is imperative due to the influence of fragmentation on the cost of downstream processes.

### 1.4 Justification and significance of the research

Due to the influence of fragmentation on mine costs and process efficiency, it is imperative to understand factors affecting fragmentation at Sishen Mine. Literature shows that fragmentation is affected by factors that can be controlled by blasting engineers and factors that they cannot control. Delay timing is amongst one of the controllable factors that influence fragmentation.

There is lack of knowledge at the mine pertaining to the influence of the burden response range on fragmentation hence the need for this research. This research defined the optimal burden response for the ore geological domain that will deliver optimal fragmentation at Sishen Mine. Optimal fragmentation will improve loading rates and reduce crusher blockages. Furthermore, this will improve the lump to fine ratio, which is one of the mine's KPIs as indicated in the previous section. Given that there is a

premium received when there are more lumps than fines, the aim is to also ensure that the plant receives more lumps than fines. However, this will be done whilst ensuring that the fragment sizes are not larger than the crusher opening of 1500 mm.

Findings of the research will improve the company's profit margins. A profitable mine leads to more job creation and promotes sustainable development in local communities. Thus, South Africans will also benefit. The research will also add onto the knowledge pertaining to the influence of burden response (delay timing) on fragmentation and how it can be used to optimise fragmentation.

## 1.5 Research aim and objectives

The aim of the research was to evaluate the impact of similar timing between the ore and waste domains, and the impact of fragmentation on downstream processes. The objectives of the research were to:

- Review literature on factors affecting fragmentation in open pit mines.
- Understand the relationship between burden response and fragmentation of the ore and waste geological domains at Sishen Mine.
- Deduce whether current timing guidelines result in the mine's required crusher feed fragmentation size.
- Determine whether it is advisable for the mine to assume that waste and ore can be blasted using the same burden response.
- Investigate the impacts of fragmentation on loading rates.

## 1.6 Research scope

In order to study the influence of burden response on fragmentation, the study was conducted from March 2022 to December 2023. The study was conducted in the North and South Mine pits, in the ore and waste domains.

A total of 18 blocks were studied: nine in the North Mine and nine in the South Mine.

In the North Mine, five blocks were in the ore domain and four in the waste domain. In the South mine, six were in the ore domain and three in the waste domains. The total blocks studied for the ore domain were 11 and 7 for the waste domain. The number of study blocks was uneven between waste and ore due to availability of blocks as per the mining schedule. The burden responses used in the study ranged from 14 ms/m to 18 ms/m at increments of 1 ms/m.

## 1.7 Summary of Chapter 1 and structure of the research report

This research report is made up of five chapters. Chapter 1 described the background and context of the research topic, problem statement, justification of the research and research objectives. The chapter introduced the background and context of the problem experienced at Sishen Mine. The problem statement and justification of the research was discussed.

Chapter 2 reviews available literature pertaining to mechanisms of rock breaking using explosives. The literature review also unpacks the controllable and uncontrollable factors that influence fragmentation. A review on how fragmentation influences downstream processes and fragmentation analysis methods is also discussed.

Chapter 3 describes the research methodology. The chapter discusses the research design and data collection processes used and the data used thereof. As part of the data collection process, the pre-blast data, post-blast data and application of Split-Desktop for fragmentation analysis is also discussed. The data validation process followed, and the data analysis approach are also outlined in the chapter.

Chapter 4 presents and analyses the research results. Chapter 5 provides conclusions and recommendations. It includes the summary of the

research, research observations, research limitations and recommendations.

# 2 LITERATURE REVIEW

## 2.1 Overview of Chapter 2

This chapter reviews literature on factors affecting fragmentation, the influence of fragmentation on downstream processes and tools used to analyse fragmentation. The chapter starts by discussing the mechanisms of rock breaking with explosives. Following that, controllable and uncontrollable factors influencing fragmentation are discussed. The uncontrollable factors are outlined whilst the controllable factors including previous studies conducted on how delay timing influences fragmentation are reviewed. Furthermore, the influence of fragmentation on downstream processes as well as fragmentation analysis methods are discussed in the chapter.

## 2.2 Mechanism of rock breaking with explosives

During the drilling and blasting process in open pit mines, blastholes are drilled to the designed depth. A detonator is inserted into a booster to create a primer which is then lowered into the blasthole to about +/- 1 m from the bottom of the blasthole as shown in Figure 2.1 which shows a cross section of a charged blasthole.

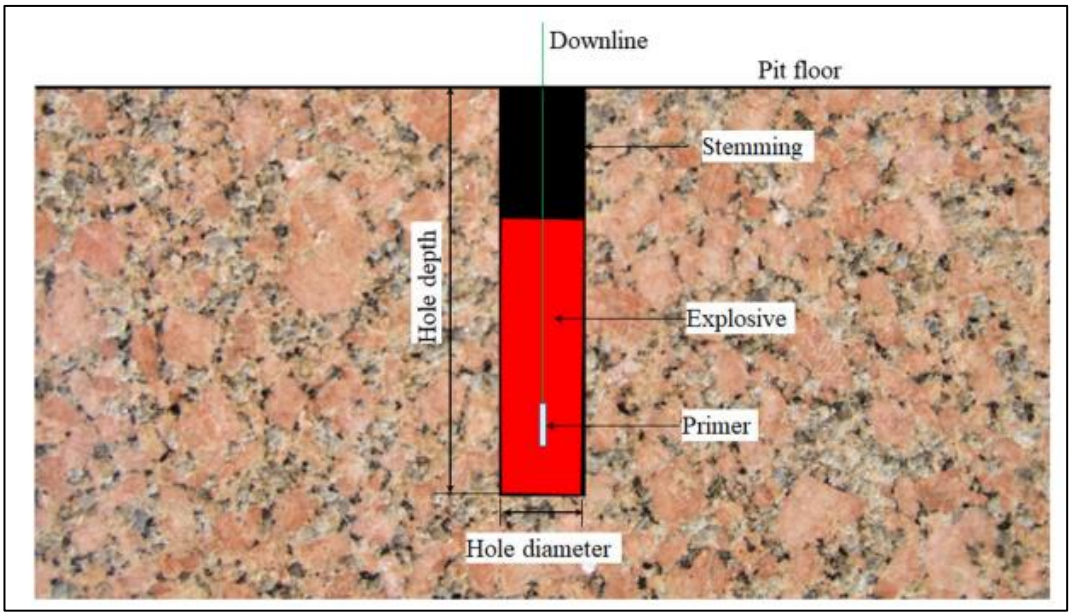



***Figure 2.1: Section view illustration of a charged blasthole***

(Source: Lawal, *et al*., 2023)

The blastholes are then charged with explosives and stemmed as per the blast design. This is done on all blastholes which are then assigned a delay timing based on the ToR. During blasting, the holes fire according to the assigned timing sequence fragmenting the rock. According to Blast Management International (2021), the rock breakage process consists of detonation, blasthole expansion and radial cracking as a result of shockwave propagation, shock wave reflection, gas driven crack expansion and burden relief.

There are two schools of thoughts and theories pertaining to rock breaking mechanisms with explosives (Hyldahl, 2018). These are reflection theory and the gas expansion theory. There are other theories that believe that both reflection and expansion occur at the same time, and these have been found to better describe the mechanism of rock breakage (Hyldahl, 2018). Figure 2.2 illustrates the breakage of the rock based on the gas expansion theory.

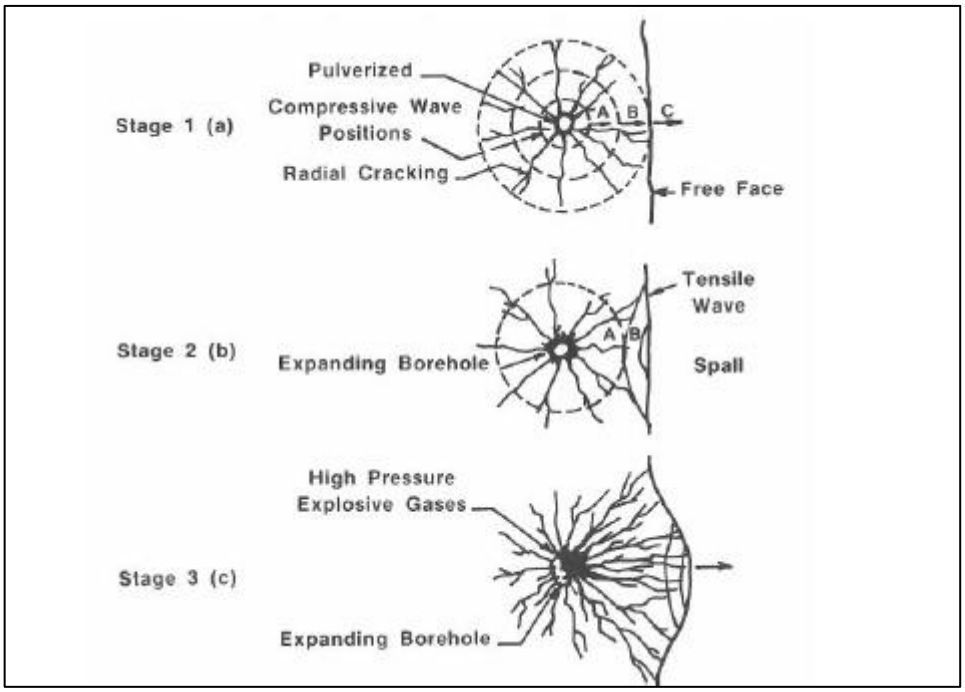



***Figure 2.2: Gas expansion theory***

(Source: Hyldahl, 2018)

The gas expansion theory is a combination of induced fracturing by stress wave and gas expansion around a blasthole. This happens in three stages. In stage 1 (a), the rock around the blasthole is shattered by high pressure and radial cracks (tangential stress) formed by the outgoing shock wave. In stage 2 (b), the outgoing shock wave creates positive pressure which reduces in magnitude as it moves away from the centre of the blasthole and drops upon reaching a free face. At the free face, the shock wave is reflected as a tensile wave towards the centre of the hole (Hyldahl, 2018). The rock consequently fails in tension creating primary failure cracks. In stage 3 (c), the actual breakage takes place. The breakage takes place through a slower reaction that is caused by the expanding gases. The radial cracks formed in stage 1 (a) are then rapidly enlarged. The breakage process that started in stage 2 (b) is completed once the mass in front of the blasthole produces high compressive stress that unloads the rock and induces high tensile stress (Hyldahl, 2018). The reflection theory is illustrated in Figure 2.3.

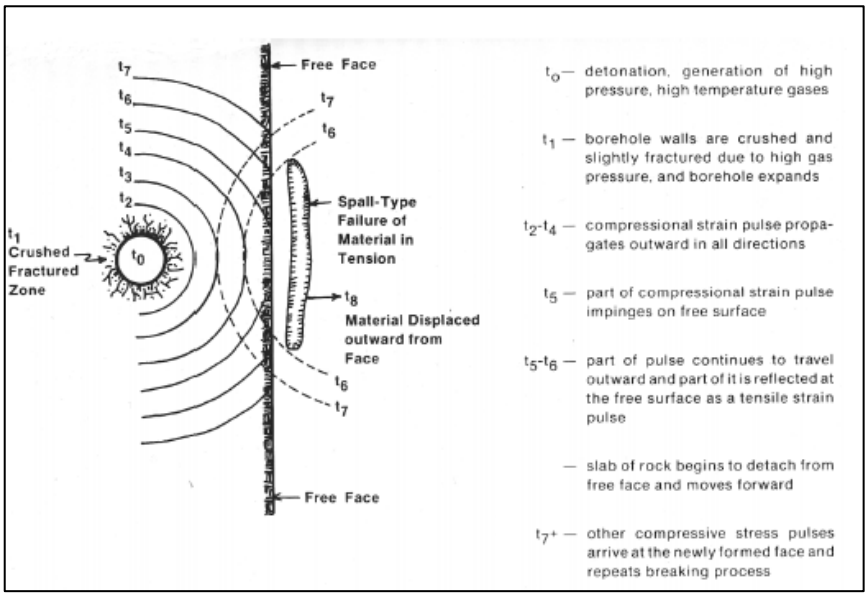



***Figure 2.3: Reflection theory***

(Source: Hyldahl, 2018)

In simple terms, the theory is based on the fact that rock is broken in compression. The compressive strength of the rock is always higher than the tensile strength of the rock (Hyldahl, 2018). An outgoing compressive wave is generated during detonation of an explosive charge. This compressive wave is then reflected back towards the blasthole as a tensile wave as soon as it reaches a free face. Based on this theory, high-pressure and expanding gases do not play a significant role in the fracturing of the rock (Hyldahl, 2018).

## 2.3 Influence of fragmentation on downstream processes

Blasting is the first step in the rock breaking process and accounts for about 15% to 20% of the total mining costs for most open pit mines (Kechik, 2018). It has a significant impact on loading, hauling, crushing and grinding (Demenegas, 2008). Therefore, it is important to understand the relationship between the outcome of blasting and downstream processes in order to achieve high productivity. This makes the evaluation of fragmentation essential to the efficiency of mining operations (Jethro, *et al*., 2016).

Kechik (2018) states that when drilling and blasting costs increase (usually due to high explosives charge value), subsequent operations costs may decrease. This is because as the explosive charge increases, the resulting fragments are finer. Figure 2.4 shows the relationship between fragmentation size and mining operational costs such as drilling and blasting, loading and hauling, crushing and grinding.

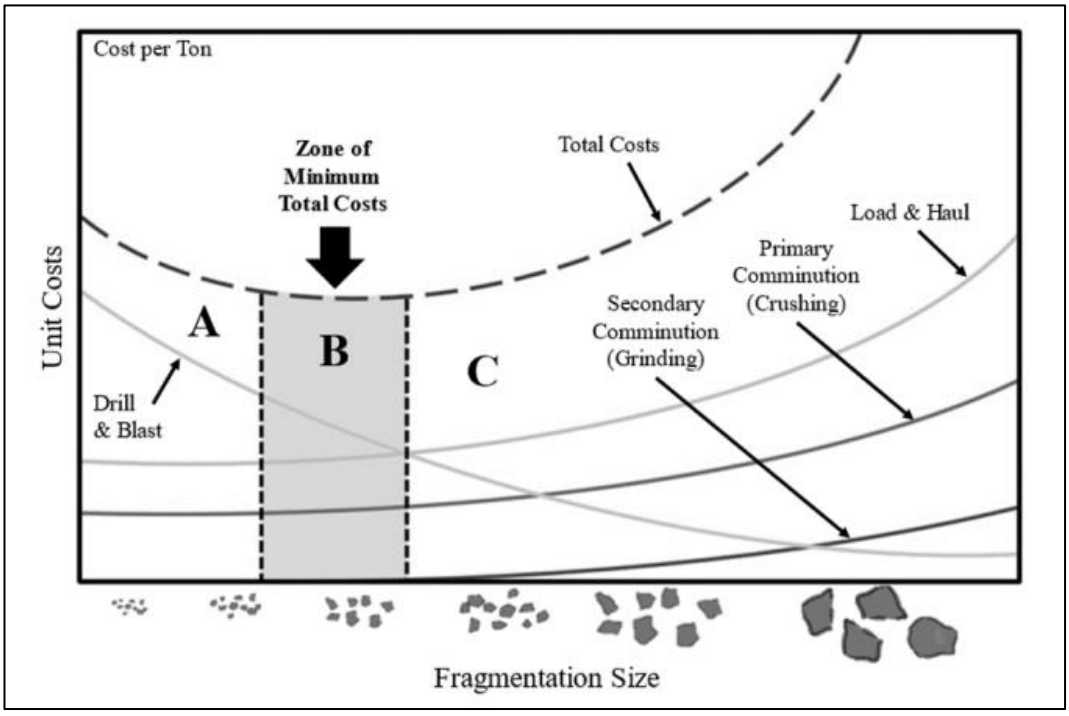



***Figure 2.4: Relationship between fragmentation size and mining operational costs***

(Source: Ikeda, *et al*., 2023)

The diagram shows three zones; namely, A, B and C. In Zone A, fragmentation size is fine with higher drilling and blasting costs compared to grinding, crushing and loading and hauling. Finer fragmentation implies that either more explosives were used or the drilling pattern was reduced thus increasing the drilling and blasting cost. However, finer fragmentation improves loading and hauling efficiencies and lowers its costs because maneuvering becomes easier consequently reducing cycle times. The

energy consumption during crushing and grinding is also reduced because with finer fragmentation, less crushing and grinding is required. The opposite of this is shown in Zone C where drilling and blasting costs are lower whilst grinding, crushing and loading and hauling costs are higher for coarser fragmentation (Ikeda, *et al.*, 2023). This is because coarser fragmentation and boulders translate into an increment of resources and time required for effective handling by mining equipment (Demenegas, 2008). These may include secondary blasting and hydraulic rock breaking. In addition, excavators cycle time increase because extensive maneuvering is required to load coarse rocks (Kechik, 2018). Furthermore, coarser fragmentation leads to increased energy consumption during crushing and grinding. In this instance, the volume of material to be downsized decreases the primary crusher throughput (Demenegas, 2008). Zone B is the optimal region and is the most economical for mining operations. This zone has lower total costs. It is important to note that each mine's optimal zone is unique and is defined by the mine's preferred fragmentation sizes and requirements for downstream processes.

Blasted rock fragments have to be of the required size distribution due to the impacts on loading, hauling, crushing and grinding (Mutinda, *et al*., 2021). This makes the size distribution of blasted fragments an important parameter to be examined (Demenegas, 2008). If fragmentation is not assessed regularly, production costs and delays could increase due to unnecessary secondary drilling and blasting (Kechik, 2018).

## 2.4 Factors influencing fragmentation

There are several factors that influence fragmentation. Kinyua *et al*. (2022), grouped these into controllable and uncontrollable factors as shown in Figure 2.5.

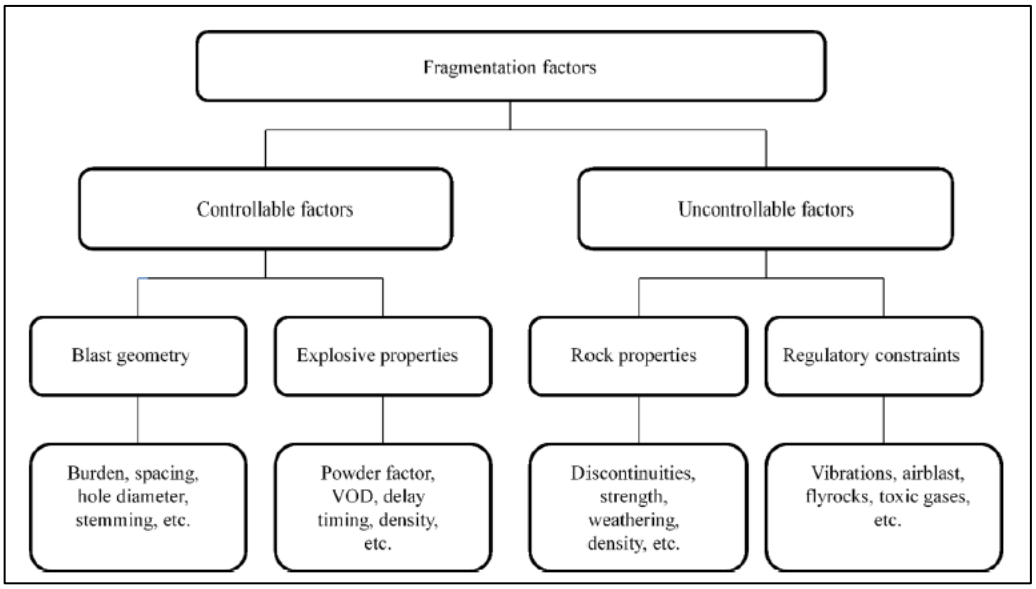



***Figure 2.5: Factors that have an influence on fragmentation***

(Source: Kinyua, *et al*., 2022)

Controllable factors are associated with the blast design geometry and explosive properties. On the other hand, uncontrollable factors are associated with rock properties and regulatory constraints.

### 2.4.1 Uncontrollable factors

Uncontrollable factors are those factors a blast engineer cannot adjust to vary fragmentation size. They are broadly categorised as either technical or legal. The technical factors are controlled by the behaviour and properties of the *in-situ* rock and include rock characteristics and geological properties. An example of the legal factors is regulations pertaining to the minimum blasting distance to the nearest sensitive structure. In most cases, the engineer would need to modify standard designs to accommodate these conditions (Gadikor, 2018). According to Mulenga (2020), the rock characteristics that influence rock fragmentation include uniaxial compressive strength (UCS), density, porosity, fractures and discontinuities. The following subsections discuss how these factors affect fragmentation.

### Uniaxial compressive strength

UCS is one of the most commonly used measures of rock strength. It is a measure of how easily a rock can generate fractures in a medium. It also has an influence on the blastability of the rock. When explosives energy is kept constant, rocks with higher UCS result in coarser fragmentation (Kinyua, et al., 2022). This is because rocks with higher strength require more explosives energy to fragment finely as compared to weaker rocks.

### Density of rock

Density of a rock mass is the mass per unit volume expressed in $t/m^3$ (Parida, 2016). The density of rock has an impact on the rock's blastability. Low density rocks break easily requiring low energy explosives to fragment finely. On the other hand, denser rocks need more explosive energy with a higher Velocity of Detonation (VOD) to break sufficiently (Kinyua, et al., 2022). When explosive energy is kept constant, denser rocks yield coarser fragmentation and vice versa for lower density rocks.

### Porosity

Porosity is defined as the measure of open spaces in a rock mass (Louisiana Department of Environmental Quality, n.d.). According to Kinyua*, et.al*. (2022), porosity has an impact on rock fragmentation. For the same water saturation conditions and amount of explosives, highly porous rocks results in coarser fragmentation. This is because greater energy dissipation takes place through the pores.

### Fractures and discontinuities

Fractures and discontinuities play a pivotal role during blasting. During blasting, explosives take the least resistant route provided by the fractures and discontinuities (Waheed, 2019). Thus, when charging blastholes where the rock has fractures and discontinuities, explosive gasses escape. In this instance, the explosives' energy can be underutilised as a result of energy escaping through the fractures (Waheed, 2019). This may result in larger

fragment sizes. It is common practice to orientate the free face in the direction of the fractures and discontinuities to maximise throw.

### 2.4.2 Controllable factors

Controllable factors can be controlled or varied by the blast engineer in order to achieve a specific blast result. These are geometric and explosive parameters (Gadikor, 2018). They are varied in an attempt to overcome challenges presented by the uncontrollable factors.

**Blasthole diameter**

According to Olofsson (1988), blasthole diameter dictates the charge diameter and controls the amount of explosives in a blasthole for any explosive type. The diameter of a blasthole affects fragmentation because it controls the explosives distribution in the blasthole (Cardu, et al., 2015). For example, for the same burden, spacing and height, a large diameter blasthole leads to a higher shock energy during blasting as opposed to a small diameter blasthole resulting in finer fragmentation size. This is because the linear charge mass (kg/m) in a large diameter blasthole is higher than in a small diameter blasthole. This results in finer fragmentation. Smaller diameter blastholes are good for highly jointed rocks and in softer geology (Gadikor, 2018). This is because highly jointed rock and softer rock formations require less explosive energy compared to competent rocks. The linear charge mass (kg/m) of smaller diameter blastholes is lower and thus the amount of explosive energy is reduced.

Blastholes with larger diameters are associated with larger burdens and spacings (Cardu, *et al*., 2015). The calculation of suitable blasthole diameter is directly influenced by the bench height as per blasting geometry rules of thumb. Equation 2.1 is used to estimate the blasthole diameter in relation to the bench height (AECI Mining Explosives, n.d):

$$Blasthole\ diameter\ (mm)\ =\ Bench\ height\ (m)\ \times\ 15 \qquad (2.1)$$

The first step towards determining the quantity of explosives per blasthole is determining the linear charge mass in kg/m. This is calculated using Equation 2.2 (AECI Mining Explosives, n.d).

$$M_c = \frac{\rho \times D^2}{1273} \quad (2.2)$$

Where: $M_c$ = Linear charge mass (kg)

$\rho$ = Density of explosive's used (g/cc)

D = Blasthole diameter (mm)

If a larger blasthole diameter is used for shorter bench heights, powder factor can increase thus leading to finer fragmentation. On the other hand, if a smaller blasthole diameter is used for a bigger bench height, powder factor can decrease thus resulting in coarse fragmentation.

**Burden and spacing**

Burden is the perpendicular distance from the axis of a blasthole to the free face, and spacing is the distance between blastholes within the same row. Burden and spacing are dependent on blasthole diameter, powder factor, bench height, fragmentation requirements and displacement requirements (Rajpot, 2009).

Tao *et al*. (2020) state that blocks with smaller burdens shatter into much finer but consistent fragments due to the pervasively distributed cracks thus resulting in finer fragmentation. Equation 2.3 is used to calculate burden (AECI Mining Explosives, n.d):

$$B = \sqrt{\frac{L \times M_C}{a \times H \times K_t}} \quad (2.3)$$

Where: B = Burden (m)

L = Charge length (m)

$M_c$ = Linear charge mass (kg/m)

a = Spacing to burden ratio

H = Bench height (m)

$K_t$= Technical powder factor (kg/m³)

According to Tao *et al.* (2020), as spacing decreases, fragment sizes also reduce. This is mainly because as the spacing decreases, there is an equivalent increase in energy density. Therefore, finer particles are formed as the potential for crack branching increase.

Smaller spacings result in premature linking of charged blastholes resulting in a fractured plane between the blastholes. Gases can escape prematurely through these fractured planes resulting in air blast, excessive fly rock, finer fragmentation and formation toes (Agyei & Owusu-Tweneboah, 2019). On the other hand, larger spacings result in coarser fragmentation, toes and non-uniform walls. This is due to the fact that blastholes that are far apart result in loss of interaction between detonating charges.

For the same geology, bench height and diameter, an increase in burden and spacing will result in coarser fragmentation. This is because the powder factor will reduce due to the larger volume of rock that needs to be broken by less explosives than required. A reduction in burden and spacing will result in finer fragmentation due to the increment in powder factor. Spacing is a function of burden which is calculated using Equation 2.4 (AECI Mining Explosives, n.d):

$$Spacing = a \times burden \tag{2.4}$$

Where a = Spacing to burden ratio

Spacing is directly proportional to burden as seen in Equation 2.4. For a constant spacing to burden ratio, when the burden is increased, the spacing must also be increased.

**Spacing to burden ratio**

Spacing to burden ratio has a direct impact on fragmentation size achieved during blasting (Lijojo, 2021). It ranges between 1 and 2. The optimal ratio

for staggered and rectangular patterns is 1.15 and 1.25, respectively (Lijojo, 2021). Equation 2.5 is used to calculate spacing to burden ratio (AECI Mining Explosives, n.d):

$$a = \frac{Spacing}{Burden} \tag{2.5}$$

Where: a = spacing to burden ratio

When spacing is substantially less than burden (when a << 1), stemming material loosens earlier than expected and premature splitting between blastholes occurs (Gadikor, 2018). This is because when blastholes are closely spaced, they interact prematurely resulting in stemming ejections and premature fracturing of the planes between blastholes. This results in high pressure explosives gases being released into the atmosphere at a rapid rate and excessive back break (Gadikor, 2018). When spacing is significantly higher than burden (a >> 1.5), charges do not interact well to break the *in-situ* rock between blastholes thus resulting in boulders (Gadikor, 2018).

**Stemming length**

Stemming is a non-explosive material which is used to fill the top portion of a blasthole from the top of the explosives deck to the collar of the blasthole (Coulibaly, 1982). Figure 2.6 shows stemming relative to the blasthole length and explosive column.

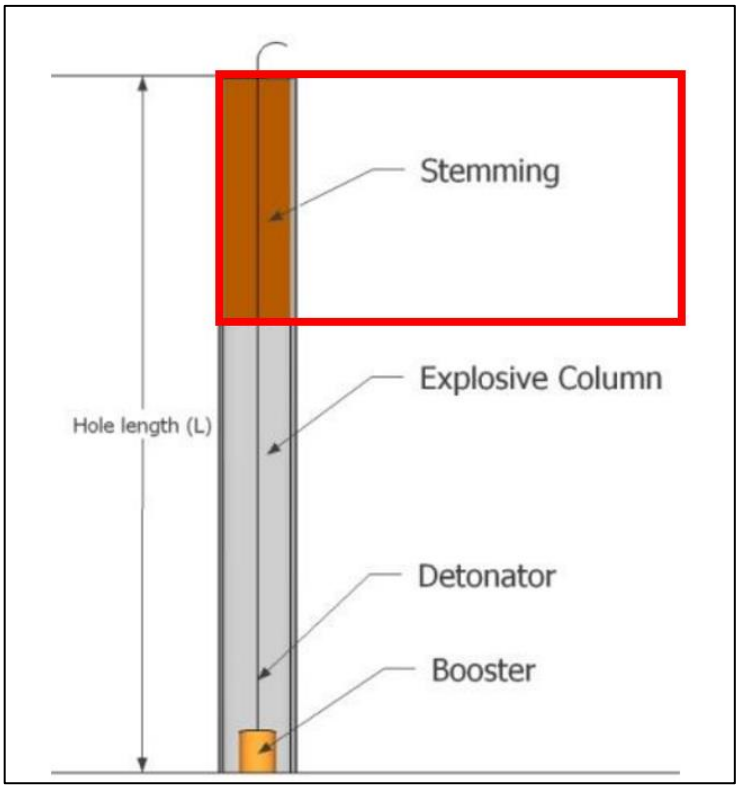



***Figure 2.6: Illustration of stemming relative to an explosive column and blasthole length***

(Source: Domingo*, et al.,* 2015)

The purpose of stemming is to promote sufficient fracturing of the rock mass by retaining the explosives' energy for an adequate time to improve explosive performance consequently improving fragmentation and reducing environmental issues (Oates & Spiteri, 2021). Hence, if stemming is insufficient, explosives gases and energy prematurely escape into the atmosphere resulting in coarse fragmentation, airblast and flyrocks (Lijojo, 2021). On the other hand, excessive stemming results in large boulders in the collar region of the bench or capping in some situations, poor swelling of the muckpile and increased ground vibration (Lijojo, 2021). Laboratory and field tests have proven that the efficiency of a blast increases by almost 50% if adequate stemming is used (Uttarwar & Devendar, 2020).

There has been a suggestion that optimum stemming length increases with a decrease in the rock mass competence and varies between 20D and 60D

where D refers to blasthole diameter (Lijojo, 2021). Some researchers have recommended that stemming length should be 25D. However, Konya and Walter (1991) suggested that stemming length should be 0.7 x burden if crushed rock is being used as stemming material and 1.0 x burden if drill chippings are being used as stemming material (Lijojo, 2021). Table 2.1 indicates stemming length rules of thumb recommended for normal and controlled blasts.

**Table 2.1: Stemming length rules of thumb**

(Source: AECI Mining Explosives, n.d.)

| Rock type | Normal (mm) | Controlled (mm) | Stemming material |
|---|---|---|---|
| Hard (competent) | 20D | 30D | Crushed stone |
| Hard (competent) | 30D | 40D | Drill cuttings |
| Medium (weathered) | 25D | 35D | Crushed stone<br>Drill cuttings |
| Soft | 15D | 25D | Drill cuttings |

Normal blasts refer to general blasts that have low risk and impact while controlled blasts are sensitive blasts whereby the risk and impact are high. For example, blasting in close proximity to a residential area.

For each rock type, stemming length should be longer for controlled blasts as compared to normal blasts. The type of stemming material used also affects stemming length. For instance, for hard rock, stemming length should be longer when drill cuttings are used as compared to when crushed stone is used. However, for medium weathered rock, the stemming length differs only depending on whether blasting is controlled or normal. The kind of stemming material used does not influence the stemming length. The calculation of the stemming length using the variables indicated in Table 2.1 is illustrated by Equation 2.6 (AECI Mining Explosives, n.d).

$$Stemming\ length\ (m) = coefficient \times blasthole\ diameter\ (mm) \qquad (2.6)$$

### Stemming material properties

The properties of stemming material such as size, aspect ratio, angularity, compaction, and cohesion influence the confining capability of the stemming material (Sazid, 2014). Stemming material should have high density and high shear strength to improve the effectiveness of a blast. It should be of a shape and size with superior interlocking capabilities during blasting (Mpofu, *et al.*, 2021).

The most widely used and preferred stemming material are drill cuttings and angular crushed stone because they are cheaper and readily available (Sazid, 2014). However, angular crushed stone is mostly recommended due to its ability to interlock making it effective as stemming material. The angularity creates frictional resistance between the stemming material and the wall of the blasthole (Sazid, 2014) thus containing explosive energy in the hole longer than with drill cuttings (Lijojo, 2021). Proper stemming material can lead to a reduction in stemming length and improve powder factor (Sazid, 2014).

The stemming material should confine explosives energy to ensure that gases do not escape prematurely. This will achieve maximum use of the energy on the rock mass. Lijojo (2021) indicates that the ratio of blasthole diameter to stemming material should be between D/10 to D/20 where D is the blasthole diameter in mm. This is applicable to angular material with minimum fines. Equation 2.7 is used to calculate the size of stemming material to use (Mpofu, *et al.*, 2021):

$$Stemming\ material\ size = \frac{1}{8} \times Blasthole\ diameter \qquad (2.7)$$

According to Oates and Spiteri (2021), fragmentation improves significantly when crushed aggregate is used to stem blastholes as compared to drill cuttings. A study was conducted at Red Dog Mine in Alaska and it was found that the mean fragmentation size ($X_{50}$) of holes stemmed with drill cuttings was significantly higher than that of blastholes stemmed with crushed

aggregate. Additionally, a 21.2% improvement in the muckpile throw was achieved when using crushed aggregate. Loading and hauling productivity also improved by 18%. The improvement pertaining to fragmentation led to a 20% longer period between crusher liners due to the reduction in wear and tear of the crusher (Oates & Spiteri, 2021).

**Powder Factor**

Mohamed, *et al.* (2015) define powder factor as the quantity of explosives required to fragment 1 $m^3$ of rock. Powder factor is expressed as $kg/m^3$. It is one of the most crucial variables that is used to predict efficient blast design parameters (Agyei & Nkrumah, 2021). According to Salati and Mark (2020), powder factor can be used as an indicator of how hard the rock is, explosives cost and/or as a guide to the blast design.

There are two different kinds of powder factors, namely actual powder factor and technical powder factor. Technical powder factor excludes sub-drill and is used in the blast design to predict fragmentation. On the other hand, actual powder factor includes sub-drill and is used to calculate the quantity of explosives and subsequently explosives costs (Lijojo, 2021). The classification of technical powder factors used in blasting per rock type, blasting category, rock factor and uniaxial compressive strength (UCS) is shown in Table 2.2.

**Table 2.2: Rock types and their technical powder factors**

(Source: AECI Mining Explosives, n.d.)

| Blasting category | Rock type | Technical powder factor (kg/m³) | Rock factor | UCS (MPa) |
|---|---|---|---|---|
| Hard | Andesite<br>Dolerite<br>Granite<br>Ironstone<br>Silcrete | 0.70 – 0.90 | 12 – 14 | >250 |
| Medium | Dolomite<br>Hornfels<br>Quarzite<br>Serpentine<br>Schist | 0.40 – 0.50 | 10 – 11 | 100 – 250 |
| Soft | Sandstone<br>Calcrete<br>Limestone<br>Shale | 0.25 – 0.35 | 8 – 9 | 50 – 100 |
| Very Soft | Coal | 0.15 – 0.25 | 6 | <50 |

Table 2.2 shows that powder factor increases with increasing rock hardness which indicates that softer rocks require less amount of explosives to break 1 m³ of rock (Kechik, 2018). Moreover, massive rocks with fewer planes of weakness require higher powder factors to break as compared to rock with closely spaced joints and fractures which require lower powder factors (Kechik, 2018). Hayati and Abroshan (2017) state that a high powder factor results in smaller fragments whereas, a lower powder factor results in coarser fragmentation which could generate boulders that require secondary blasting. The actual powder factor $(K_a)$ is calculated using Equation 2.8 (AECI Mining Explosives, n.d):

$$K_{\mathrm{a}} = \frac{(L+U) \times M_c}{B \times S \times H} \tag{2.8}$$

Where: L = Charge length (m)

U = Sub-drill (m)

$\mathrm{M_c}$ = Linear charge mass (kg/m)

B = Burden (m)

S = Spacing (m)

H = Bench height (m)

The equation illustrates that actual powder factor is directly proportional to explosives quantity used and inversely proportional to burden, spacing and bench height (volume of broken rock). Figure 2.7 illustrates the relationship between powder factor and mean fragmentation size.

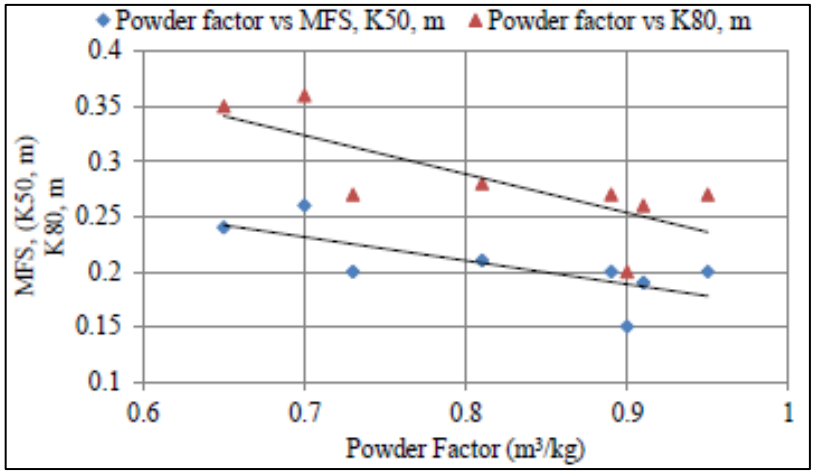



***Figure 2.7: Relationship between rock fragment sizes and powder factor for a mine in India***

(Source: Prasad, *et al*., 2017)

The figure was drawn from a study conducted at a coal mine in Jharkhand, India. The graph shows that the mean and maximum fragmentation sizes decrease as the powder factor increases. Another study was conducted at a limestone quarry. Figure 2.8 shows the results of the study.

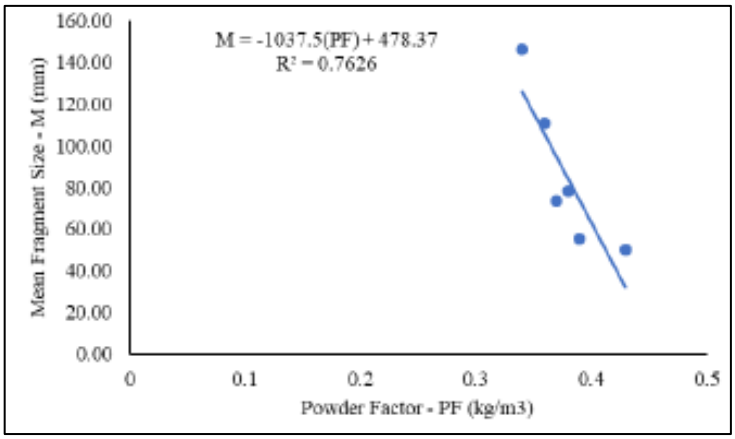



***Figure 2.8: Relationship between rock fragment sizes and powder factor for a limestone quarry***

(Source: Shehu, *et al*., 2020)

Figure 2.8 also shows that as powder factor increases, the mean and maximum fragmentation sizes decrease. This is because a higher powder factor means that more explosives are used to break a certain volume of rock thus increasing the explosives energy. This then decreases fragmentation sizes (Shehu, *et al.*, 2020).

**Delay timing**

Nie (2016, p. 8) defines delay timing as "*the timing interval between detonations"*. The aim during detonation is that when blastholes are fired, a free face for subsequent blastholes to break into is created, which is achieved by utilising the correct firing pattern and delay intervals between blastholes (Kinyua, *et al*., 2022). Delay timing plays a crucial role in the blasting process and has been shown to have a direct impact on fragmentation, back break, ground vibrations and muckpile characteristics (Kinyua, *et al*., 2022). Nie (2016) further elaborates that there are two types of delay timings namely, inter-row and inter-hole timing as shown in Figure 2.9.

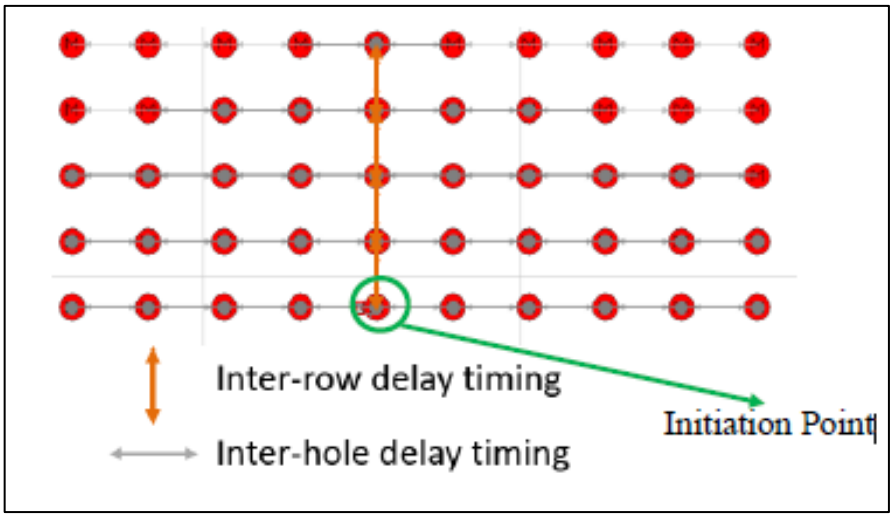



***Figure 2.9: Inter-hole delay timing and inter-row delay timing***

(Source: Kinyua, *et al*., 2022)

Inter-row timing refers to the time interval between rows and inter-hole timing refers to the time interval between holes in the same row. The sequence in which blastholes are fired is determined by the firing pattern used (Kinyua, *et al*., 2022). Burden response which is also referred to as burden relief is a factor that has to do with the initiation sequence of a blast. It is measured in millisecond per metre (ms/m) of the firing burden in the blast (Martin, 2018). Burden response is then multiplied by burden to get the inter-row delay timing. This is the delay interval between rows (Bender, 1999).

According to Yang and Rai (2011), inter-row timing plays a vital role in the systematic utilisation of energy that has to do with burden movement. Also, it plays a role in ensuring that there is momentum, and the desired coherence of blastholes is maintained during blasting. Furthermore, controlling and properly sequencing delay timing is the easiest way to improve fragmentation and ensure blast consistency (Tang, *et al*., 2022).

In cases were shorter inter-row delay timing is used, the front row burden does not move before the second-row fires. This leads to poor relief and over confinement of the consecutive rows. Upward cratering (vertical uplift)

then takes place due to poor relief. As a result, fragmentation will be coarse and the muckpile will be tight close to the face (Yang & Rai, 2011). On the other hand, if longer inter-row delay timing is used, front row blastholes fail to act as a screen and do not confine the consecutive rows. This results in undesired lateral scattering and fine fragmentation. Ideally, the burden preceding any row should move sufficiently by the time subsequent rows fire (Yang & Rai, 2011).

Yang and Rai (2011) conducted a study at a limestone quarry to investigate the influence of delay timing on fragmentation. The study was conducted on different firing patterns using 17 ms and 25 ms inter-row delays. These equated to effective firing delays of 8 ms/m and 12 ms/m per firing burden, respectively. Blasts fired using shorter inter-row delays (17 ms) yielded finer fragmentation compared to blasts fired using longer inter-row delays (25 ms). These results indicate that shorter inter-row delay timings are most effective in strong and hard rock formations (Yang & Rai, 2011).

Another study was conducted by Choudhary, *et al*. (2021) at a limestone mine on the effects of stemming material and inter-row delay timing on blast results. The delay intervals between successive rows in the study varied from 5 ms/m to 23.4 ms/m of burden. The results of the study indicated that inter-row delay timings of 8 ms/m to 14 ms/m of the burden between the first and second row along with a gap of 5 ms/m of burden between the last two rows resulted in uniform and finer fragmentation sizes for the entire blast (Choudhary, et al., 2021). The longer delay interval between the first two rows and an extra delay at the back rows allowed for the muckpile to displace sufficiently and prevented boulders. This is because the delay timing intervals between rows plays a significant role in inter rock collisions and the congestion of the muckpile. Without the delay between the rows, the fragment sizes were bigger and not uniform (Choudhary, et al., 2021). This indicates that softer rock types such as limestone require more time to displace the muckpile resulting in finer and uniform fragmentation.

Therefore, slower inter-row delay timing is more effective for softer rock formations.

Katsabanis *et al.* (2006) also conducted a series of small-scale tests at a granodiorite block to study the effects of timing on fragmentation. The study indicated that very long or very short delays resulted in coarse fragmentation. However, the study indicated that there is a window period that resulted in optimum fragmentation. For granodiorite, this is between 0.11 ms/m and 11 ms/m of burden.

A study conducted by Rai and Nath (2004) to investigate inter-row delay requirements for strong sandstone strata indicated that large inter-row delay timing yielded coarse fragmentation. The inter-row delay timing used was 24 ms/m and 18 ms/m. In this case the mean, coarse and maximum fragment sizes were very large. The blasts yielded mean fragmentation sizes of 632.9 mm and 706.8 mm. Blasts where the inter-row delay timing was reduced (14 ms/m and 11 ms/m) yielded better fragmentation with mean fragmentation sizes of 424.1 mm and 404.6 mm (Rai & Nath, 2004).

The studies above highlight the dependency of timing on rock strength and that each mine has unique timing hence the need to conduct this study. The inter-row delay timing should be shorter for strong and massive rocks and can be doubled for weak and highly fissured rocks (Rai & Nath, 2004). This is because greater shattering effect is imperative to ensure sufficient rock breakage in strong and hard rock formations. Shorter inter-row delays allow for the great shattering effect because the shorter delay interval between rows creates plenty opportunities for shattering by inter-rock collisions. Longer inter-row delays result in adequate relief. However, there are minimal opportunities for inter-rock collisions (Yang & Rai, 2011).

Tang *et al.* (2022) conducted an experimental study to determine the influence delay timing has on fragmentation in bench blasting. This was done by analysing the stress wave in a two-dimensional horizontal plane of

granite rock. The study showed that fragmentation size increased when delay timing is longer without any stress wave interaction. Thus, supporting the conclusion that delay timing does affect fragmentation.

Hettinger (2015) conducted a study at a granite quarry on the effects of short delay times on rock fragmentation in bench blasts. The study concluded that short hole-to-hole delays do not improve fragmentation in full scale bench blasts. Longer inter-hole delays (10 ms and 25 ms) resulted in finer fragmentation whilst shorter inter-hole delays (1 ms) resulted in coarser fragmentation (Hettinger, 2015). According to Domede *et al.* (2018), granite has high mechanical strength of up to 220 MPa. This indicates that in a case where coarser fragmentation is required, stronger rock formations require shorter delay timing.

Bender (1999) states that inter-hole delay timing should be 3.3 ms/m to 16.4 ms/m of burden and inter-row delay timing should be 2 to 3 times longer than the inter-hole timing. AECI Mining Explosives (n.d) states that inter-hole delay timing should be 3 ms/m to 6 ms/m of burden for hard to soft rock, respectively. Furthermore, inter-row delay timing should be 10 ms/m to 30 ms/m of burden for hard to soft rock, respectively (AECI Mining Explosives, n.d.). Orica (2020) states that the overall burden response should be 10 ms/m to 20 ms/m for production blasts.

**Explosive properties**

Detonation pressure, explosive density and VOD are explosive properties that affect fragmentation. Detonation pressure is located in the shock zone in front of a reaction zone. It is a function of explosive density and the square of VOD (Mulenga, 2020). Figure 2.10 shows the detonation sequence of an explosives charge. The detonation pressure is measured in the Chapman-Jouguet plane (C-J plane) of a detonation wave as it propagates through an explosive column.

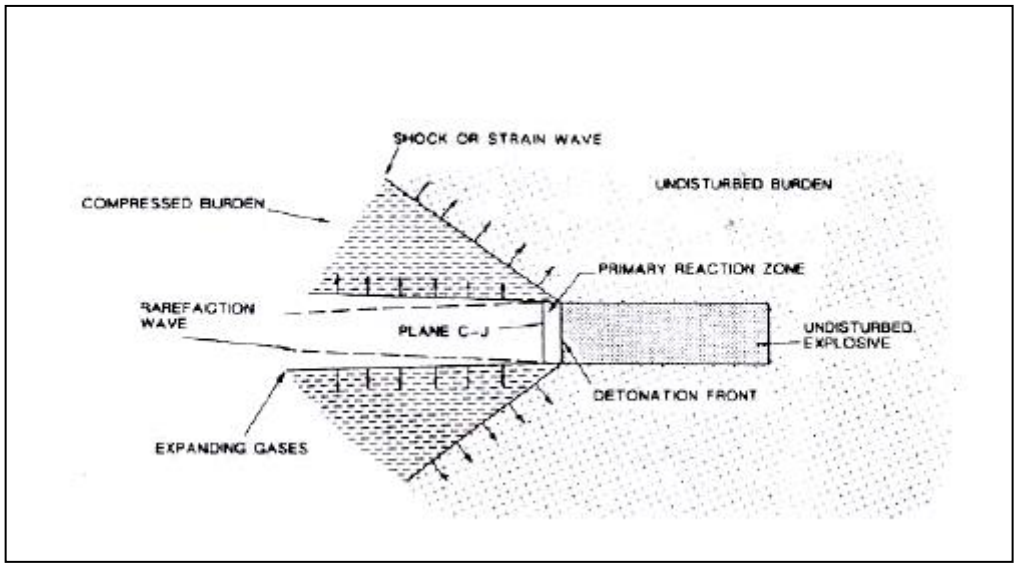



***Figure 2.10: Detonation sequence showing Chapman-Jouguet Plane***

(Source: Kondelchuk & Novikov, 2005).

Detonation pressure for commercial explosives varies from 500 MPa to 1500 MPa (Kondelchuk & Novikov, 2005). Hard and competent rocks fragment easier with high detonation pressure explosives. This is because of the direct impact of detonation pressure on rock breakage mechanisms with explosives (Kondelchuk & Novikov, 2005). Detonation pressure is calculated using Equation 2.9 (Orica, 2016):

$$P_d = 0.25 \times \rho \times VoD^2 \times 10^{-6} \quad (2.9)$$

Where: $P_d$ = Detonation pressure (GPa)

ρ = Density of explosives (g/cm³)

According to Equation 2.9, detonation pressure is dependent on explosive density and VOD. Detonation pressure increases with increasing explosive density and VOD. Explosive density refers to specific weight of explosives in g/cm³ (Kondelchuk & Novikov, 2005). Explosives with a higher density have more strength as compared to lower density explosives (Parida, 2016).

This means that high density explosives provide more breakage thus resulting in finer fragmentation (Kondelchuk & Novikov, 2005).

VOD refers to the speed in metre per second (m/s) which the detonation of explosives travels through an explosive column (Kondelchuk & Novikov, 2005). Lower VOD explosives have lower detonation pressure and lower explosive energy. Thus, explosives with a lower VOD result in coarser fragmentation compared to explosives with a higher VOD for the same rock type (Kabwe, 2018). Furthermore, because higher VOD explosives have a more shattering effect, they are more suitable for hard rock mining (Kondelchuk & Novikov, 2005).

## 2.5 Fragmentation analysis

Fragmentation is a vital KPI and has been widely used in numerous studies to understand the influence of blasting on downstream mining processes. This makes analysis of fragmentation significant when optimising blasts (Bamford, *et al*., 2021).

There are numerous methods used to analyse fragmentation. These methods include qualitative visual observation, equipment monitoring, sieving and digital image analysis. The qualitative visual analysis method involves viewing the blasted muckpile immediately after a blast. This is done by mining professionals who then decide whether secondary drilling and/or blasting is required or whether blast design parameters need to be changed or not (Nanda & Pal, 2020). This method has low accuracy as it is subjective and the hidden portion of a muckpile does not get analysed. The equipment monitoring method can be applied through shovel loading rates analysis (Nanda & Pal, 2020). This method assumes that the faster the loading rate, the better the fragmentation. However, in instances where there is no uniform fragmentation distribution, this method becomes inefficient. Sieving is the most accurate method of fragmentation analysis. With this method, different sieves with different mesh numbers for different fragment sizes are

used to screen rock fragments. The screened rock fragments are then grouped by size. However, sieving is costly, time consuming and requires the loading and hauling process to be halted during the analysis (Nanda & Pal, 2020). As a result, sieving is not economically viable, as it affects production.

Digital image analysis is the widely used method though it has limitations (Bamford, *et al*., 2021). The method uses data processing techniques and different sensors to analyse fragmentation size distribution. These techniques include stereo photography, laser scanning and photography. The techniques have limitations including quality of the images and the fact that that they only sample surface fragmentation to estimate internal characteristics, estimating amount of fines and fragments delineation. Additionally, the technique involves extensive manual editing to delineate fragments correctly from the images of the fragments captured. This can be very time consuming (Bamford, *et al*., 2021).

One of the programs utilised to digitally analyse fragmentation images is Split-Desktop. According to Esen, *et al.* (2000), Split-Desktop refers to a desktop version software of a program known as SPLIT which is user-assisted and can be used by mining engineers on mining sites. The software has five major parts. The first part is the scaling of images in the field using an object of known size. The second part is the automatic delineation of fragmentation images. The third part is manual editing of automatically delineated fragments to improve quality of results. The fourth part is the calculation of the size distribution within the program from the delineated fragments information. The fifth part of the program involves plotting and exporting of the size distribution results (Esen, *et al.*, 2000). The digital image analysis method was used to conduct fragmentation analysis for the study. This is because as a widely used method, it is readily available.

## 2.6 Chapter summary

This chapter reviewed literature pertaining to fragmentation in surface mines. Rock is fragmented with explosives through the gas expansion theory and/or the reflection theory. The size of the fragments has an impact on downstream mining processes such as loading, hauling, crushing and grinding. It is thus important to understand factors that influence fragmentation.

Factors that influence fragmentation are classified as uncontrollable and controllable. Rock properties such as UCS, density, porosity and fractures and discontinuities are examples of uncontrollable factors. When all parameters are kept constant, higher UCS and density yields coarser fragmentation. Whereas highly porous rocks result in finer fragmentation. Fractures and discontinuities lead to explosives energy escaping thus result in larger fragment sizes.

Controllable factors include blasthole diameter, burden and spacing, burden to spacing ratio, stemming length, stemming material properties, powder factor, delay timing and explosive properties. When all factors are kept constant, an increase in blasthole diameter and powder factor yields finer fragmentation. On the other hand, an increase in burden, spacing and stemming length results in larger fragment sizes. Also, blastholes should be preferably stemmed with crushed angular rock to ensure that explosive energy is retained long enough to break the rock sufficiently.

Another controllable factor is delay timing. Delay timing refers to inter-hole and inter-row delay timing. When burden response is applied, it is multiplied by burden to get inter-row delay timing. Multiple studies indicated that inter-row delay timing should be shorter for stronger rocks and longer for softer rocks.

Explosives properties also have an influence on fragmentation. These properties are explosives density, VOD and detonation pressure. All these

factors have a similar influence on fragmentation. As they increase, the fragment sizes reduce.

Following the understanding of factors affecting fragmentation, it is imperative to understand how fragmentation is analysed. There are multiple methods of fragmentation analysis. However, the most commonly used method is digital imaging. This can be done using Split Desktop software.

# 3 RESEARCH METHODOLOGY

## 3.1 Overview of chapter 3

This chapter describes the research method used for the study. The research design used to conduct the study is presented. The data collection method is also discussed looking into the pre- and post-blast data collected and how it was collected. As part of the data collection process, the delay timing design process and application of Split-Desktop for fragmentation analysis is discussed. This chapter also discusses the data validation process that was followed to ensure validity of the data used for the study and introduces how the collected data was analysed.

## 3.2 Research design

Research design is a plan for a study which outlines the framework for data collection. It is a plan that is used for selecting subjects, research sites and the data collection process used to answer the research question(s). Essentially, research design is a bridge between the research question and execution (Mafuwane, 2011) .

The two types of research methods are qualitative and quantitative research approaches. This research study used the quantitative approach. Quantitative research is conducted by collecting data that can be analysed numerically. Furthermore, the results can be presented through tables, graphs and statistics (Acaps, 2012). There are four types of methods under quantitative research approach namely survey, correlational, experimental, and casual-comparative research (Apuke, 2017). Survey research involves applying the scientific sampling method using questionnaires to deduce a selected population’s characteristics through statistical methods. Correlational research is utilised to ascertain if there is a relationship between two or more variables within a sample or population and if so to what degree. This relationship is determined through correlation coefficients

which range from +1.00 to -1.00 (Apuke, 2017). Figure 3.1 illustrates the spectrum that can be used to interpret correlation coefficients.

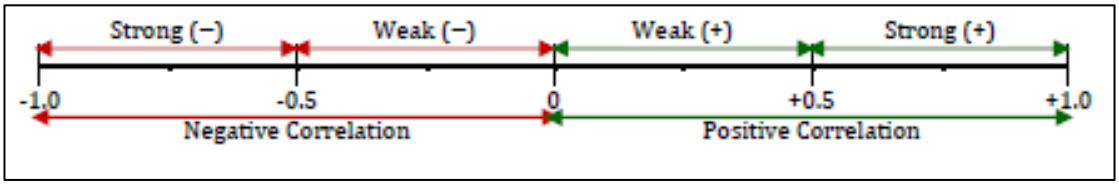



***Figure 3.1: Spectrum for interpreting correlation coefficients***

(Source: Senthilnathan, 2019)

A correlation between two variables can be positive or negative. This is dependent on the correlation coefficient (Senthilnathan, 2019). A correlation coefficient of +1 indicates a strong positive correlation and a correlation coefficient of -1 indicates a strong negative correlation (Gogtay & Thatte, 2017). A positive correlation means that the two variables being studied are directly proportional and a negative correlation means that the two variables are inversely proportional (Corporate Finance Institute, n.d.).

Casual-comparative research is also known as ex post facto which means "*from after the fact*" (Apuke, 2017, p. 45). This simply means that the researcher studies variables in retrospect to investigate a problem under study. With this method, the cause and consequence of the relationship between two or more variables are identified and established. Experimental research is research where the influence of an independent variable on a dependent variable is observed. Independent variables are altered to track their impacts on the dependent variable (Mozumder, 2021). The experimental, correlational, and casual comparative methods were selected and used in this research because these are the most suitable methods based on the aims and objectives of the research.

The aim of this research was to deduce whether similar timing guidelines for both waste and ore currently used at Sishen Mine result in ore being fragmented to the required crusher feed size. This was done through

experimental research whereby the independent variable (burden response) was altered to monitor its effects on fragmentation (the dependent variable) while some variables were kept constant. Geometric design parameters (burden, spacing and diameter) were kept constant. This is because these variables also have an impact on fragmentation. However, the research only focused on the relationship between burden response and fragmentation.

Following on the discussion in Section 2.3, fragmentation size has an influence on loading, hauling, crushing and grinding. Therefore, it is essential to determine the relationship between fragmentation size and loading rates. This relationship was analysed using the correlational research method. A casual-comparative research method was used to determine whether it is advisable for the mine to blast waste and ore using a similar timing. This was done by investigating the consequence of burden response for a certain rock density on fragmentation.

### 3.3 Data collected and the collection process

The data collection process details the process used to gather data required to achieve the research objectives. The process is important to ensure that data is collected and captured correctly and to ensure that the data can be used properly to answer the research question(s) (Lijojo, 2021).

Data can either be secondary or primary in nature. Secondary data is data that has been collected from an already published source or from other existing sources. Primary data is firsthand data collected by the researcher which has not been published. Primary data is deemed to be more reliable (Kabir, 2016). Both primary and secondary data were used for this study. Table 3.1 indicates which data was classified as primary and which was classified as secondary data. It also indicates the source of each data type that was collected.

**Table 3.1: Type of data collected and data source**

| Primary data | Data source | Secondary data | Data source |
|---|---|---|---|
| Geometric design | Rockma software | Geological information | Reconcilor Data Entry cloud storage system |
| Timing design | ViewShot 3D software | Average UCS | Rockma software |
| Charge data | BlastLogic software | Fragmentation analysis data | Split-Desktop software |
| | | Loading rates | Tableau Server cloud storage system |
| | | Lump to fine ratio | DMS Plant Metallurgist |

Data was collected in two sets which are, the pre-blast data and post-blast data. The two data sets are different and serve different purposes. The data was collected in the waste and ore geological domains in the North and South Mine pits from March 2022 to November 2023. A total of 11 blocks were studied in the ore domain and 7 in the waste domain as stated in Section 1.6.

### 3.3.1 Pre-blast data

Pre-blast data is the first set of data that was collected. This data set is blast design data. The data included average UCS, geological information, geometric design, and timing design data. The geological data gathered pertains to the rock type(s) on the blast block and density of the material. The densities of ore and waste were captured on Microsoft Excel. The data was captured directly from Reconcilor Data Entry. This was also used to collect rock types found in each block. Reconcilor Data Entry is the mine's internal data entry cloud storage system used by the geology department to store geological information. The geological information was also used in determining the blasthole diameter, burden and spacing used as per the already existing mine's ToR. Furthermore, the average UCS recorded by the drill rig sensors during drilling was captured from Rockma software.

The geometric design data gathered was the burden, spacing and blasthole diameter. For the purpose of this research, the blocks analysed had the same geometric design which was kept constant throughout the study. This was done to ensure consistency throughout the study. It was also to ensure

that only certain variables are altered to be able to achieve the research objectives. However, two different kinds of explosives were used due to the mine's contractual obligations with explosive suppliers. To ensure consistency, the data was grouped by explosive type. This data was collected from Microstation software and BlastLogic software which are used by the mine to design blasts and to assign charges.

Burden response timing data was collected prior to blasting. This was collected from ViewShot 3D which is the timing design software used by the mine. The software is also used to simulate blasts on a computer before transferring the timing onto the initiation systems used. The timing was applied in the form of burden response and was varied between 14 ms/m to 18 ms/m at 1ms/m intervals for both domains. This data and the geometric design data is primary data.

**Blast design parameters**

The study was conducted on production blocks with the same geometric design. Blast design parameters were kept constant on all these blocks as discussed in Section 1.6. These are shown in Table 3.2.

**Table 3.2: Blast design parameters**

| Design parameter | Value |
|---|---|
| Blasthole diameter (mm) | 311 |
| Burden (m) | 7 |
| Spacing (m) | 8 |
| Spacing to burden ratio | 1.14 |
| Sub-drill (m) | 2.5 |
| Bench height (m) | 12.5 |
| Final stemming length (m) | 6 |
| Initiation system | IntelliShot |
| Booster (pentolite booster) (g) | 400 |

Parameters stipulated in Table 3.2 were based on the ToR used to design drill and blast patterns at the mine. These were kept constant because all

these parameters influence fragmentation. However, one of the research objectives was to analyse the influence of burden response on fragmentation. Thus, the need to ensure all other parameters remain constant throughout the study. The two explosive products used for during the study are Powergel Eco 35 and Innovex EGA. The properties of these explosives are as shown in Table 3.3.

**Table 3.3: Explosive properties**

| **Product name** | **Innovex EGA** | **Powergel Eco 35** |
|---|---|---|
| **Type of explosive product** | Bulk | Bulk |
| **Average VOD (m/s)** | 5 142 | 5 000 |
| **Average in-hole density (g/cm³)** | 1.28 | 1.15 |
| **Calculated detonation pressure (GPa)** | 8.46 | 7.19 |

Powergel Eco 35 is doped emulsion with 35% Ammonium Nitrate Porous Prills and Innovex EGA is emulsion. Innovex EGA has a higher average VOD, in-hole density and detonation pressure. According to the discussion in Section 2.4.2, higher VOD, in-hole density and detonation pressure result in finer fragmentation.

### Ore domain data

A total of 11 blocks were studied in the ore domain. As indicated, these were further grouped by explosive product used. The first set of eight study blocks were charged with Powergel Eco 35. The pit name, average rock density, average UCS and burden response used are shown in Table 3.4. The UCS for each rock type is presented in Appendix C.

**Table 3.4: Ore domain pre-blast data for blocks charged using Powergel Eco 35**

| Block ID | Pit name | Average rock density (t/m³) | Average UCS (MPa) | Burden response used (ms/m) |
|---|---|---|---|---|
| 241023 | South Mine | 4.09 | 192 | 15 |
| 241127 | South Mine | 3.91 | 148 | 15 |
| 952206 | North Mine | 4.10 | 192 | 16 |
| 761807 | North Mine | 4.07 | 182 | 17 |
| 761808 | North Mine | 4.07 | 204 | 18 |
| 241129 | South Mine | 3.97 | 205 | 15 |
| 4311336 | South Mine | 3.90 | 203 | 14 |
| 4311337 | South Mine | 4.10 | 200 | 14 |

Three of the study blocks charged with Powergel Eco 35 were based in the North Mine and five in the South Mine pit. The average rock density was calculated as the average of the different rock densities on a specific block. The burden response used on these set of blocks ranged from 14 ms/m to 18 ms/m. Three blocks were charged with Innovex EGA and the pre-blast data collected is shown in Table 3.5.

**Table 3.5: Ore domain pre-blast data for blocks charged with Innovex EGA**

| Block ID | Pit name | Average rock density (t/m³) | Average UCS (MPa) | Burden response used (ms/m) |
|---|---|---|---|---|
| 311397 | South Mine | 4.68 | 221 | 15 |
| 952119 | North Mine | 3.96 | 178 | 18 |
| 1042106 | North Mine | 4.19 | 181 | 18 |

One block was based in the South Mine and two in the North Mine. Only two burden responses were applied to these set of blocks which are 15 ms/m and 18 ms/m. The geology and timing plans for all ore blocks are as shown in Appendix D and E, respectively.

**Waste domain data**

A total of seven blocks were studied in the waste domain. The blocks were designed and drilled on the same geometric design parameters as the ore

blocks. Table 3.6 shows the pit location, burden response, rock types, average rock densities and average UCS for the waste blocks that were charged with Powergel Eco 35.

**Table 3.6: Waste domain pre-blast data for blocks charged using Powergel Eco 35**

| Block ID | Pit name | Average rock density (t/m³) | Average UCS (MPa) | Burden response used (ms/m) |
|---|---|---|---|---|
| 952214 | North Mine | 3.27 | 168 | 17 |
| 952220 | North Mine | 4.10 | 202 | 15 |
| 771802 | North Mine | 4.22 | 139 | 17 |

All blocks in the waste domain that were charged with Powergel Eco 35 were located in the North Mine. These blocks were fired using 15 ms/m and 17 ms/m burden response. Blocks 952220 and 771802 had higher average rock density due to the small pockets of ore bearing rock types in the blocks. Table 3.7 shows the pre-blast data for blocks charged with Innovex EGA.

**Table 3.7: Waste domain pre-blast data for blocks charged with Innovex EGA**

| Block ID | Pit name | Average rock density (t/m³) | Average UCS (MPa) | Burden response used (ms/m) |
|---|---|---|---|---|
| 4310906 | South Mine | 2.70 | 205 | 15 |
| 4311102 | South Mine | 3.02 | 172 | 18 |
| 231263 | South Mine | 2.95 | 146 | 16 |
| 1051405 | North Mine | 2.68 | 161 | 18 |

Three of the bocks charged with Innovex EGA were based in the South Mine and one in the North Mine. These blocks were fired using 15 ms/m, 16 ms/m and 18 ms/m burden responses. These set of blocks had the lowest average rock densities compared to all the blocks that were studied. These ranged from 2.68 t/m³ to 3.02 t/m³. All these blocks were fully waste blocks and Fe was less than 40%. The average rock densities for the waste blocks are lower compared to ore blocks. This is due to the low Fe percentage in waste blocks. The geology and timing designs for all waste blocks are presented in Appendix F and G, respectively. According to Kulula, *et al.,* (2017), high

density rocks have higher strength and hardness and tend to result in coarser fragmentation. In this case, based on the study blocks, waste blocks generally have lower density and lower strength.

### 3.3.2 Post-blast data

The post-blast data that was collected pertains to the fragmentation analysis, loading rates and DMS crusher ROM lump to fine ratio. Fragmentation analysis images were collected directly from the pit. These were transferred to Split Desktop software which was used to produce the fragmentation size distribution curves and the uniformity index per block. This data was collected by the explosives supplier thus it is secondary data. Loading rates data was also collected to understand the influence of fragmentation on loading. This was collected from the mine's Tableau Server which collects the data directly from the shovels making it primary data. The lump to fine ratio was collected to analyse the ratio during the investigation and after assigning the optimal burden response from the study. This was provided by the mine's metallurgist making it secondary data.

### 3.3.3 Application of Split-Desktop for fragmentation analysis

Split-Desktop is designed to analyse digital fragmentation images obtained from a digital camera which are captured from blasted muckpiles in the pit. The software then produces the fragmentation size distribution curve (Tavakol Elahi & Hosseini, 2017). The system was utilised to analyse fragmentation post blasting. The software was applied in four of the five stages described in Section 2.5. The second stage was not applied because the images were delineated manually and automatic delineation was not applied. The four stages are discussed in the next subsections.

#### Stage 1: Capturing and scaling images

Images were collected from the blocks selected for the study using a digital camera directly from the blasted muckpile. According to Esen *et al*. (2000), images from muckpiles are collected by placing two objects of a known size

for scaling. One is placed at the top of the slope and the other at the bottom of the slope. A total of 8 to 20 images are sufficient depending on the size of the blast (Esen, *et al*., 2000). An example of a fragmentation image with two scales is indicated in Figure 3.2.



***Figure 3.2: Captured image for fragmentation analysis***

(Source: Bulk Mining Explosives, 2023)

Two 230 mm diameter basket balls were used for this study. On average 10 images were taken per study block. One ball was placed at the bottom of the slope and another at the top of the slope.

**Stage 3: Delineation of fragmentation images**

Once the images were captured, they were firstly automatically delineated by the software. An example of a delineated image is shown in Figure 3.3.

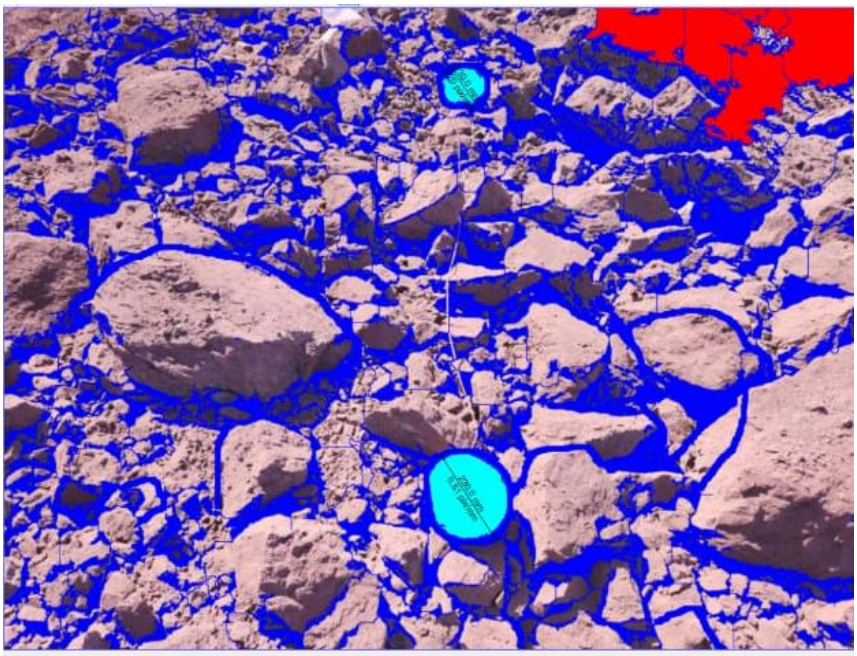


***Figure 3.3: A delineated fragmentation analysis image***

(Source: Bulk Mining Explosives, 2023)

After the automatic delineation it is always necessary to manually delineate the images. This is because automatic delineation has some limitation. The first limitation is that the software may mistakenly consider a large patch of fines as a boulder. Secondly, the software may divide a single fragment into smaller fragments due to bedding planes and rock textures (Esen, *et al*., 2000). Lastly, the software may delineate particles which should not be included in the final size distribution that are neither fines nor rock fragments (Esen, *et al*., 2000). During the manual delineation, each rock fragment was traced out in blue and a red paint bucket was used to fill in the fines and items that were not identified as rock fragments.

**Stage 4: Calculation of results**

Once the images were delineated and scaled, the software was prompted to show results. The software utilises the characteristics of the delineated fragments to calculate the size distribution of each analysed image (Esen, *et al*., 2000). These characteristics are the area and dimensions of each rock fragment in comparison to the scale. The software offers two

calculation options; a Schumann distribution and a Rosin-Rammler distribution. For this study, a Rosin-Rammler distribution calculation method was used because it provides the most reasonable description of the fragmentation sizes (Abioye, 2018).

**Stage 5: Fragmentation size distribution curve**

The fragmentation size distribution curve along with percentage passing were exported onto Microsoft Excel and saved in a computer. Figure 3.4 shows an example of the size distribution curve produced by the software for block 241127.

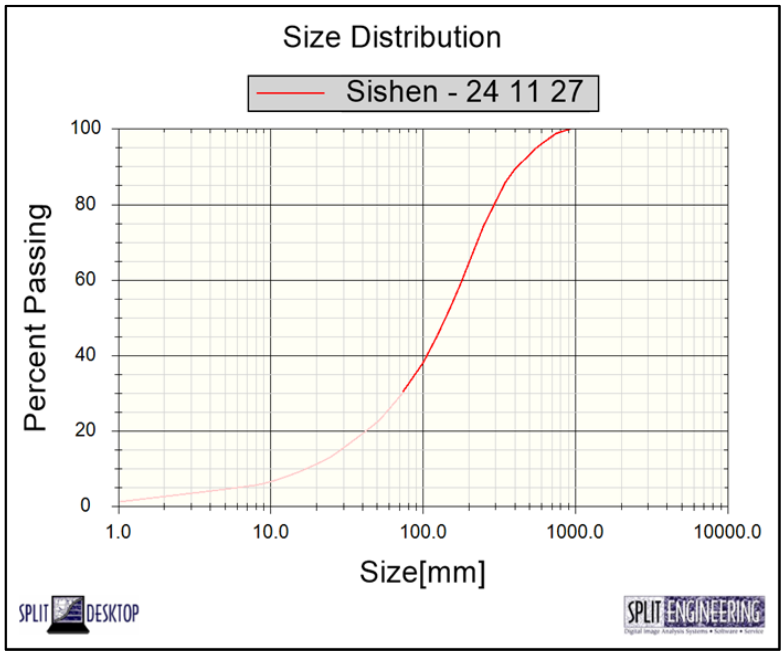



***Figure 3.4: Fragmentation size distribution curve for block 241127***

(Source: Bulk Mining Explosives, 2023)

A similar curve was plotted for all blocks. The size distribution curve is based on the cumulative percentage passing and size (mm) exported from the software. The results were then tabulated. The uniformity index, mean fragmentation size and the top size were exported from the software.

## 3.4 Data validation process

The data used in the research was collected directly from the timing and design software to ensure validity. This was to ensure that actual drilling and timing data was used. Geological data and loading rates were collected from the mine's database servers to ensure that the data was not altered in any form. Fragmentation was analysed in conjunction with the explosive supplier. To ensure that the data was valid, the unfiltered results exported from the software was provided for the research. Nonetheless, the analysis was carried out manually, thus there was human intervention involved in the process. Therefore, there is potential of errors in the analysis.

## 3.5 Data analysis approach

A quantitative data analysis is a systematic process of collecting and evaluating quantifiable data. This can be done in two ways which are inferential and descriptive. The inferential data analysis approach is inductive (Ali, 2021). This approach tests hypotheses to deduce the probability of whether or not a hypothesised effect, difference or relationship is true or not (Kotronoulas, et al., 2023). A descriptive approach presents data in a quantitative and an easily accessible form (Ali, 2021). This method simply describes how samples look in the form of tables or graphs (Kotronoulas, et al., 2023). According to Ali (2021), descriptive data analysis compares variables against other variables to answer the research question(s). A descriptive data analysis approach was chosen for the study because the collected data was quantitative and presented in tables and graphs.

The data analysis started with clearly defining research objectives. This was followed by data collection that was captured in a spreadsheet on Microsoft Excel. Graphs and tables were produced to describe the collected data. These consisted of the relationship between burden response and 80%

passing fragmentation size ($X_{80}$) for ore blocks to determine the influence of burden response on fragmentation.

The fragmentation size distribution of the study blocks was overlaid with the mine's required crusher feed fragmentation size distribution. Additionally, this analysis determined whether current timing guidelines result in the mine's required crusher feed fragmentation size or if the guidelines should be changed. The data was further analysed to determine whether waste and ore blocks should be blasted using the same burden response. It was also imperative to further understand the influence of fragmentation size on downstream processes. This was done by analysing the relationship between fragmentation and loading rates in the form of a graph.

## 3.6 Chapter summary

This chapter describes the approach that was used to investigate the influence of burden response (inter-row delay timing) on fragmentation at Sishen Mine. The research design was discussed, describing how the research was conducted. The research design indicated that experimental, correlational and causal-comparative research methods approaches were the appropriate quantitative methods to achieve the research objectives. The manner in which the pre and post blast data was collected throughout the study was presented elaborating which set of data was primary and which was secondary. The application of the fragmentation analysis method was described. Furthermore, the data validation process that was followed during the study was discussed along with the approach that was used to analyse the collected data.

# 4 RESULTS AND ANALYSIS OF RESULTS

## 4.1 Overview of chapter 4

This chapter presents the results of the study and the analysis thereof. Two different kinds of explosive products were used during the study. Therefore, the results are grouped by geological domain and further by explosive product.

## 4.2 Ore domain results

The post-blast results analysed in the study was the fragmentation size achieved at $X_{80}$ and loading rates. $X_{80}$ for ore blocks is the most crucial post-blast variable because it is a measure of fragmentation distribution that are send to the plant. With ore blocks, it is imperative to ensure that the $X_{80}$ is as close as possible to 600 mm. This enables the plant to produce more lumps than fines post crushing and grinding. Generally, finer fragments result in shorter cycle times and improved loading rates. However, having shorter cycle times but wrong fragmentation sizes does not assist in terms of revenue generation. Optimal fragmentation is more preferred. Table 4.1 shows the post-blast results of ore blocks that were charged with Powergel Eco 35. The fragmentation results PSD for all study blocks are presented in Appendix H and I for ore and waste blocks, respectively.

**Table 4.1: Ore domain post-blast results for blocks charged using Powergel Eco 35**

| Block ID | Average rock density (t/m³) | Average UCS (MPa) | Burden response used (ms/m) | $X_{80}$ (mm) | Loading rate (t/hr) |
|---|---|---|---|---|---|
| 241023 | 4.09 | 192 | 15 | 330.13 | 6 399 |
| 241127 | 3.91 | 148 | 15 | 292.04 | 10 340 |
| 952206 | 4.10 | 192 | 16 | 210.42 | 19 046 |
| 761807 | 4.07 | 182 | 17 | 201.95 | 5 895 |
| 761808 | 4.07 | 204 | 18 | 191.48 | 20 694 |

The table shows that $X_{80}$ ranged from 191.48 mm to 330.13 mm. The finer and coarser $X_{80}$ of the set was achieved using a burden response of 18 ms/m and 15 ms/m, respectively. Loading rates ranged from 6 399 t/hr to 20 694 t/hr. The coarser $X_{80}$ resulted in lower loading rates and the smaller $X_{80}$ resulted in the highest loading rates. This is because coarser fragments are more difficult to load and take longer compared to finer fragments.

The fragmentation results of these blocks were plotted against the crusher feed PSD guidelines. This was to compare the results against the plant fragmentation requirements. This is shown in Figure 4.1 which was extracted from Appendix H.

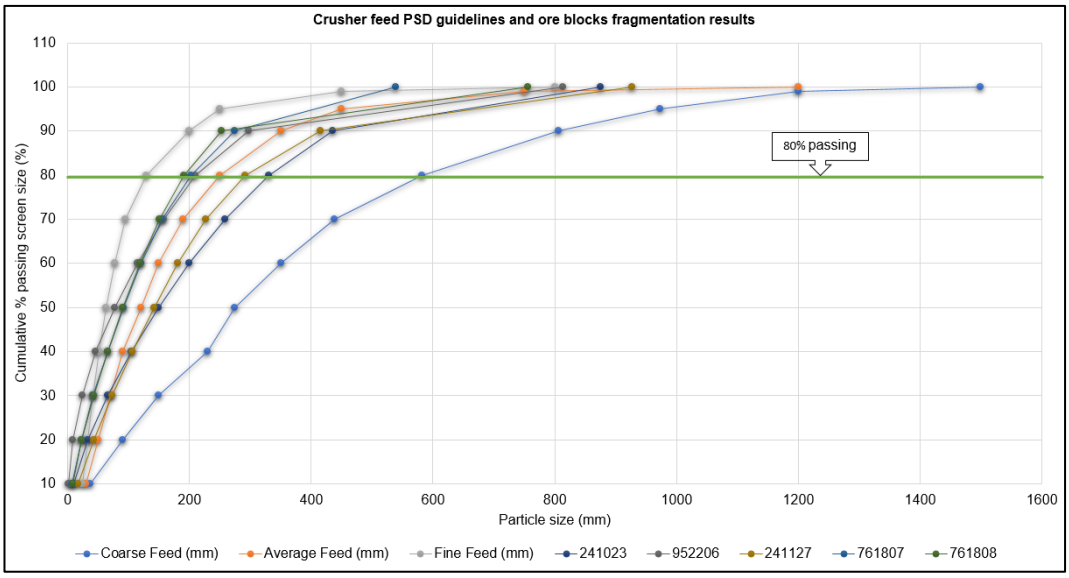



***Figure 4.1: Crusher feed PSD guidelines and ore blocks fragmentation results for ore blocks charged using Powergel Eco 35***

An average feed graph was added on Figure 4.1. The mean fragmentation is 250 mm. The PSD for blocks 241023 and 241127 are above the average feed PSD. The other three blocks achieved PSD below the average feed. Block 761808 PSD is closer to the fine feed which is followed by blocks 761807 and 952206 with fragmentation sizes lower than 230 mm. Fragmentation sizes finer than 230 mm are considered fines. From the five blocks, block 241023 resulted in better fragmentation. This block was fired using 15 ms/m burden response. Block 241127 was also blasted using 15 ms/m burden response and resulted in $X_{80}$ finer than block 241023 by 38.09 mm. This is because block 241023 was denser than block 241127. Thus block 241127 resulted in finer fragmentation compared to block 241023. The post-blast results for ore blocks charged with Innovex EGA are shown in Table 4.2.

**Table 4.2: Ore domain post-blast results for blocks charged using Innovex EGA**

| Block ID | Average rock density (t/m³) | Average UCS (MPa) | Burden response used (ms/m) | $X_{80}$ (mm) | Loading rate (t/hr) |
|---|---|---|---|---|---|
| 311397 | 4.68 | 221 | 15 | 220.24 | 8 950 |
| 952119 | 3.96 | 178 | 18 | 161.65 | 15 484 |
| 1042106 | 4.19 | 181 | 18 | 165.39 | 12 600 |

Only three blocks were studied in this case. This is because two of the other blocks charged with Innovex EGA were not accessible post the blast. The blasts were taken late in the afternoon when it was dark. The following morning, loading and hauling had already begun, thus due to safety reasons access to the blasted blocks was impossible.

The $X_{80}$ results for the three blasts ranged from 161.65 mm to 220.24 mm. The two blocks blasted using 18 ms/m burden response resulted in finer fragmentation compared to block 311397. Block 311397 achieved a coarser $X_{80}$. This block was blasted using 15 ms/m burden response. Loading rates ranged from 8 950 t/hr to 15 484 t/hr. Block 952119 achieved the highest loading rate with the finest fragmentation. Block 311397 achieved the lowest loading rate with coarser fragmentation. This indicates that finer fragmentation yields higher loading rates. The fragmentation results for these blocks were also plotted against the plant crusher feed PSD guidelines for comparison. This is shown in Figure 4.2.

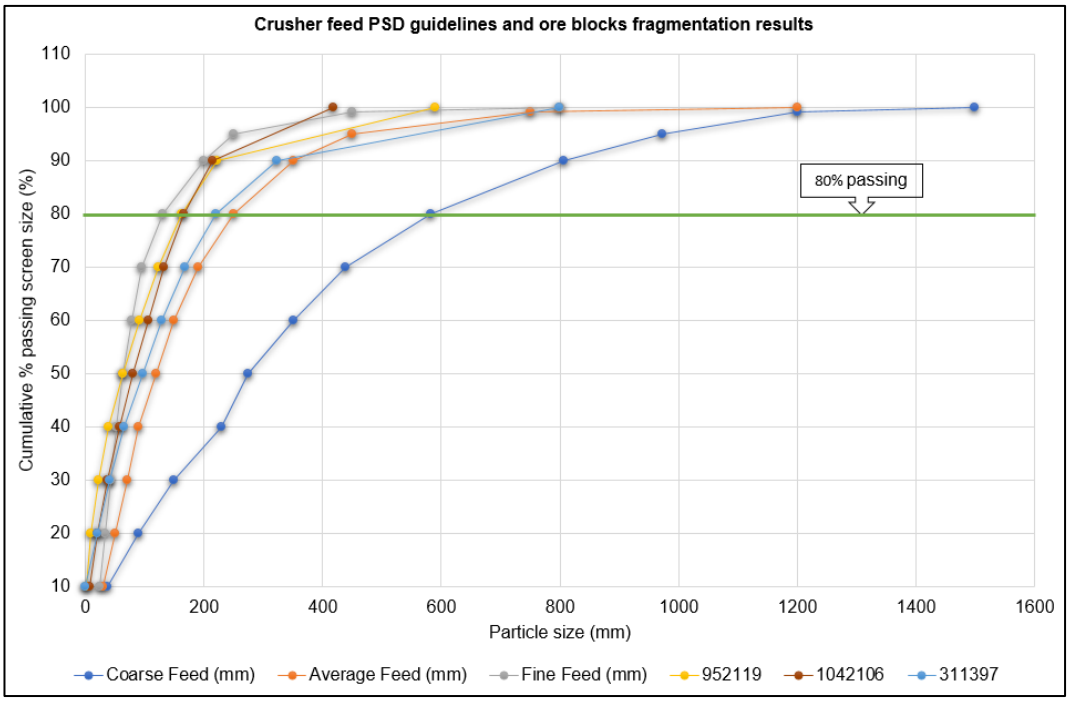



***Figure 4.2: Crusher feed PSD guidelines and ore blocks fragmentation results for ore blocks charged using Innovex EGA***

All the ore blocks blasted with Innovex EGA resulted in a finer fragmentation distribution size lower than 230 mm. As discussed in Section 1.2, fragment sizes below 230 mm are considered fine feed and undesirable at Sishen Mine. The finer fragmentation is because of the high detonation pressure of 8.46 GPa for Innovex EGA compared to 7.19 GPa for Powergel Eco 35. The detonation pressure was calculated using Equation 4.1 (Orica, 2016):

$$P_d = 0.25 \times \rho \times VoD^2 \times 10^{-6} \quad (4.1)$$

Where: $P_d$ = Detonation pressure (GPa)

ρ = Density of explosives (g/cc)

Based on the post blast results, 15 ms/m was chosen as the optimal burden response. This was due to the fact that 15 ms/m burden response resulted in fragmentation distribution size closer to the target compared to blocks blasted using burden responses between 16 ms/m and 18 ms/m. This was

the case for all ore blocks charged with both Powergel Eco 35 and Innovex EGA. Therefore, 15 ms/m was applied to block 241129 in the South Mine. The block was charged with Powergel Eco 35 because Innovex EGA has a higher detonation pressure thus resulting in finer fragmentation. The aim was to achieve a PSD closer to the coarse feed PSD with $X_{80}$ of 600mm. The block's rock types and density are shown in Table 3.4. The block achieved $X_{80}$ of 200.28 mm and 11 241 t/hr loading rates. The block's fragmentation results plotted against the crusher feed PSD guidelines are shown in Figure 4.3.

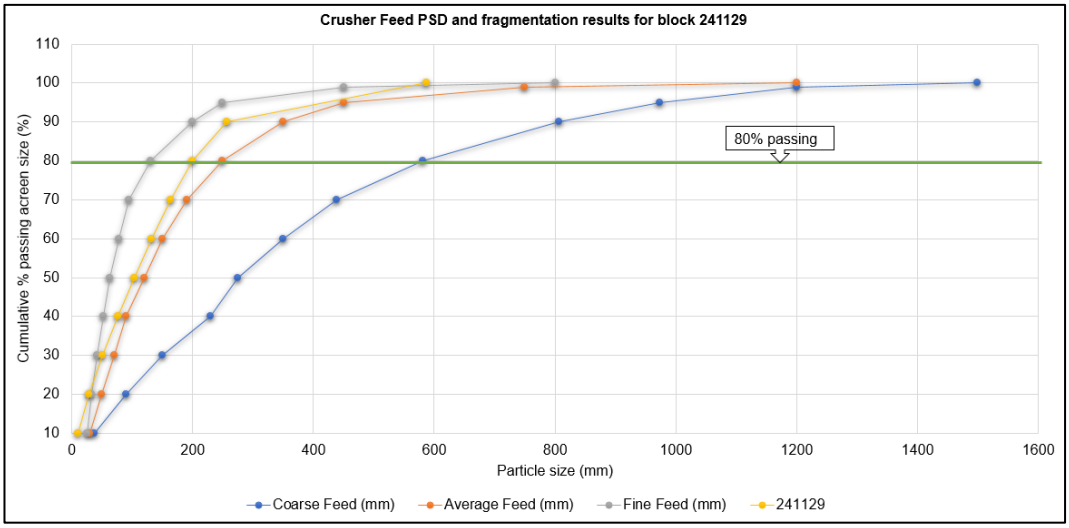



***Figure 4.3: Crusher feed PSD guideline and fragmentation results for block 241129***

The block's PSD was below average and closer to the fine feed PSD. This is because extra holes were added for smaller drill rigs onto the block due to undulations. This then resulted in a higher powder factor. Thus, optimal fragmentation was not achieved. Due to this, two more blocks were added to the study namely blocks 4311336 and 4311337. However, these blocks were fired using a faster burden response of 14 ms/m. This was because 15 ms/m burden response was achieving coarser fragmentation results but still not resulting in PSD closer to the coarse feed PSD. The blocks were both charged with Powergel Eco 35 and based in the South Mine.

Rock types and densities of the blocks are shown in Table 3.4. Block 4311336 achieved a higher X80 of 354.63 mm and block 4311337 achieved $X_{80}$ of 234.82 mm. The fragmentation results against the crusher feed PSD guidelines are shown in Figure 4.4.

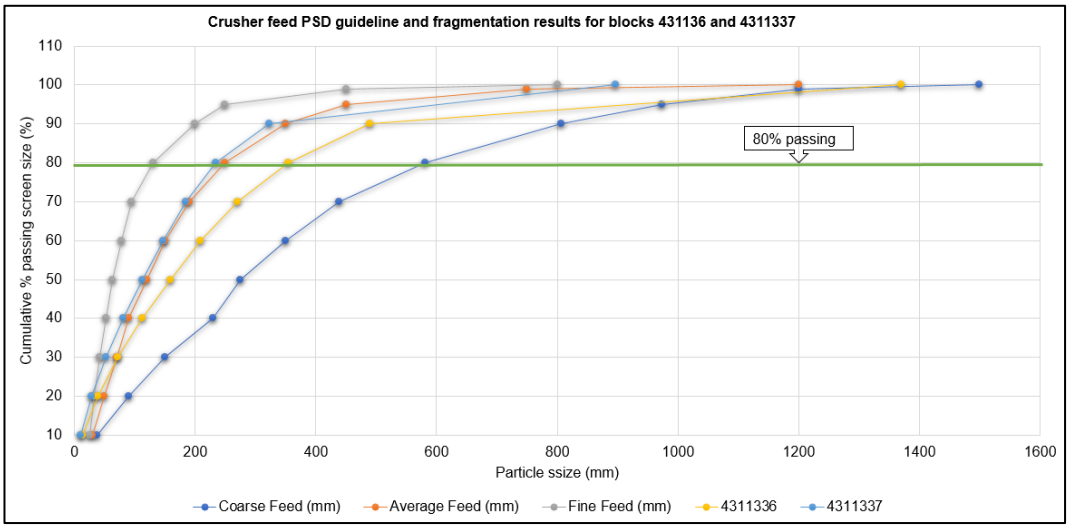



***Figure 4.4: Crusher feed PSD guideline and fragmentation results for blocks 4311336 and 4311337***

The PSD curves show that block 4311337 results were slightly below average. Block 4311336's PSD was closer to the coarser feed. When compared to all the ore blocks that were studied, block 4311336 achieved coarser $X_{80}$ hence the best fragmentation results.

The research aim was to investigate how burden response affects fragmentation. Given that the data was grouped by explosive product and geological domain, the analysis was also grouped as such. Figure 4.5 shows the relationship between burden response and fragmentation for the ore blocks charged using Powergel Eco 35.

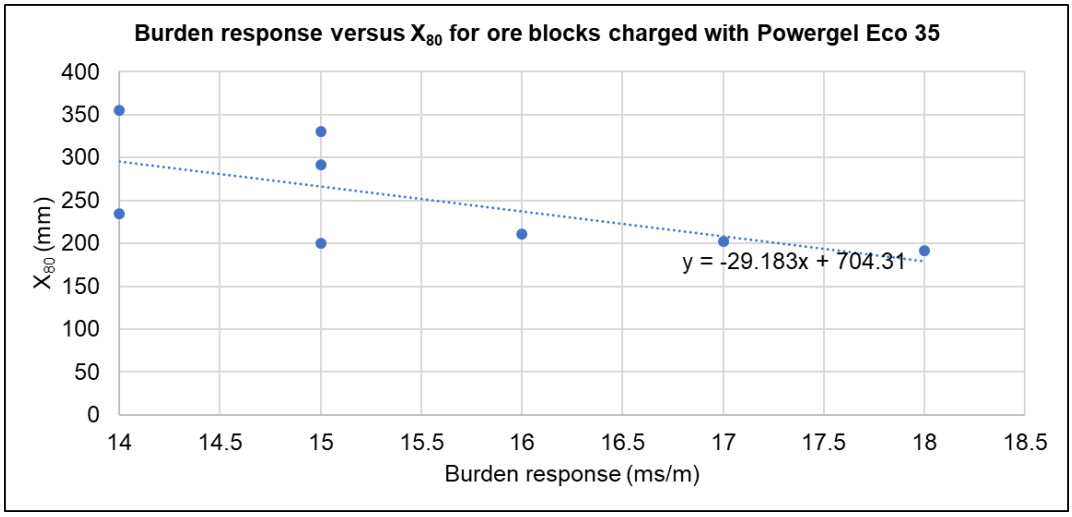



***Figure 4.5: Burden response versus $X_{80}$ for ore blocks charged using Powergel Eco 35***

The graph shows $X_{80}$ achieved by all eight ore blocks charged using Powergel Eco 35 that were used for the study. This was for the purpose of analysing the overall impact of burden response on fragmentation. The linear trendline in the graph shows that the $X_{80}$ decreases as burden response increases. The largest $X_{80}$ was achieved at 14 ms/m. As discussed in Section 2.4.2, this is because shorter burden responses do not afford enough time for the front row of blastholes to move sufficiently before the second row of blastholes fire. This then yields coarser fragmentation due to poor relief. The influence of burden response faster than 14 ms/m on fragmentation could not be studied due to time limits constraints. Equation 4.2 from the linear trendline on Figure 4.5 was used to estimate the burden response where $X_{80}$ of 600 mm may be achieved:

$$y = -29.183x + 704.31 \quad (4.2)$$

Where: y = $X_{80}$ (mm)

x = Burden response (ms/m)

Using Equation 4.2, $X_{80}$ of 600 mm was estimated to be achieved at 3.6 ms/m burden response for ore blocks charged using Powergel Eco 35. Figure 4.6 shows the relationship between burden response and fragmentation for ore blocks charged using Innovex EGA.

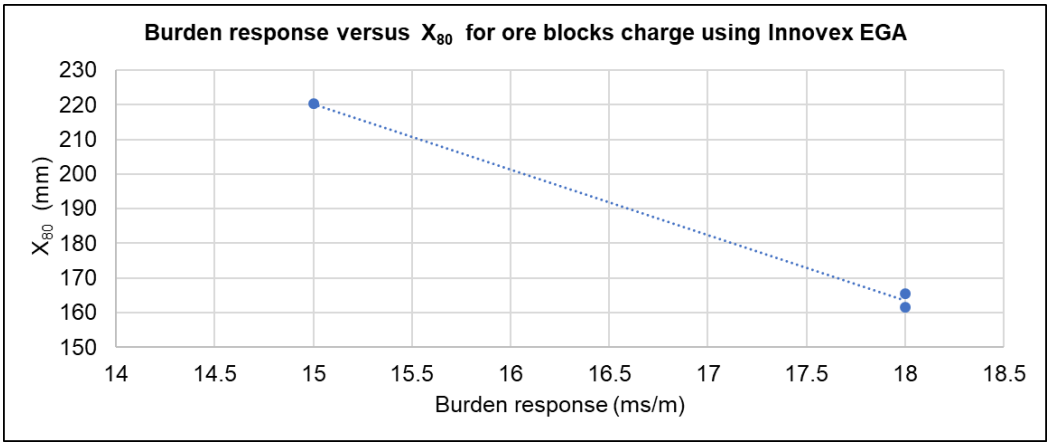



***Figure 4.6: Burden response versus $X_{80}$ for ore blocks charged with Innovex EGA***

The graph shows a similar trend as with blocks charged with Powergel Eco 35. The largest $X_{80}$ was achieved at the fastest burden response of 15 ms/m. However, the fragmentation results of all these blocks are finer compared to blocks charged with Powergel Eco 35. This is shown in Figure 4.7 which shows the comparison of burden response versus $X_{80}$ between the two explosive products for all studied ore blocks.

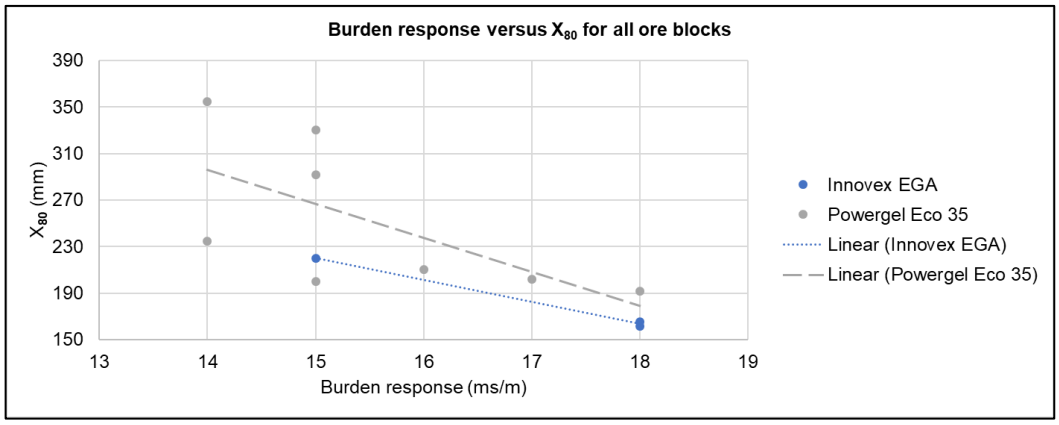



***Figure 4.7: Burden response versus $X_{80}$ for all ore blocks***

At 15 ms/m and 18 ms/m, Powergel Eco 35 achieved the largest $X_{80}$. This shows that overall, Powergel Eco 35 resulted in coarser fragmentation sizes. This is because Innovex EGA has a higher in-hole density of 1.28 g/cm³ (Brits, 2024) compared to Powergel Eco 35 with an in-hole density of 1.15 g/cm³ (MacVay, 2024). Therefore, Innovex EGA has more shattering effect hence the finer fragmentation results. Thus, for lumpier fragments, Powergel Eco 35 yielded better results.

The mine plant aims to provide customers with more lumps than fines. Their preference is to get a feed with an $X_{80}$ of 600 mm. The blocks in the study did not achieve this. However, the study demonstrated that the burden response for ore blocks should be faster than 15 ms/m to result in a lump to fine ratio of 79%. The study also demonstrated that Powergel Eco 35 which has a lower in-hole density thus lower VOD, gives coarser fragmentation results for ore blocks.

### 4.3 Waste domain results

The aim of the research was to investigate whether it is reasonable for the timing guidelines for ore and waste to be the same. To determine this, fragmentation results for waste blocks were required. In order to improve the drilling and blasting process for waste, cycle times is one of the key variables to optimise. Unlike ore, waste is removed from the face to the

waste dump without any processing required. Therefore, loading rates are more important for waste. Additionally, open-pit mines move more waste than ore. Therefore, even though lump to fine ratio is not a KPI for waste optimal fragmentation is still important. The faster waste is loaded and hauled, the quicker ore blocks are exposed hence the quicker profit is made. Therefore, burden response for waste should be optimal to get the correct fragmentation size to get optimal loading and hauling efficiencies. These results are shown in Tables 4.3 and 4.4 for waste blocks charged with Powergel Eco 35 and Innovex EGA, respectively.

**Table 4.3: Waste domain post-blast results for blocks charged using Powergel Eco 35**

| Block ID | Average rock density (t/m³) | Average UCS (MPa) | Burden response used (ms/m) | $X_{80}$ (mm) | Loading Rates (t/hr) |
|---|---|---|---|---|---|
| 952220 | 4.10 | 202 | 15 | 231.8 | 14 407 |
| 952214 | 3.27 | 168 | 17 | 299.9 | 6 285 |
| 771802 | 4.22 | 139 | 17 | 203.48 | 14 167 |

The three blocks in this group yielded $X_{80}$ that ranged from 203.48 mm to 299.9 mm. Loading rates ranged from 6 285 t/hr to 14 407 t/hr. The burden response versus $X_{80}$ for these blocks is shown in Figure 4.8.

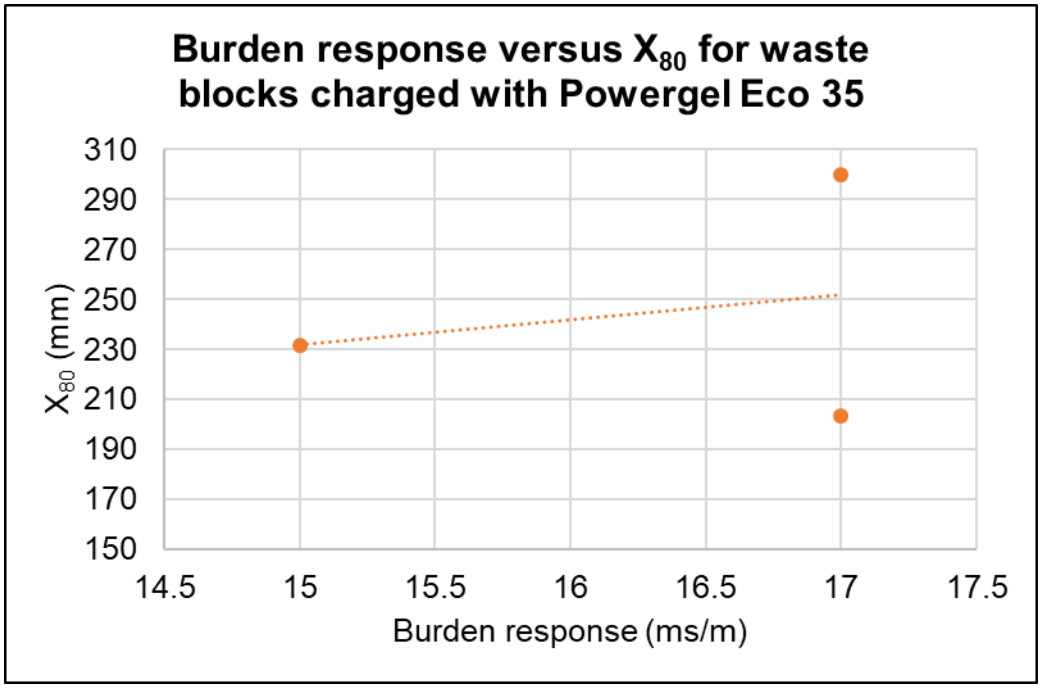



***Figure 4.8: Burden response versus $X_{80}$ for waste blocks charged using Powergel Eco 35***

The trendline shows that $X_{80}$ becomes coarser with increasing burden response. This trend is due to the coarser $X_{80}$ achieved on block 952214 which was blasted using 17 ms/m burden response. However, this resulted in the lowest loading rate because of the coarser fragment sizes which reduced loading rates.

**Table 4.4: Waste domain post-blast results for blocks charged using Innovex EGA**

| Block ID | Average rock density (t/m³) | Average UCS (MPa) | Burden response used (ms/m) | $X_{80}$ (mm) | Loading rate (t/hr) |
|---|---|---|---|---|---|
| 4310906 | 2.70 | 205 | 15 | 268.96 | 26 937 |
| 231263 | 2.95 | 146 | 16 | 349.88 | - |
| 4311102 | 3.02 | 172 | 18 | 215.36 | 9 685 |
| 1051405 | 2.68 | 161 | 18 | 245.31 | 14 107 |

The four blocks charged with Innovex EGA yielded $X_{80}$ from 215.36 mm to 349.88 mm. Loading rates ranged from 9 685 t/hr to 26 937 t/hr. Block 231263's loading rate was not recorded because the block was loaded by a contractor. The contractor's shovels do not record loading rates as with the mine's shovels. Burden response versus $X_{80}$ for waste blocks charged with Innovex EGA is shown in Figure 4.9.

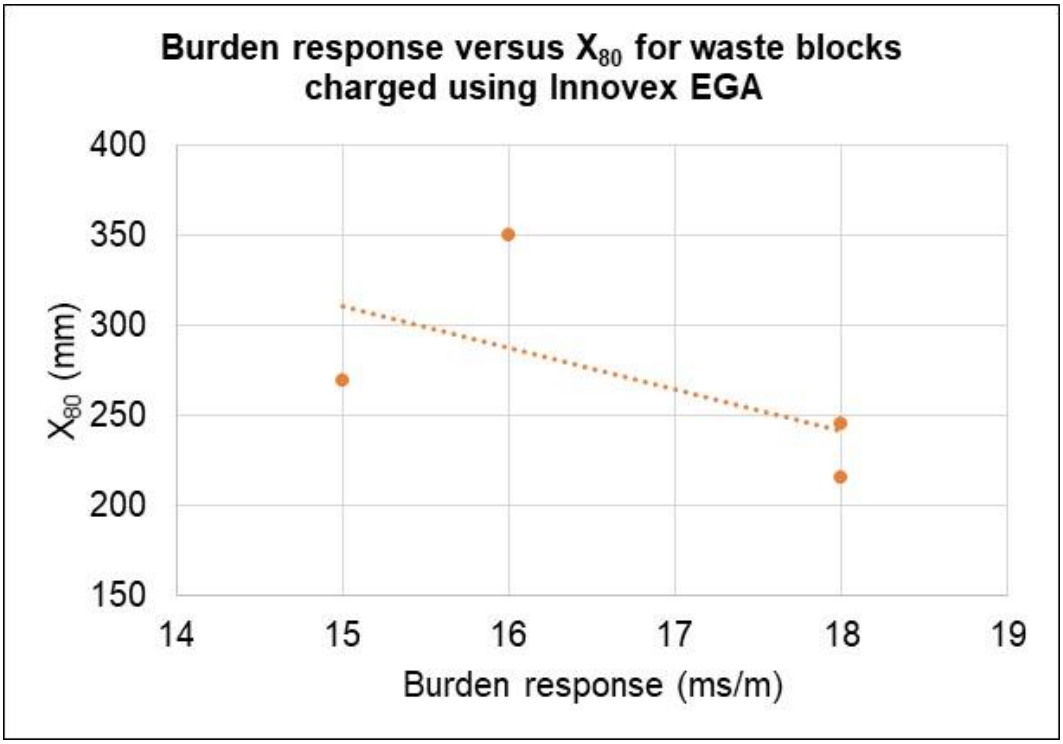



***Figure 4.9: Burden response versus $X_{80}$ for waste blocks charged using Innovex EGA***

Figure 4.9 shows that fragmentation sizes reduce as the burden response becomes slower. Unlike all previous results, the lowest loading rate was achieved on a block with the lowest $X_{80}$. This is because the particular block (4311102) did not have any free faces during blasting. Thus, the block was chocked. The block had a hard face due to poor movement and over confinement which affected loading rates. The largest $X_{80}$ resulted from the block 231263 which did not have loading rates. However, block 4310906 which had the 2$^{nd}$ coarser fragmentation after block 231263 had the highest loading rate. This was because the block was weak and less dense with an average rock density of 2.70 t/m$^3$ thus easy to load. Even though the block had coarser fragments, the geology made it easy for loading. Thus, increasing loading rates.

## 4.4 Ore and waste comparison

A comparison of burden response versus $X_{80}$ for ore and waste is shown in Figures 4.10 and 4.11. The aim of the comparison was to investigate whether it is reasonable for the mine's timing guidelines to use the same burden response for both waste and ore blocks.

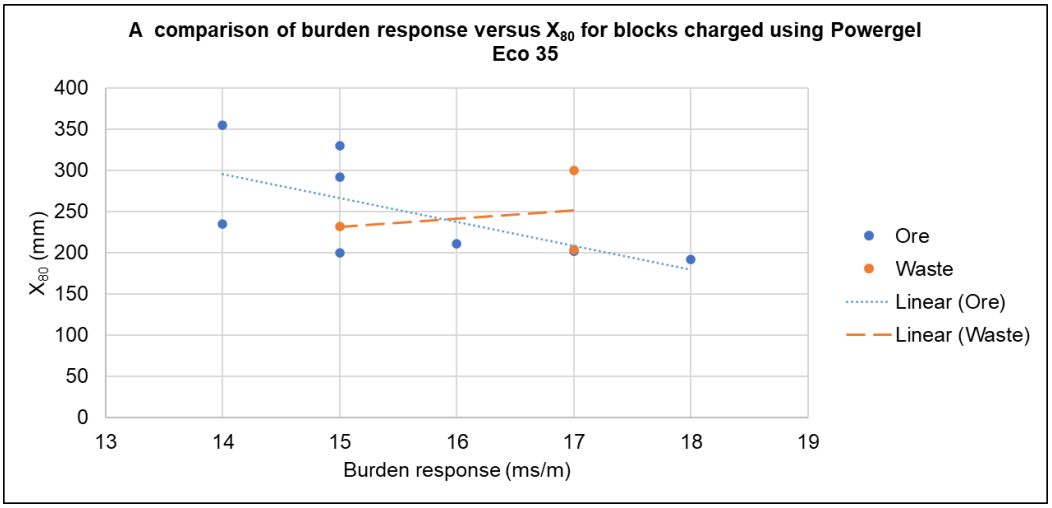



***Figure 4.10: A comparison of burden response versus $X_{80}$ for ore and waste blocks charged with Powergel Eco 35***

The trendline for ore shows that $X_{80}$ becomes finer as burden response increases. However, the trendline for waste shows that $X_{80}$ becomes coarser as burden response increases. This is because ore blocks are denser than waste blocks. The average rock density for ore blocks is 4.09 t/m³ compared to waste blocks with an average rock density of 3.28 t/m³. Furthermore, ore blocks are more competent compared to waste blocks with average UCS recorded during drilling of 191.45 MPa and 170.43 MPa, respectively. Thus, for the same timing and same quantity of explosives, waste blocks should result in finer fragmentation as discussed in Section 2.4.1 because ore blocks are denser and have a higher UCS. Therefore, as discussed in Section 2.4.2, faster burden responses are more suitable for ore blocks as these are more competent rock formations. Shorter burden responses allow for more shattering effect and sufficient breakage in competent rock formations. Figure 4.10 shows that at 15 ms/m, waste block resulted in finer fragmentation compared to majority of the ore blocks at this burden response. However, at 17 ms/m the $X_{80}$ for waste is coarser than that of ore blocks. The waste block that resulted in coarser $X_{80}$ was block 771802. This block was very dense with an average rock density of 4.22 t/m³ (Table 4.3). The block consisted of small pockets of ore with an average rock density of 4.74 t/m³ thus increasing the overall block density.

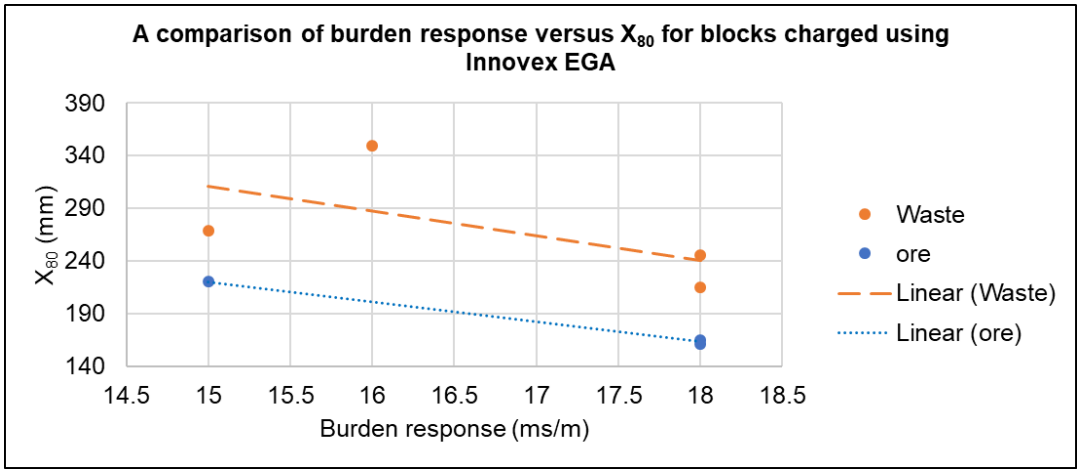



***Figure 4.11: A comparison of burden response versus $X_{80}$ for ore and waste blocks charged using Innovex EGA***

Figure 4.11 shows that the trendline for both ore and waste blocks is similar. However, ore blocks generally resulted in a finer $X_{80}$ compared to waste blocks. The aim is to ensure that ore blocks are designed and blasted to achieve a coarse feed $X_{80}$ of 600 mm to achieve the desired lump to fine ratio. This can be achieved when the burden response is faster than 15 ms/m. At 15 ms/m, the $X_{80}$ achieved was still fine. However, for waste blocks, the aim is to ensure that the blocks are designed and blasted in a manner that results in finer fragmentation which is achieved at slower burden response. Thus, the burden response for waste blocks should be slower than that of ore blocks. In this case, the timing guidelines should therefore have different ranges for ore and for waste.

## 4.5 The influence of fragmentation on loading rates

The literature has shown that fragmentation size has an influence on loading, hauling and crushing processes. To investigate that, $X_{80}$ was plotted against loading rates to determine this relationship. The results are shown in Figures 4.12 and 4.13 for blocks charged using Powergel Eco 35 and Innovex EGA, respectively.

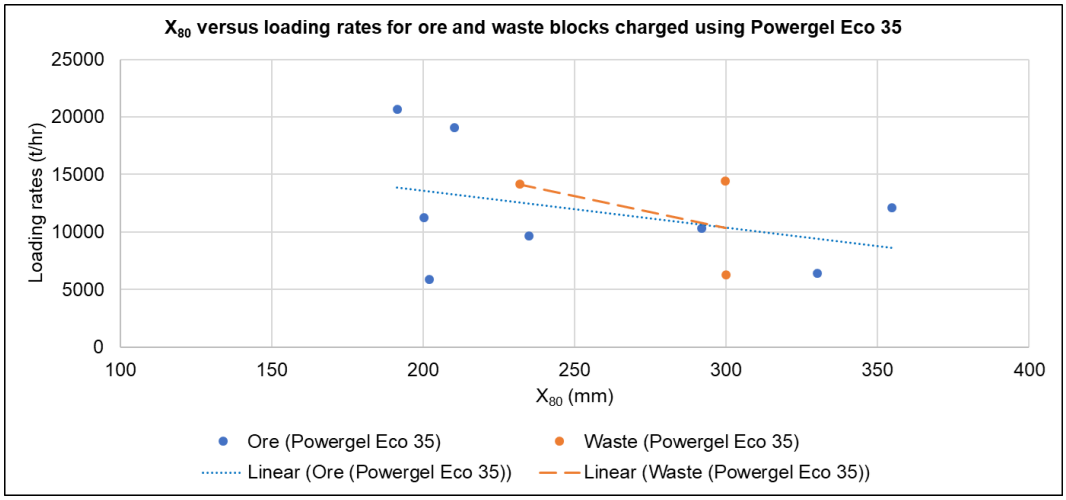



***Figure 4.12: $X_{80}$ versus loading rates for ore and waste blocks charged using Powergel Eco 35***

Figure 4.12 shows that for blocks charged with Powergel Eco 35, a higher $X_{80}$ resulted in lower loading rate. The correlation coefficient of $X_{80}$ against loading rate for ore blocks and waste blocks charged with Powergel Eco 35 is -0.6 and -1.0, respectively. The correlation for waste blocks is much stronger compared to one for ore blocks. However, both coefficients indicate a negative correlation. As discussed in Section 3.2, this indicates that fragmentation size and loading rate are inversely proportional. As fragmentation size increases, loading rate decrease which subsequently reduces loading efficiencies and increases costs and vice versa. This is because boulders are more difficult to load than fine material.

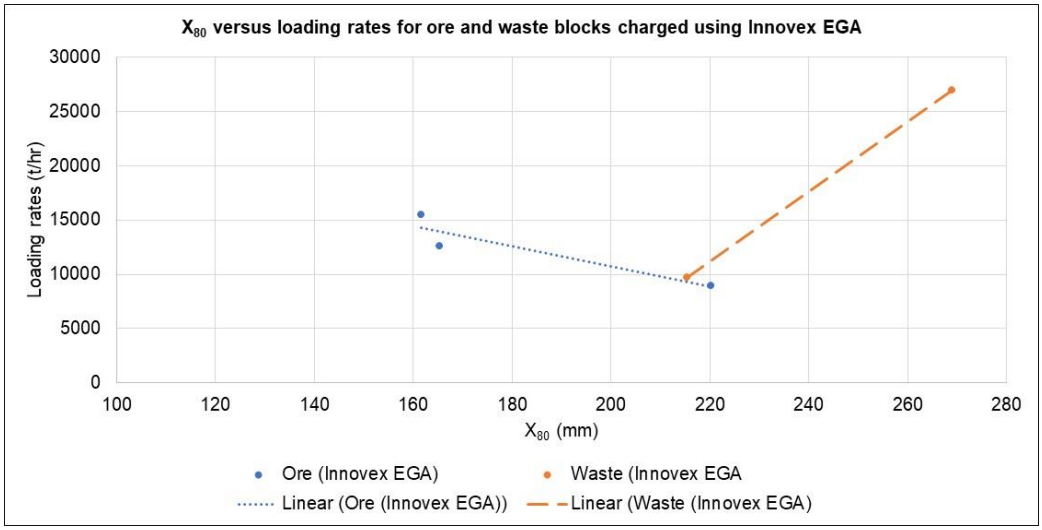



***Figure 4.13: $X_{80}$ versus loading rates for ore and waste blocks charged using Innovex EGA***

Figure 4.13 shows a similar relationship as with Powergel Eco 35 for ore blocks. The loading rates reduced with increasing $X_{80}$ and the correlation coefficient of $X_{80}$ against loading rate for these blocks is -0.9 which indicates a strong inversely proportional correlation. However, the same relationship was not observed for waste blocks charged with Innovex EGA. The loading rates increased with increasing $X_{80}$. The correlation coefficient for these blocks is +0.94 which is a strong directly proportional correlation. This is because the particular block (4310906) is weaker than all waste blocks with an average rock density of 2.7 t/m³. The block recorded an average UCS of 205 MPa due to the QTZ which has a UCS of 202 MPa. However, the rock formation was very friable and thus fairly easy to load. This block achieved loading rates of 26 937 t/hr. However, three of the four study blocks demonstrate that an increase in $X_{80}$ reduces loading rates.

Generally, majority of the blocks indicated a strong negative correlation between loading rates and fragmentation sizes. Thus, as fragmentation size increases, loading rate decreases. Thus, to achieve faster loading rates, waste blocks should be blasted with a burden response slower than 18 ms/m. This is because the relationship between burden response and $X_{80}$ showed that $X_{80}$ reduces with slower burden response.

## 4.6 DMS ROM lump to fine results

The ROM lump to fine ratio is a direct interpretation of the fragmentation feed into the crusher. The aim was to measure if there was any improvement or not after determining the best burden response for the ore domain. This was compared against 2021 results and against the 79% lump to fine ratio target. The results are shown in Figure 4.14.

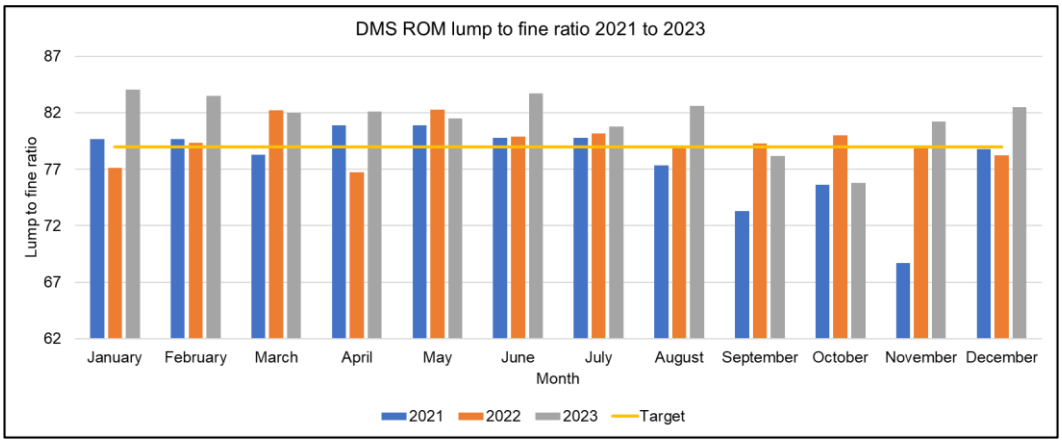



***Figure 4.14: DMS ROM lump to fine 2021 to 2023***

The average ratio achieved in 2021, 2022 and 2023 was 77.74%, 79.43% and 81.50%, respectively. In 2021, the target of 79% was achieved in 6 of the 12 months of the year (these were not consecutive). There was an improvement in 2022. However, the target was achieved in 8 of the 12 months. In 2023, the target was achieved for all months except September and October 2023. The graph shows that since March 2022 there has been an improvement in the DMS ROM lump to fine ratio. For most of 2023, the lump to fine ratio was above 80%. This shows that adjustments to the burden response has greatly improved fragmentation fed into the plant. This shows that there was an improvement in terms of fragmentation sizes post blasting.

## 4.7 Chapter summary

This chapter presented the results and analysis of the study. The analysis of the results demonstrated that ore fragmentation size increases when burden response is faster. A burden response of 14 ms/m resulted in coarser $X_{80}$. Thus, to yield the preferred $X_{80}$ of 600mm, the burden response for ore blocks should be faster than 14 ms/m. Furthermore, the analysis indicated that Powergel Eco 35 is more suitable for ore blocks of the same blast design as compared to Innovex EGA. This is because it resulted in coarser fragmentation compared to blocks charged with Innovex EGA.

The ore and waste burden response versus $X_{80}$ relationships were compared. This comparison demonstrated that waste blocks should be blasted with slower burden responses compared to ore blocks. This is because majority of the burden response versus $X_{80}$ relationships illustrated a reduction in fragment sizes for slower burden responses than 15 ms/m. Finer fragments are preferred for waste because waste is not sent to the plant but affect loading and hauling rate. The loading rates versus $X_{80}$ relationships indicated that loading rates increase with a lower $X_{80}$. Thus, finer fragment sizes are more favourable for waste. Due to the great shattering effect of explosives with higher in-hole density and VOD, Innovex EGA would aid with resulting in finer fragmentation sizes for waste blocks.

The analysis demonstrated that ore and waste should not be timed using similar burden responses. This is due to the fact that waste blocks had better fragmentation for loading and hauling when the burden response was slower than 14 ms/m. Better fragmentation for ore blocks for the plant was achieved when burden response was faster than 15 ms/m. Furthermore, in 2022 and 2023 the DMS ROM lump to fine average was 79.43% and 81.50%, respectively. This was an improvement compared to 2021's average of 77.74%. The target was 79% which was achieved in 2022 and 2023. This indicates that faster burden response improved plant crusher feed lump to fine at the DMS crusher by more than 2% in 2023.

# 5 CONCLUSIONS AND RECOMMENDATIONS

## 5.1 Overview of chapter 5

Chapter 5 presents the conclusions drawn from the research and provide recommendations. It starts by presenting the summary of the research. This is then followed by research conclusions, research limitations and recommendations.

## 5.2 Summary of the research

Sishen Mine is an iron ore open pit mine based in the Northern Cape. The mine is divided into three pits, namely North Mine, South Mine and Lyleveld pit. All these pits have five geological domains. Clay is mined out first, followed by calcrete, then a combination of the two. This is then followed by the waste and ore. The predominant rock types in the waste and ore are BIF, CGB, chert, chert breccia, shale, quartzite and hematite (HB, HL, HM). In some cases, a block can contain both waste and ore. A block is classified as an ore block when the majority of the block contains rock types with an Fe percentage of more than 40%.

The ore is extracted by means of drilling and blasting. In this process, blastholes are assigned delay timing. At Sishen Mine this is by means of burden response. According to the mine's guidelines developed from historic data, waste and ore blocks are blasted using similar burden responses between 12 ms/m and 18 ms/m. These guidelines form part of the blast design ToR. However, high Fe percentage bearing ore blocks are denser than waste blocks. Thus, the need for this research to determine whether ore and waste burden responses should be similar or not.

The fragment sizes of the ore extracted post blasting should be between 230 mm to 600 mm. The plant's optimal $X_{80}$ is 600 mm. This is as per the coarser feed PSD guidelines into the crusher. Furthermore, the DMS feed

preferred lump to fine ratio is 79%. In 2021, the average lump to fine ratio achieved was 77.74% which was below the target. This could have possibly been due to incorrect burden response being used to blast ore blocks. Hence the need for this research to review the burden response guidelines and investigate the influence of burden response on fragmentation. Furthermore, the need to determine the optimal burden response that delivers optimal fragmentation at Sishen Mine. Fragmentation affects other downstream operations. Therefore, it was necessary to also investigate how fragmentation further affects loading rates. The DMS ROM lump to fine ratio was also captured to determine whether the project assisted the plant to achieve the 79% lump to fine target.

The investigation was conducted from March 2022 to December 2023. This was conducted on 18 blocks in both North and South Mine pits. The burden response studied was from 14 ms/m to 18 ms/m.

The investigation began with a literature review on factors affecting fragmentation in open pit mines. The two theories that describe how rock is fragmented using explosives were described. These are gas expansion theory and reflection theory. These are essential to the research because to deliver optimal fragmentation, it was important to understand factors that affect fragmentation and how rock is fragmented. The factors are divided into controllable and uncontrollable factors. The literature review detailed how uncontrollable factors such as rock UCS, density, porosity and fractures and discontinuities affect fragmentation. Higher rock UCS and density result in larger fragment sizes when all factors are kept constant. On the other hand, highly porous rocks yield smaller fragment sizes. Fractures and discontinuities result in coarser fragmentation because explosives energy escapes through them.

The literature review further indicated that controllable factors such as blasthole diameter, burden and spacing, spacing to burden ratio, stemming length, stemming material properties, powder factor, delay timing and

explosive properties also affect fragmentation. In the case of these controllable factors, the impacts on fragmentation can be seen when one factor is being altered at a given time and all parameters are kept constant. Larger blasthole diameters results in smaller fragment sizes. This is because an increase in blasthole diameters results in an increase in the linear charge mass. This then translates into an increase in powder factor thus yielding finer fragmentation.

Larger burden and spacing yield coarser fragmentation. As the burden and spacing increase, this increases the volume of rock to be broken by a certain amount of explosive. Powder factor is thus reduced hence the coarser fragmentation. In the case where a longer stemming length is used, fragmentation becomes coarse. This is because the less explosives than what is required to sufficiently break the rock will be charged in the blasthole. Explosives energy will therefore not be sufficient to break the rock in the collar thus resulting in larger fragments in the collar of the blastholes. Blastholes stemmed with crushed angular rock result in better fragmentation compared to blastholes stemmed with drill chippings. Angular crushed rock contains energy long enough to ensure that the rock mass surrounding the blastholes breaks sufficiently.

As per the literature review, delay timing is also one of the controllable factors that affect fragmentation. This is the inter-hole and inter-row delay timing. The study's main focus was on the inter-row delay timing which is obtained by multiplying burden response and burden. In stronger rocks, shorter inter-row delay timing results in better fragmentation compared to longer inter-row delay timing. Greater shattering effect is important to break stronger rocks hence the need for shorter inter-row delay timing. Furthermore, longer inter-row delay timings do not offer sufficient inter-rock collisions. In softer rocks, the P-wave velocity is lower and thus requires higher delays as compared to stronger rocks.

Explosive density, VOD and detonation pressure are explosives properties that also affect fragmentation. When all parameters are kept constant, as these properties individually increase, fragmentation becomes finer. Higher density explosives have higher energy which reduces fragmentation. Higher VOD explosives contain higher detonation pressure and shock energy which breaks the rock mass to smaller fragments compared to lower VOD explosives.

The method of analysing fragmentation was also described. Though there are several fragmentation analysis methods, digital imaging is the widely used method. One of the software that analyses fragmentation through digital imaging is Split Desktop. This software entails capturing images of the muckpile after a blast. A scaling object of a known size must be used when capturing these images. These are either delineated automatically by the software or manually by the end user. The delineated fragment sizes are compared against the scale and PSD results are exported.

The literature review was followed by a description of the research methodology used to carry out the research. The research was conducted using three quantitative methods to achieve the research objectives. These are experimental, correlational and casual-comparative research methods. Firstly, the experimental method was used to monitor the influence of burden response on fragmentation when all geometric design parameters are kept constant. Secondly, the correlational method was used to determine the relationship between loading rate and fragmentation. The correlation was a strong negative correlation. However, waste blocks charged with Innovex EGA demonstrated a strong positive correlation. And lastly, the casual-comparative method was used to deduce if it is advisable for waste and ore to be blasted using similar burden response.

The quantitative data collection process and analysis used for the research was described. Pre- and post-blast data was collected and analysed. The data was both primary and secondary data. The geometric design and

timing design data was primary data. The geological information, fragmentation analysis data, loading rates and DMS Rom lump to fine were secondary data.

The results and their analysis thereof were presented following the research methodology. The pre- and post-blast results were grouped by domain (ore and waste) and explosive product used. This is because two explosive types were used due to availability on the day of charging. The explosives have different properties which affect fragmentation. Essentially, the research methods used required that certain variables remain constant while burden response is altered. Thus, the need to group the data by explosive product to ensure a homogenous comparison between blocks.

## 5.3 Research conclusions

The research found that within the ore domain, a faster burden response increases fragmentation sizes. However, $X_{80}$ of 600 mm was not achieved during the study. This is because the fastest burden response applied during the study was 14 ms/m which yielded $X_{80}$ of 354.63 mm. Additionally, the analysis indicated that Powergel Eco 35 results in coarser fragmentation for ore blocks as compared to Innovex EGA. Furthermore, the DMS plant ROM lump to fine ratio was improved from 77.74% in 2021 to 79.43% and 81.50% in 2022 and 2023, respectively.

Based on the research, ore and waste should not be assigned similar burden response as demonstrated by the results and analysis. Waste blocks should be blasted using a burden response slower than 15 ms/m and ore blocks should be blasted using a burden response faster than 14 ms/m. As discussed in the literature review, shorter inter-row delay timing is more effective for harder rocks. The literature review further demonstrated that shorter delays in stronger rock types result in coarser fragmentation. Additionally, for softer rock types, longer inter-row delay timing results in finer fragmentation. The estimated burden response where $X_{80}$ of 600 mm

may be achieved for ore blocks charged with Powergel Eco 35 is 3.6 ms/m, which is faster than 14 ms/m.

Waste is sent to the waste dump thus the fragmentation sizes post blasting need to improve loading and hauling efficiency. It was found that loading rates decrease with an increment in fragmentation sizes. Additionally, Innovex EGA is more suitable to blast waste blocks due to its great shattering effect as a result of its high detonation pressure.

## 5.4 Research limitations

Challenges beyond the control of the researcher were encountered during the research. Firstly, the inability to focus on blocks charged with one explosive product. This could not be done as ordering and assigning of explosive product to blocks was done by the mine's blasting manager. The allocation of explosive product was limited by contractual obligations and availability of the explosive product. As a result, the number of blocks charged with Innovex EGA were reduced from ten (initially planned) to seven. Secondly, the fragmentation analysis was carried out manually, thus requiring human intervention. Due to this, there was potential for errors during the analysis.

Thirdly, there was a challenge experienced with accessing blasted muckpiles to capture fragmentation analysis images. This led to only three blocks charged with Innovex EGA being used for the study instead of five. The fourth limitation was the fact that block 231263's loading rates were not recorded because the block was loaded by a contracting company. These contractor shovels are not fitted with the system that collects loading rates data.

The fifth limitation was using linear regression statistical analysis method on a small sample size to estimate burden response where $X_{80}$ is achieved at

600 mm. Different results (in terms of $X_{80}$ being achieved at 600 mm) may be obtained if the sample size is increased.

## 5.5 Recommendations

Based on the analysis and research observations, the timing guidelines at Sishen Mine should be changed. Ore and waste blocks should not be blasted using the same burden response as currently practised. Ore blocks should be blasted using burden response faster than 14 ms/m and waste blocks should be blasted using 16 ms/m to 18 ms/m burden response. This is because ore is harder and requires faster timing to result in lumpier fragmentation. In addition, softer waste blocks require longer inter-row delay timing to result in finer fragmentation.

The study did not include blocks blasted faster than 14 ms/m due to time limits constraints. More experiments should be conducted on ore blocks as $X_{80}$ of 600 mm was still not achieved in the study. It was estimated that $X_{80}$ of 600 mm may be achieved at 3.6 ms/m burden response thus the need for more experiments. Furthermore, increasing the sample size would increase the confidence of the data and results.

Currently, the mine assigns explosives product to a block according to availability of explosive product and contractual obligations. The mine should take geological properties and fragmentation requirements into consideration when assigning explosive products to blocks. The study indicated that Powergel Eco 35 is more suitable for blasting ore blocks, and Innovex EGA for waste blocks.

Timing guidelines at Sishen Mine do not include inter-hole delay timing guidelines. A burden response when applied, assigns inter-row delay timing. This means that inter-hole delay timing is decided by the timing software used. However, delay timing is an effective way of controlling fragmentation. Therefore, the mine should consider inter-hole delay timing as well.

Furthermore, inter-hole delay timing does have an impact on fragmentation as well.

## References


Abioye, A.V., Babatunde, A. and Oyedele, A.E., 2018. Fragmentation prediction models: Is there a relationship between Rosin-Rammler and Swebrec distribution functions parameters?. In *ISRM International Conference on Advances in Rock Mechanics-TuniRock*

Acaps, 2012. Qualitative and quantitative research techniques for humanitarian needs assessment: An introductory brie*f.* [Online] Available at: http://www.govtgirlsekbalpur.com/Study_Materials/Sociology/Sociology_GE_Sem-IV_Qualitative_and_Quantitative_Research_Techniques.pdf [Accessed 13 August 2023].

AECI Mining Explosives, n.d. Surface Blasting Handbook. Johannesburg

Agyei, G. & Nkrumah, M.O, 2021. A review on the prediction and assessment of powder factor in blast fragmentation. *Nigerian Journal of Technology,* 40(2), pp. 275-283.

Agyei, G. & Owusu-Tweneboah, M., 2019. A comparative analysis of rock fragmentation using blast prediction results. *Ghana Mining Journal,* 19(1), pp. 49-58.

Ali, A., 2021. Quantitative data analysis. [Online] Available at: http://dx.doi.org/10.13140/RG.2.2.23322.36807 [Accessed 13 August 2023].

Anglo American, n.d. Plant ROM requirements.

Anglo American, 2023a. What we do*.* [Online] Available at: https://www.angloamericankumba.com/about-us/what-

we-do
[Accessed 11 June 2023].

Anglo American, 2023b. Kumba External Data Entry. [Online]
Available at:
http://aissisrec01.angloiit.net/ReconcilorDataManagement/BlastVisualisation
[Accessed 04 July 2023].

Apuke, O., 2017. Quantitative research methods: A synopsis approach. *Kuwait Chapter of Arabian Journal of Business and Management Review,* 6(10), pp. 1-8.

Balasubramanian, A., 2017. Rock blasting for mining. Centre for Advanced Studies in Earth Science. University of Mysore

Bamford, T., Esmaeili, K. & Schoellig, A.P, 2021. A deep learning approach for rock fragmentation analysis.. *International Journal of Rock Mechanics and Mining Sciences,* (145), p. 104839.

Bender, W.L., 1999. *Back to basics:* The fundamentals of blast design. In *Workshop of the Golden West Chapter of the International Society of Explosives Engineers*.

Blast Management International, 2021. Chapter 3: Explosives rock interactions. s.l.:Unpublished.

Brits, K., 2024. Innovex EGA explosive properties [Interview] (30 January 2024).

Bulk Mining Explosives, 2023. Fragmentation analysis. s.l.:Bulk Mining Explosives.

Cardu, M., Seccatore, J., Vaudagna, A., Rezende, A., Galvão, F., Bettencourt, J and Tomi, GD, 2015. Evidences of the influence of the detonation sequence in rock fragmentation by blasting–Part I. *REM: Revista Escola de Minas, 68 (3)* pp. 337-342.

Choudhary, B.S., Agrawal, A. and Arora, R., 2021. Stemming material and Inter-row delay timing effect on blast results in limestone mines. *Sādhanā*, *46*, pp.1-12.

Corporate Finance Institute, n.d. Negative correlation. [Online] Available at: https://corporatefinanceinstitute.com/resources/data-science/negative-correlation/ [Accessed 14 February 2024].

Coulibaly, D.A., 1982.Effects of stemming on open pit bench blasting. Master's thesis. University of Nevada, Reno.

Demenegas, V., 2008. Fragmentation analysis of optimized blasting rounds in the Aitik mine - effect of specific charge. [Online] Available at: https://www.diva-portal.org/smash/get/diva2:1026690/FULLTEXT01.pdf [Accessed 29 June 2023].

Domede, N., Parent, T. and Sellier, A., 2019. Mechanical behaviour of granite: a compilation, analysis and correlation of data from around the world. *European Journal of Environmental and Civil Engineering*, *23*(2), pp.193-211.

Domingo, J., Leite, F., Mirada, V. and Carrasco, I., 2015. Dilution, ore grade and blast movement calculation model. In *Proceedings of 11th International Symposium on Rock Fragmentation by Blasting, Fragblast* 11, pp. 71-78.

Esen, S., Bilgin, H. A & BoBo, T., 2000. Effect of explosive on fragmentation. *The 4th Drilling and Blasting Symposium 2000, Ankara, Turkey,* 6372.

Gadikor, J.E.K, 2018. Optimization of drilling and blasting practices at a Western US open pit copper mine. Master of Science Thesis, Montana Tech of the University of Montana.

Gogtay, N.J & Thatte, U.M, 2017. Principles of correlation analysis. *Journal of the Association of Physicians of India,* 65, pp. 78-81.

Hayati, M. & Abroshan, M.R, 2017. Providing a model to determine of powder factor using principal component analysis technique. *Indian Journal of Science and Technology,* 10(24), pp. 1-7.

Hettinger, M.R, 2015. The effects of short delay times on rock fragmentation in bench blasts. Master of Science Thesis, Missouri University of Science and Technology.

Hyldahl, J., 2018. Effects of jointing on fragmentation design and influence of joints in small scale testing. Masters Thesis, Luleå University of Technology.

Ikeda, H., Sato, T., Yoshino, K., Toriya, H., Jang, H., Adachi, T., Kitahara, I. and Kawamura, Y., 2023. Deep learning-based estimation of muckpile fragmentation using simulated 3D point cloud data. *Applied Sciences*, *13*(19), p.10985.

Jethro, M.A, Shehu, S.A & Kayode, T.S, 2016. Effect of fragmentation on loading at Obajana cement company plc, Nigeria. *International Journal of Scientific and Engineering Research,* 7(4), pp. 608-620.

Kabir, S.M, 2016. Chapter 9: Methods of data collection. In: *Basic guidelines for research: An introductory approach for all disciplines.* Bangladesh: Book Zone Publications, pp. 201-275.

Kabwe, E., 2018. Velocity of detonation measurement and fragmentation analysis to evaluate blasting efficacy. *Journal of rock Mechanics and geotechnical Engineering,* 10(3), pp. 523-533.

Katsabanis, P.D, Tawadrous, A., Brausn, C. & Kennedy, C., 2006. Timing effects on fragmentation*. Fragblast,* 10(1-2), pp. 83-93.

Kechik, N.A.H.B.A, 2018. Effect of blast designs on rock fragmentation at Lafarge Kanthan Quarry, Chemore, Perak*.* Honours dessertation, Universiti Sains Malayisa.

Kename, P., 2024. DMS ROM lump to fine ratio 2021 - 2023. Kathu.

Kinyua, E.M., Jianhua, Z., Kasomo, R.M., Mauti, D. and Mwangangi, J., 2022. A review of the influence of blast fragmentation on downstream processing of metal ores. *Minerals Engineering*, *186*, p.107743

Kondelchuk, D. & Novikov, E., 2005. Study of the mechanical properties of the granitoid rocks and the influence of blasting parameters on the quality of aggregates: literature research*.* Master of Science Thesis, Luleå University of Technology.

Konya, C. J., and Walter, E. J., 1991. Rock Blasting and Overbreak Control. United States. Federal Highway Administration.

Kotronoulas, G., Miguel, S., Dowling, M., Fernández-Ortega, P., Colomer-Lahiguera, S., Bağçivan, G., Pape, E., Drury, A., Semple, C., Dieperink, K.B. and Papadopoulou, C., 2023. An overview of the fundamentals of data management, analysis, and interpretation in

quantitative research. *Seminars in oncology nursing, 39(2)* p. 151398.

Kulula, M.I., Nashongo, M.N. and Akande, J.M., 2017. Influence of blasting parameters and density of rocks on blast performance at Tschudi Mine, Tsumeb, Namibia. *Journal of Minerals and Materials Characterization and Engineering*, *5*(06), p.339.

Lawal, A.I., Adebayo, B., Afeni, T.B., Okewale, I.A., Ajaka, E.O., Amigun, J.O., Akinbinu, V.A. and Apena, W.O., 2023. Soft Computing Applications for Optimum Rock Fragmentation: An Advanced Overview. *Geotechnical and Geological Engineering,* pp. 1-22.

Lijojo, L., 2021. Simulating the influence of blast geometry and rock geology on rock fragmentation. Master of Science Dissertation*,* University of Witwatersrand, Johannesburg.

Louisiana Department of Environmental Quality, n.d. Porosity and permeability. [Online]
Available at:
https://deq.louisiana.gov/assets/docs/Water/DWPP_forkidsandeducators/PorosityandPermeability.pdf
[Accessed 16 February 2024].

MacVay, D., 2024. Powergel Eco 35 explosive properties [Interview] (30 January 2024).

Mafuwane, B.M, 2011. The contribution of instructional leadership to learner performance*.* Doctoral disseration, University of Pretoria.

Martin, D., 2018. Assessment of blasting on the Klondyke Queen. A roost site for Pilbara-Leaf-nosed Bat and Ghost Bat*.*. [Online]

Available at:
https://www.epa.wa.gov.au/sites/default/files/PER_documentation2/3-3.%20Blasting%20Assessment%20(Blast%20It%20Global).pdf
[Accessed 05 November 2023].

Mohamed, F., Hafsaoui, A., Talhi, K. & Menacer, k., 2015. Study of the powder factor in surface bench blasting. *Procedia earth and planetary science,* 15, pp. 892-899.

Mozumder, S., 2021. Research design and its elements and types assignment. [Online]
Available at:
https://www.researchgate.net/publication/353751939_Assignment_on_Research_Design_and_its_elements_and_types
[Accessed 26 July 2023].

Mpofu, M., Ngobese, S., Maphalala, B., Roberts, D. and Khan, S., 2021. The influence of stemming practice on ground vibration and air blast. *Journal of the Southern African Institute of Mining and Metallurgy*,*121*(1), pp.1-10.

Mulenga, S., 2020. Evaluation of factors influencing rock fragmentation by blasting using interrelations diagram method. *Journal of Physical Sciences*, *2*(1), pp.1-15.

Mutinda, E.K, Alunda, B.O, Maina, D.K & Kasomo, R.M, 2021. Prediction of rock fragmentation using the Kuznetsov-Cunningham-Ouchterlony model. *Journal of the Southern African Institute of Mining and Metallurgy,* 121(3), pp. 107-112.

Nanda, S. & Pal, B.K, 2020. Analysis of blast fragmentation using WipFrag. *International Journal of Innovative Science and Research Technology,* 5(6), pp. 1561-1566.

Nie, H., 2016. Evaluation and potential application of 4D energy distribution analysis in blast design. Honours Thesis, The University of Queensland.

Oates, T.O & Spiteri, W., 2021. Stemming and best practice in the mining industry: A literature review. *Journal of the Southern African Institute of Mining and Metallurgy,* 121(8), pp. 415-426.

Olivier, P., 2022. Timing Guidelines. Kathu: Anglo American, Kumba Iron Ore: Sishen Mine.

Olofsson, S., 1988. Applied explosives technology for construction and mining. 2nd edition. Sweden: Applex.

Onederra, I. and Esen, S., 2003, September. Selection of inter-hole and inter-row timing for surface blasting–an approach based on burden relief analysis. In *Proceedings of the 2nd world conference on explosives and blasting technique, Prague. Taylor & Francis,* pp. 269-275.

Orica, 2016. *Orica drill and blast calculators -Metric.*

Orica, 2020. Pocket blast guide. [Online]
Available at: https://orica.psrstore.com.au/verve/_resources/OMS17-3328_Pocket_Blast_Guide_Sept_2020__web.pdf
[Accessed 02 November 2023].

Parida, A., 2016. Evaluation of blasting efficiency in surface mines, s.l.: National Institute of Technology Rourkela.

Prasad, S., Choudhary, B.S & Mishra, A.K, 2017. Effect of blast design parameters on blast induced rock fragmentation size–A case study.

*International Conference on Deep Excavation, Energy Resources and Production,* pp. 1-7.

Rai, P. & Nath, R., 2004. Interrow delay requirement for strong sandstone strata on high dragline benches- a case study. *IE (I) Journal-MN,* 1(85), pp. 20-24.

Rajpot, M.A, 2009. The effect of fragmentation specification on blasting cost. Master of Science Thesis, Queen's Unveristy, Canada.

Rout, M. & Parida, C., 2007. Optimization of blasting parameters in opencast mine*s.* Bachelor of Technology Thesis, National Insitute of Technology, Rourkela.

Salati, L.K & Mark, G.O, 2020. Optimum powder factor selection in *blasthole*s at dangote limestone Quarry, Obajana, North-Central Nigeria. *International Journal of Scientific & Engineering Research,* 11(1), pp. 1459-1476.

Sazid, M.O.H.D, 2014. Investigating the role of effective stemming in engineering blasting operations for open-pit mines. Doctoral disseration, Indian Institute of Technology Bombay.

Senthilnathan, S., 2019. Usefullness of correlation analysis*.* [Online] Available at: https://papers.ssrn.com/sol3/papers.cfm?abstract_id=3416918 [Accessed 14 February 2024].

Shangoni Management Services, 2017. Anglo American: Kumba Iron Ore-SIshen Mine: preliminary closure plan*.* [Online] Available at: https://minedocs.com/20/Anglo_American_Kumba_Iron_Sishen_Min

e_02282017.pdf
[Accessed 07 March 2023].

Shehu, S.A, Hashim, M.H.M, Hazirah, N.A. & Kechik, A., 2020. Preliminary assessment of the effects of blast design factors on fragmentation at Lafarge Kanthan limestone quarry, Chemor, Perak. *ASEAN Engineering Journal ,* 10(2), pp. 58-72.

Skosana, N., 2023. Plant lump to fine ratio requirements [Interview] (11 June 2023).

Tang, H.L, Liu, X., Yang, J. & Yu, Q., 2022. Experimental study on the influence of delay time on rock fagmentation in bench blasting. *Applied Sciences,* 13(1), p. 85.

Tao, J., Yang, X.G., Li, H.T., Zhou, J.W., Qi, S.C. and Lu, G.D., 2020. Numerical investigation of blast-induced rock fragmentation. *Computers and Geotechnics*, *128*, p.103846.

Tavakol Elahi, A. & Hosseini, M., 2017. Analysis of blasted rocks fragmentation using digital image processing (case study: limestone quarry of Abyek Cement Company). *International Journal of Geo-Engineering,* 8, pp. 1-11.

Uttarwar, M. & Devendar, M., 2020. Investigation into the effect of stemming on blast performance in underground excavations-a model study. *Helix-The Scientific Explorer Peer Reviewed Bimonthly International Journal,* 10(1), pp. 43-50.

Waheed, A., 2019. Optimization of kiln feed yield through an analysis of drilling and blasting parameters in a Quarry. Master of Science, The Delft University of Technology.

Worsey, T., 2020. The effect of delay and sequence on blasting fragmentation results. Doctoral dissertation, University of Kentucky.

Yang, H. & Rai, P., 2011. Characterization of fragment size vis-à-vis delay timing in quarry blasts. *Powder technology,* 211(1), pp. 120-126.

## Appendix A: Sishen Mine geology

| Sishen Mine Geology | |
|---|---|
| **Main Code** | **Description (rock type)** |
| BIF | Banded Iron Formation |
| BOS | Bostonite |
| CC | Calcrete |
| CGB | Conglomerate BIF |
| CGT | Conglomorate |
| CBR | Chert Breccia |
| CH | Chert Breccia |
| CL | Clay |
| DI | Diabase |
| DMT | Diamictite |
| DOL | Dolomite |
| FLS | Flagstone |
| GRS | Gritstone |
| HB | Hematite Brecciated |
| HC | Hematite conglomeratic |
| HD | Hematite detrital |

| Sishen Mine Geology | |
|---|---|
| **Main Code** | **Description (rock type)** |
| HG | Hematite gritty |
| HL | Hematite laminated |
| HM | Hematite massive |
| LAV | Lava |
| LAW | Weathered lava |
| PEB | Pebbles |
| QTZ | Quartzite |
| SD | Sand |
| SH | Shale |
| SHA | Shale Pirofilitic |
| SHT | Shale tech |
| SHM | Shale manganiferous |
| TIL | Tillite |
| VQ | Vein quartz |

# Appendix B: Sishen Mine ore/waste classifications

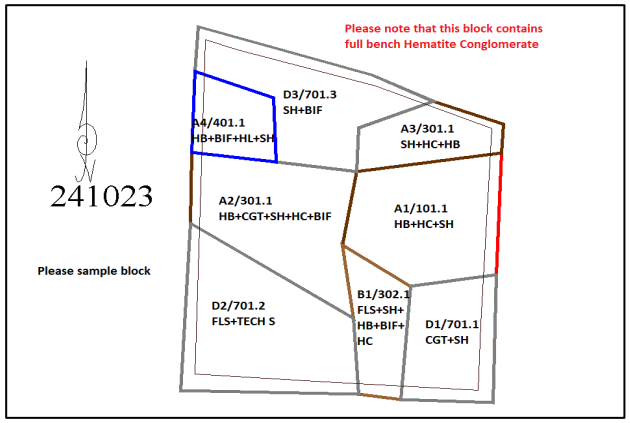
| Material Class | | Description | Grade Cut-offs | | | | | | | | | Mining Class |
|---|---|---|---|---|---|---|---|---|---|---|---|---|
| | | | Bench In Situ | | | Bench DMS | | | | Bench JIG | | |
| | | | Material Proportion | Fe | K2O | Fe | Al2O3 | K2O | Yield | Fe | Yield | |
| 101 | DMS grade ore | **High grade** | | | | >= 64.5% | < 1.9% | < 0.2% | >= 80% | | | A |
| 102 | | **High grade** | | | | >= 64.5% | >=1.9% | >=0.2% | >= 80% | | | A |
| 201 | | **Ore + high density waste** (high density BIF + CGB >= 50% of total waste) | | | < 0.3% | >= 61% | | | | | | A |
| 301 | | **Ore + high density waste** (high density BIF + CGB < 50% of total waste) | | | | | | | | | | A / K (K if Bench JIG K2O >= 0.6%) |
| 401 | | **Ore + low density waste** (weighted ave. rd of waste < 3.6) | | | | | | | >= 60% | | | A |
| 202 | Jig grade ore | **Ore + high density waste** (high density BIF + CGB >= 50% of total waste) | Ore >= 25% | | < 0.3% | | | | | >= 58.5% | >= 40% | L |
| 302 | | **Ore + high density waste** (high density BIF + CGB < 50% of total waste) | | | | | | | | | | B / K (K if Bench JIG K2O >= 0.6%) |
| 402 | | **Ore + low density waste** (weighted ave. rd of waste < 3.6) (DMS grade on Fe but DMS yield <60%) | | | | >= 61% | | | < 60% | | | B |
| 501 | | **Ore + high density waste** (high density BIF + CGB >= 50% of total waste) | Ore < 25% | | < 0.3% | | | | | >= 58.5% | | L |
| 601 | | **Ore + high density waste** (high density BIF + CGB < 50% of total waste) | | | | | | | | | | B / K (K if Bench JIG K2O >= 0.6%) |
| 502 | Low grade ore | **Low grade Si-rich Ore (High Pot.)** (BIF dominated potential UHDMS ore ) | Flagstone <= 25% | Fe >= 43% | < 0.3% | | | | | | | C |
| 602 | | **Low grade K2O-rich Ore (High Pot.)** (potential UHDMS ore ) | | | | | | | | | | C |
| 503 | | **Low grade Si-rich Ore (Low Pot.)** (BIF dominated potential UHDMS ore ) | | Fe >= 40% | < 0.3% | | | | | | | G |
| 603 | | **Low grade K2O-rich Ore (Low Pot.)** (potential UHDMS ore ) | | | | | | | | | | G |
| 701 | Waste | **Sterile Waste** (no ore potential) | | Fe < 40% | | | | | | | | D |
| 702 | | **Flagstone dominated mineralised material** | Flagstone > 25% | Fe >= 40% | | | | | | | | D |
| 801 | | **Clay- rich Material** | Clay >= 30% | | | | | | | | | E |

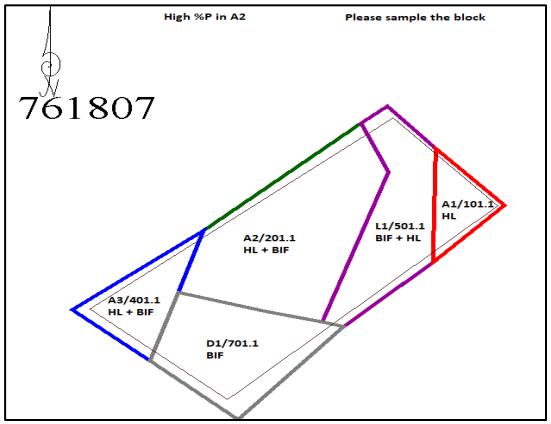
## Appendix C: UCS and hardness rating for each rock type

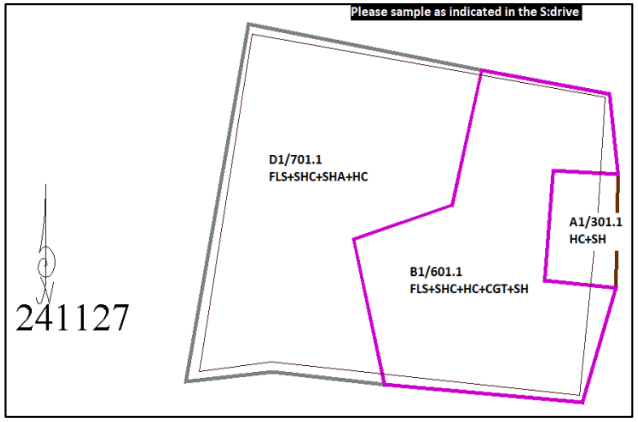
| Lithology in Block Model | UCS (MPa) | Hardness Rating |
|---|---|---|
| DOL | 167 | 4 |
| LAVF | 139 | 3 |
| CLAY | 0.2 | 1 |
| CCR | 66 | 2 |
| BIF | 231 | 5 |
| MAM | 259 | 6 |
| GAM | 73 | 2 |
| ORE | 281 | 6 |
| CGL | 100 | 3 |
| FLS | 202 | 5 |
| PEB | 0.2 | 1 |
| QTZ | 202 | 5 |
| SHTF | 73 | 2 |
| SHTL | 73 | 2 |
| DIA | 170 | 4 |
| SHTU | 73 | 2 |
| LAVW | 25 | 1 |

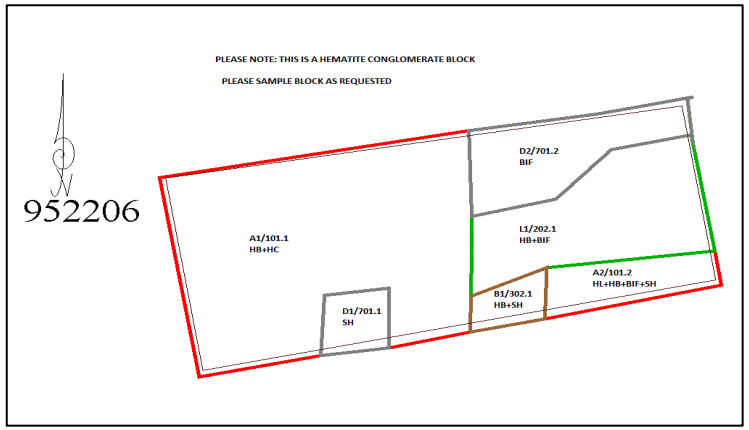
# Appendix D: Ore blocks geology

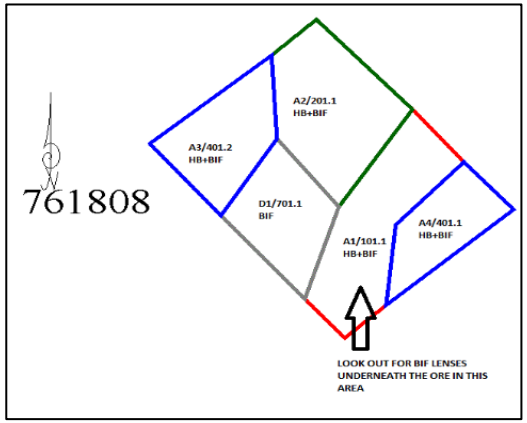
## Blocks charged using Powergel Eco 35 blocks

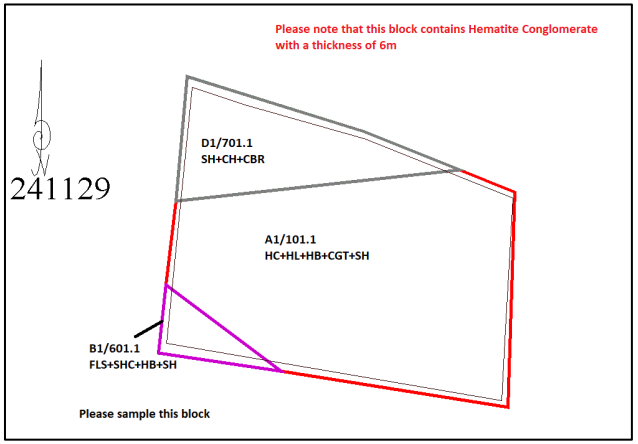


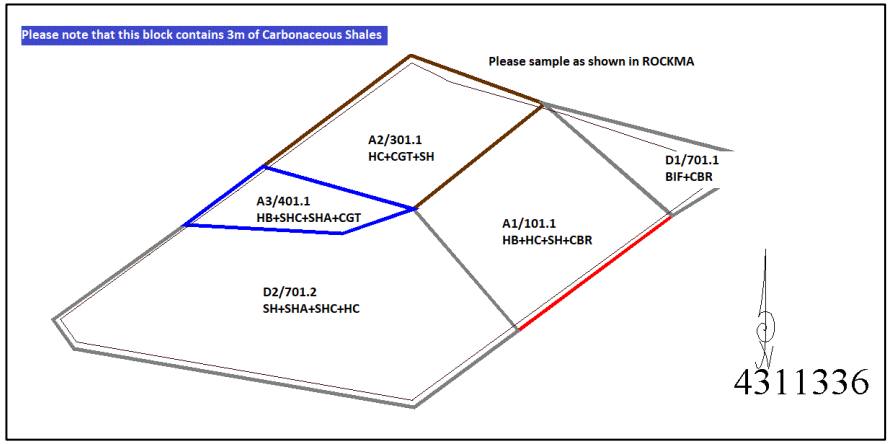



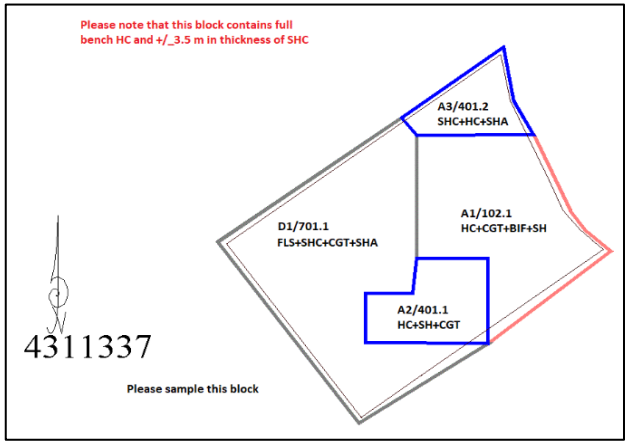



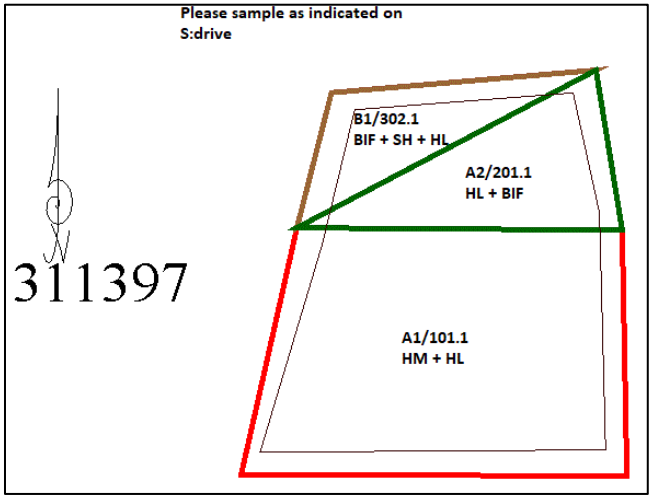



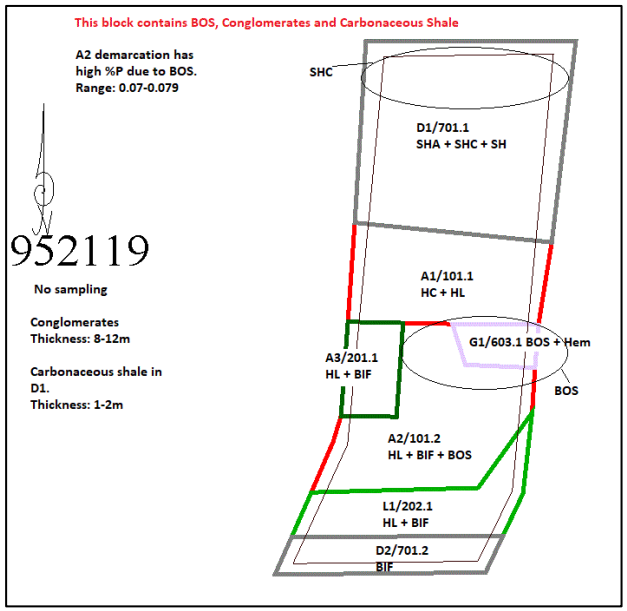

Please note that this block contains Hematite Conglomerate with a thickness of 6m
241129
D1/701.1
SH+CH+CBR
A1/101.1
HC+HL+HB+CGT+SH
B1/601.1
FLS+SHC+HB+SH
Please sample this block

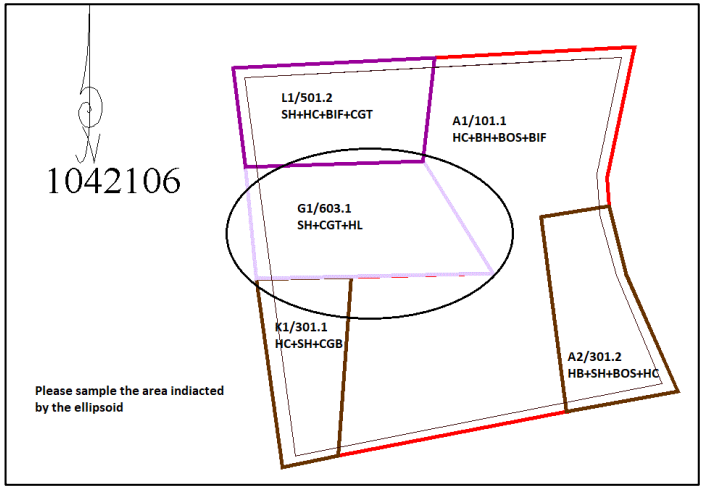

Please note that this block contains 3m of Carbonaceous Shales
Please sample as shown in ROCKMA
A2/301.1
HC+CGT+SH
D1/701.1
BIF+CBR
A3/401.1
HB+SHC+SHA+CGT
A1/101.1
HB+HC+SH+CBR
D2/701.2
SH+SHA+SHC+HC
4311336


Please note that this block contains full bench HC and +/_3.5 m in thickness of SHC
A3/401.2
SHC+HC+SHA
A1/102.1
HC+CGT+BIF+SH
D1/701.1
FLS+SHC+CGT+SHA
A2/401.1
HC+SH+CGT
4311337
Please sample this block

## Blocks charged using Innovex EGA blocks

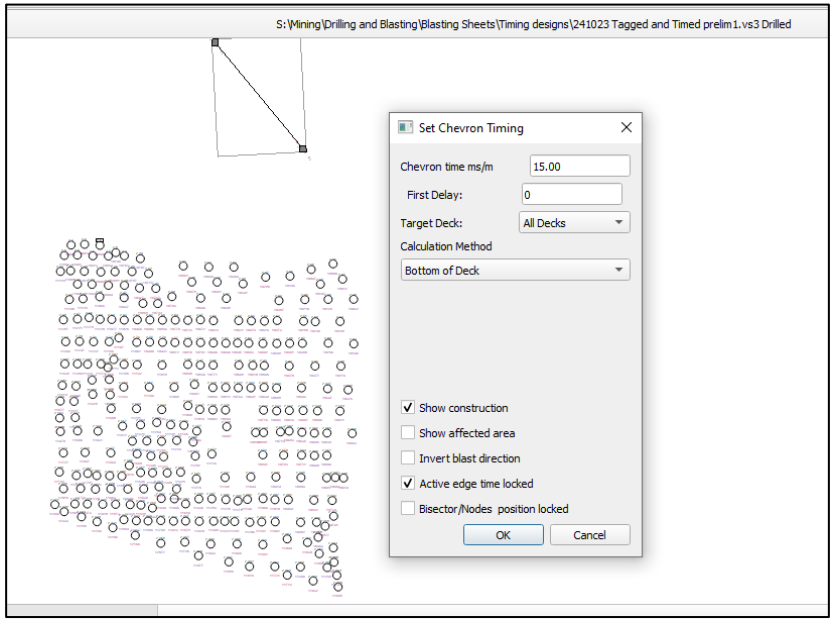


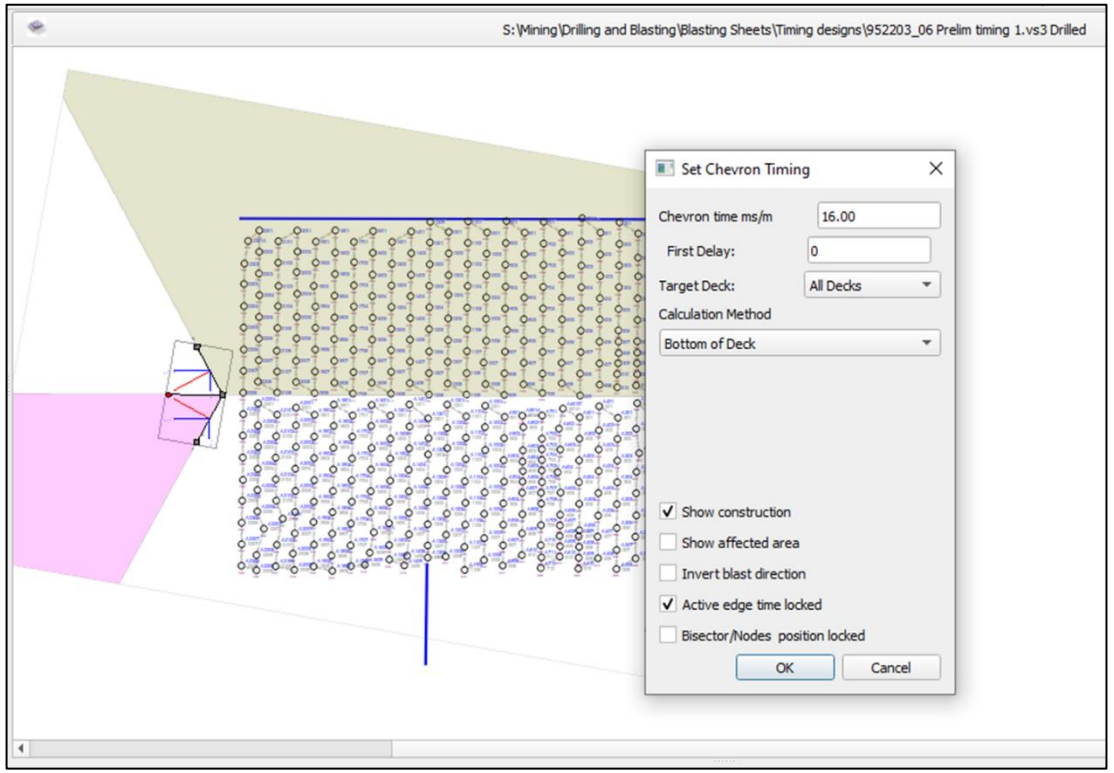



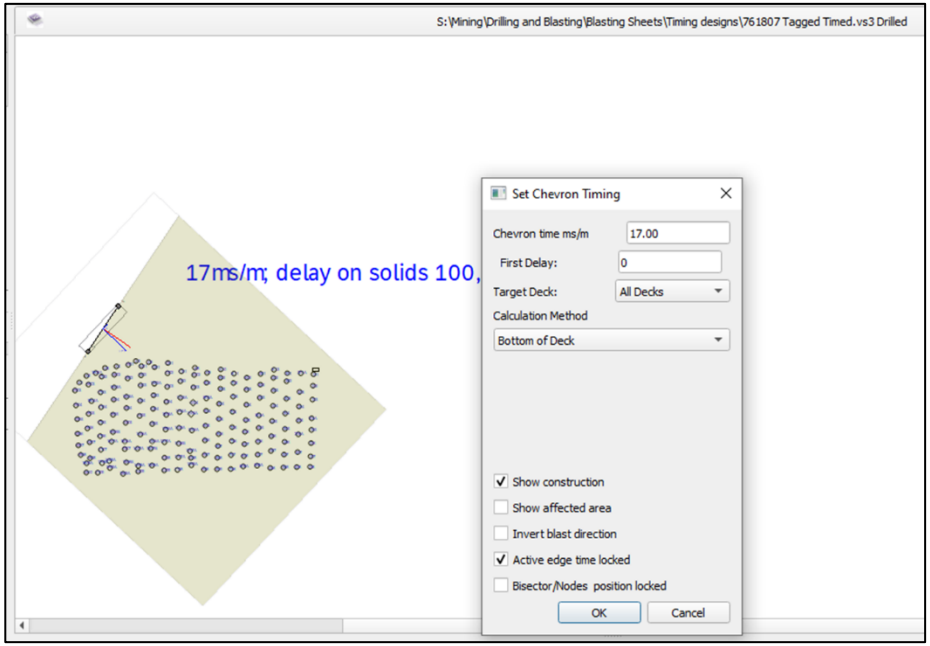



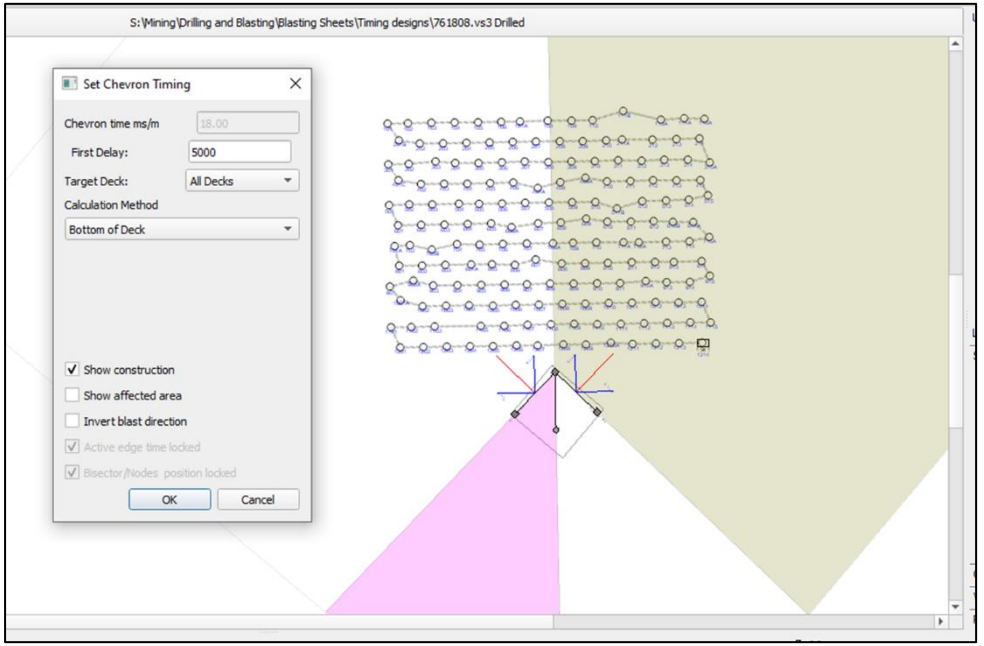
# Appendix E: Ore blocks timing plans

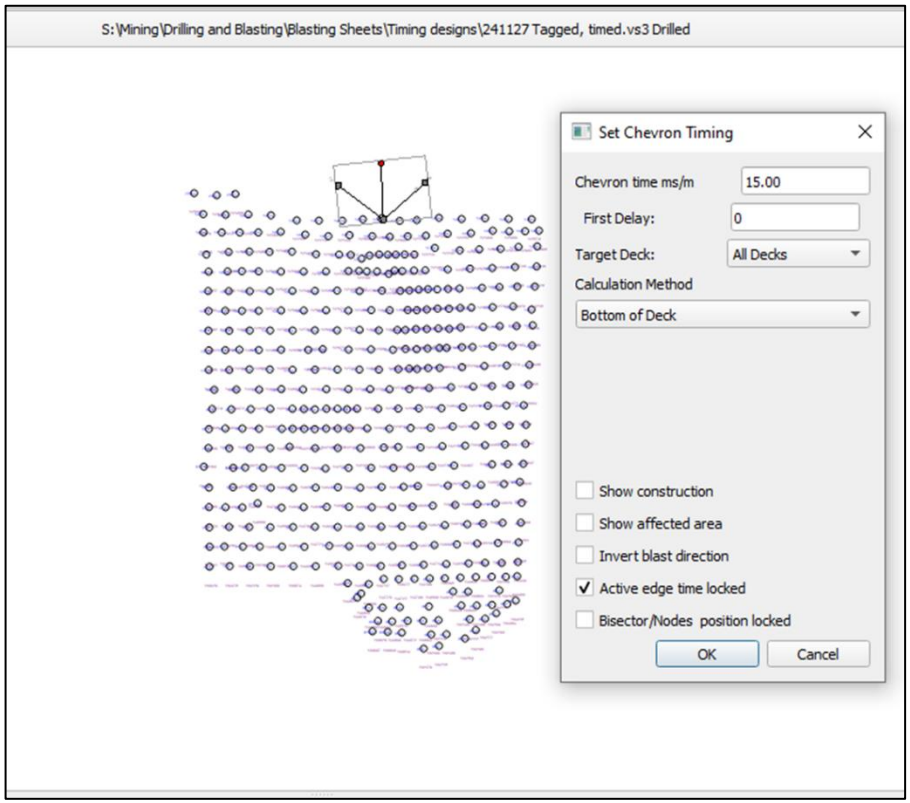
## Blocks charged using Powergel Eco 35

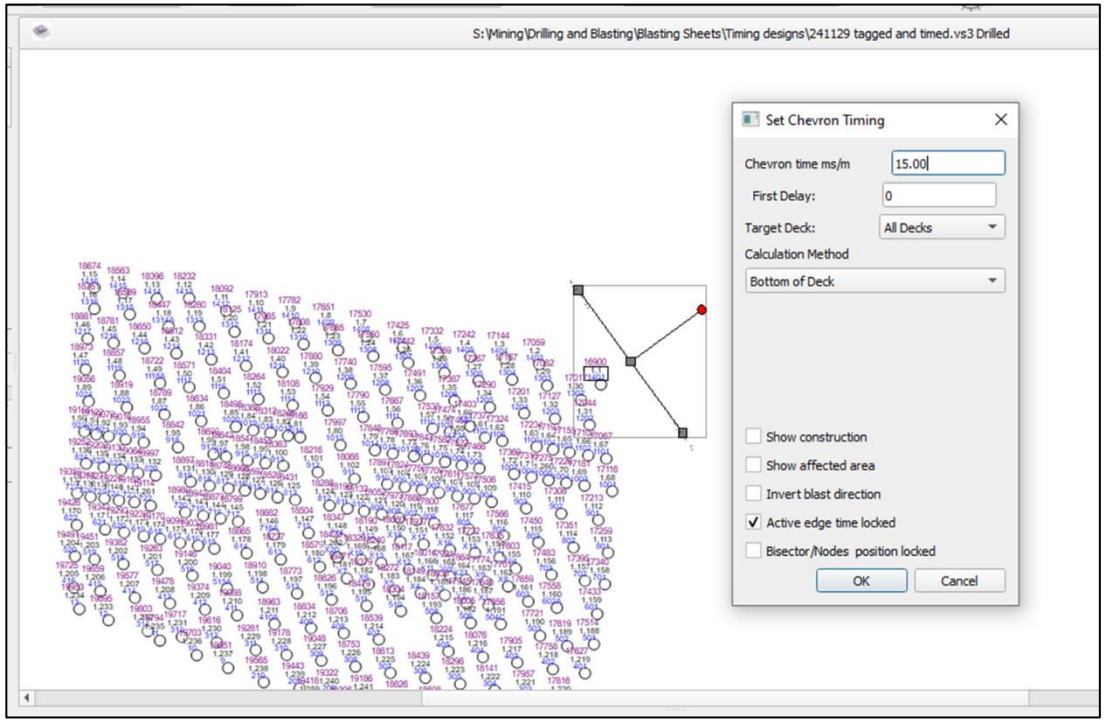


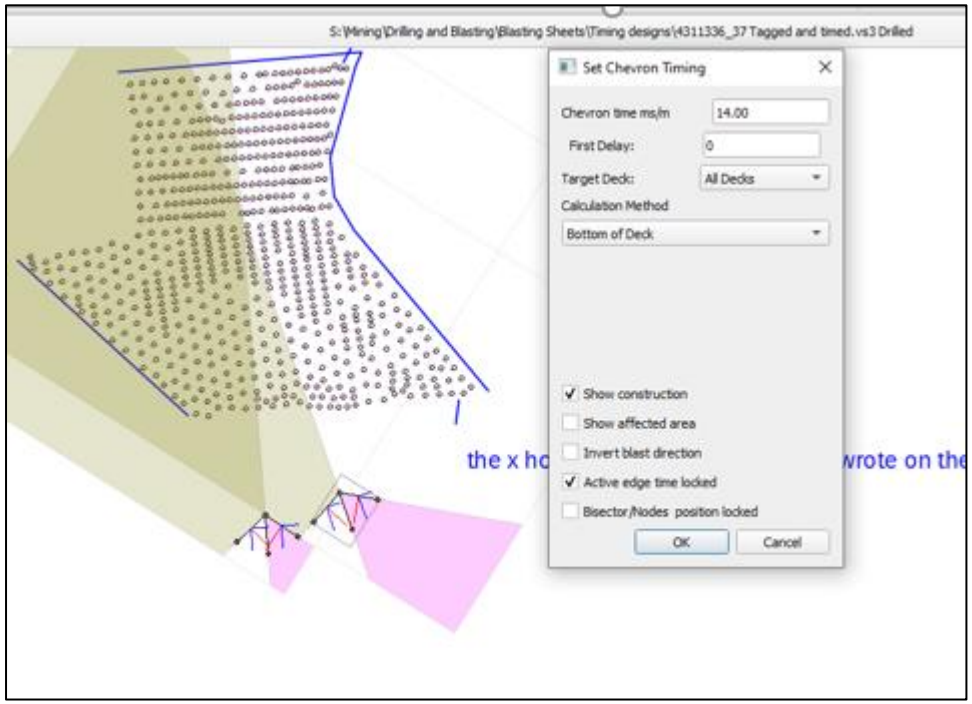




S:\Mining\Drilling and Blasting\Blasting Sheets\Timing designs\761807 Tagged Timed.vs3 Drilled
17ms/m; delay on solids 100,
Set Chevron Timing
Chevron time ms/m
17.00
First Delay:
0
Target Deck:
All Decks
Calculation Method
Bottom of Deck
Show construction
Show affected area
Invert blast direction
Active edge time locked
Bisector/Nodes position locked
OK
Cancel

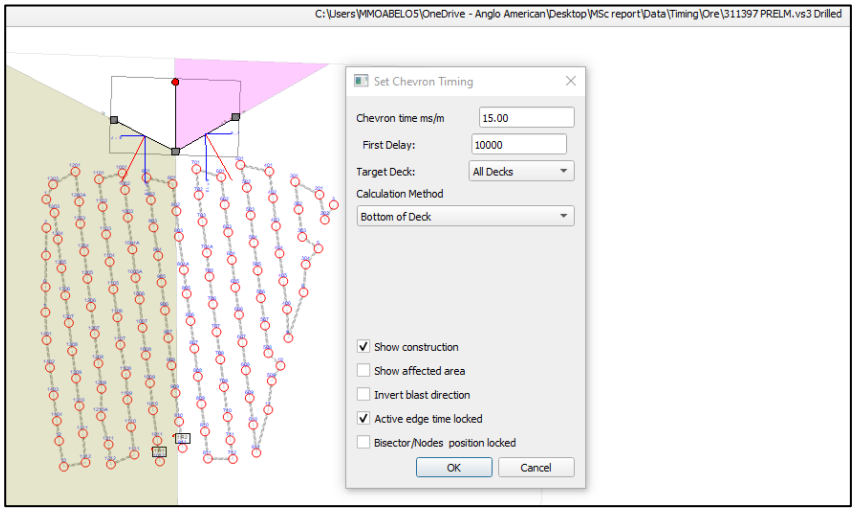

S:\Mining\Drilling and Blasting\Blasting Sheets\Timing designs\761808.vs3 Drilled
Set Chevron Timing
Chevron time ms/m
18.00
First Delay:
5000
Target Deck:
All Decks
Calculation Method
Bottom of Deck
Show construction
Show affected area
Invert blast direction
Active edge time locked
Bisector/Nodes position locked
OK
Cancel

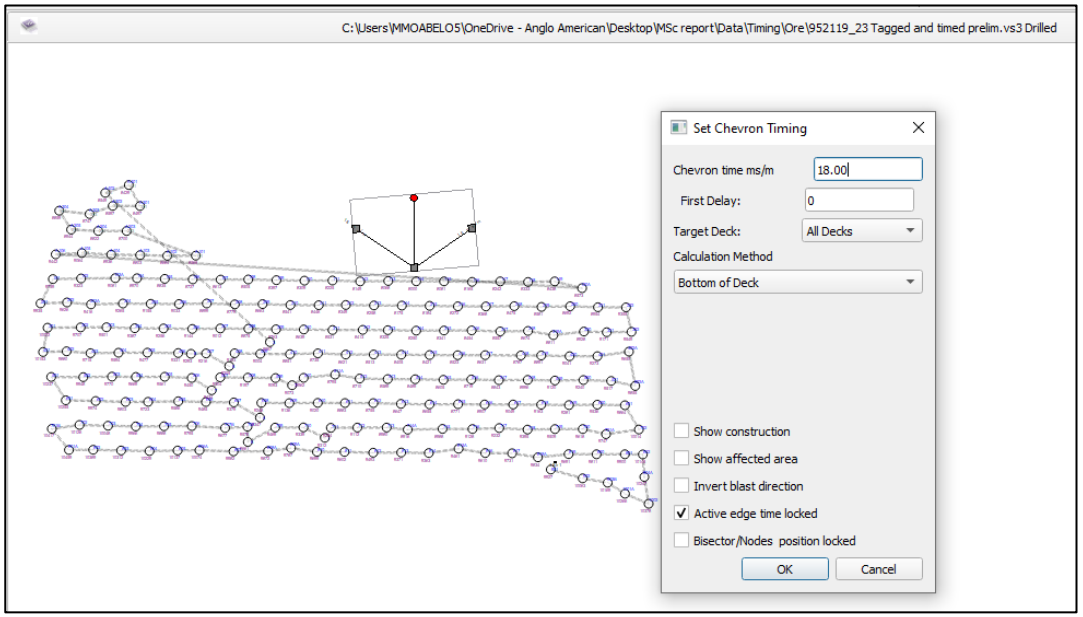

S:\Mining\Drilling and Blasting\Blasting Sheets\Timing designs\241127 Tagged, timed.vs3 Drilled
Set Chevron Timing
Chevron time ms/m
15.00
First Delay:
0
Target Deck:
All Decks
Calculation Method
Bottom of Deck
Show construction
Show affected area
Invert blast direction
Active edge time locked
Bisector/Nodes position locked
OK
Cancel

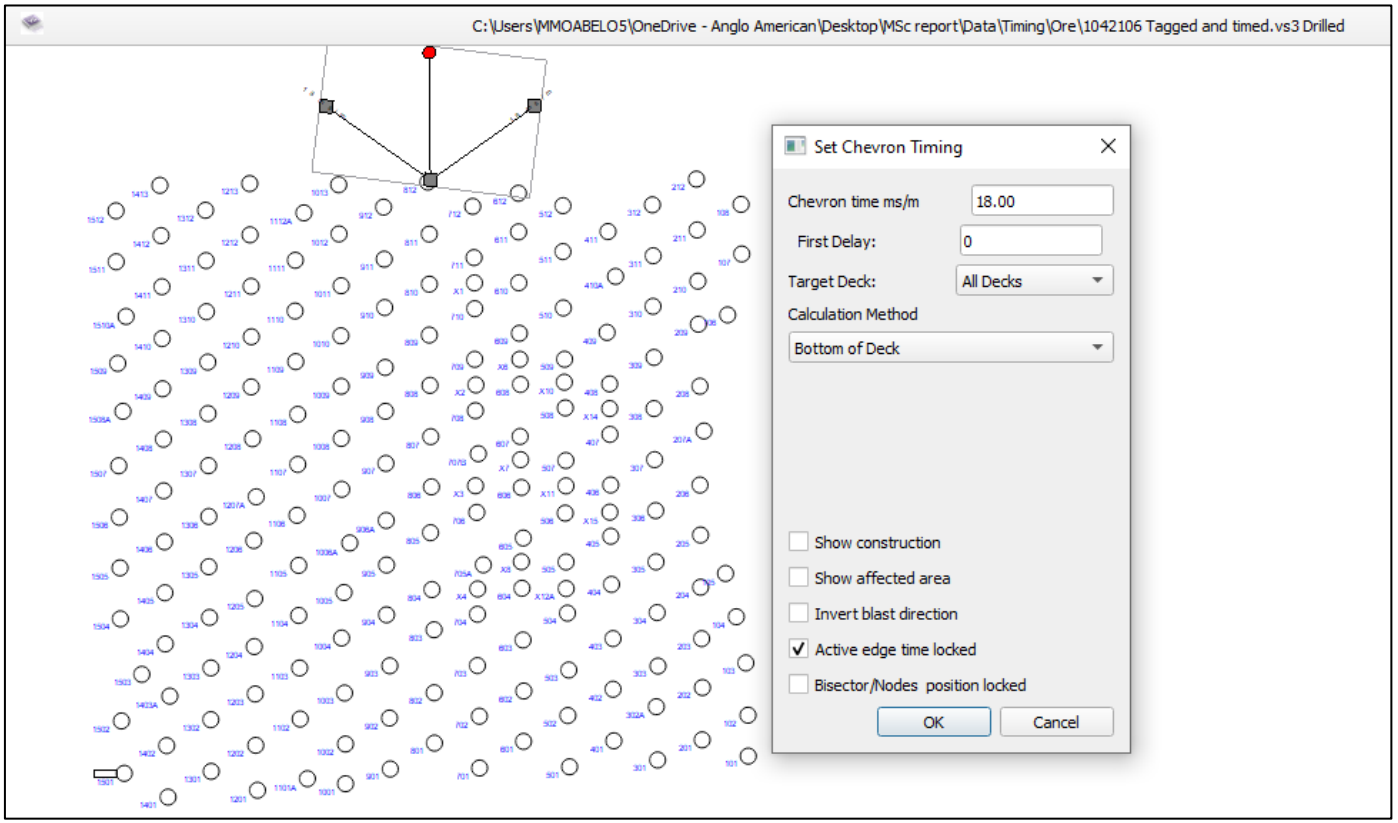

S:\Mining\Drilling and Blasting\Blasting Sheets\Timing designs\241129 tagged and timed.vs3 Drilled
Set Chevron Timing
Chevron time ms/m
15.00
First Delay:
0
Target Deck:
All Decks
Calculation Method
Bottom of Deck
Show construction
Show affected area
Invert blast direction
Active edge time locked
Bisector/Nodes position locked
OK
Cancel


S:\Mining\Drilling and Blasting\Blasting Sheets\Timing designs\4311336_37 Tagged and timed.vs3 Drilled
Set Chevron Timing
Chevron time ms/m
14.00
First Delay:
0
Target Deck:
All Decks
Calculation Method
Bottom of Deck
Show construction
Show affected area
Invert blast direction
Active edge time locked
Bisector/Nodes position locked
OK
Cancel

## Blocks charged using Innovex EGA

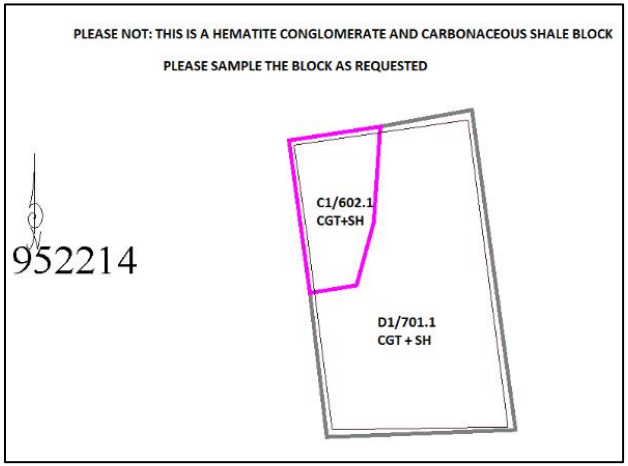


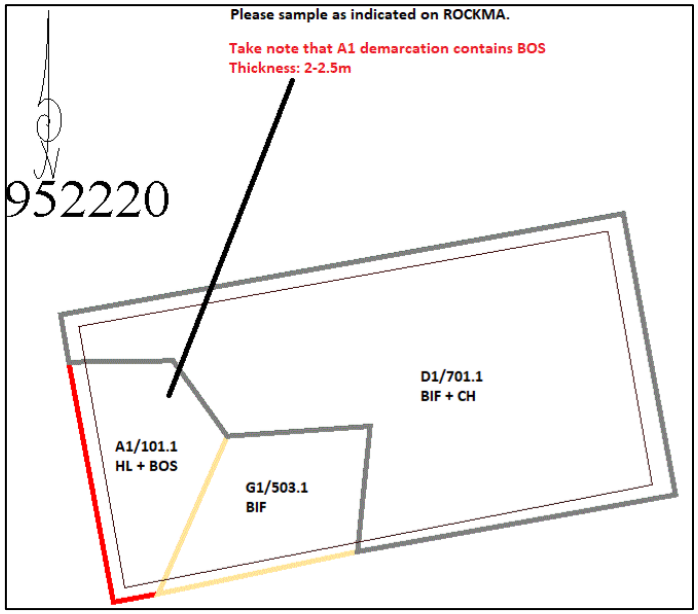



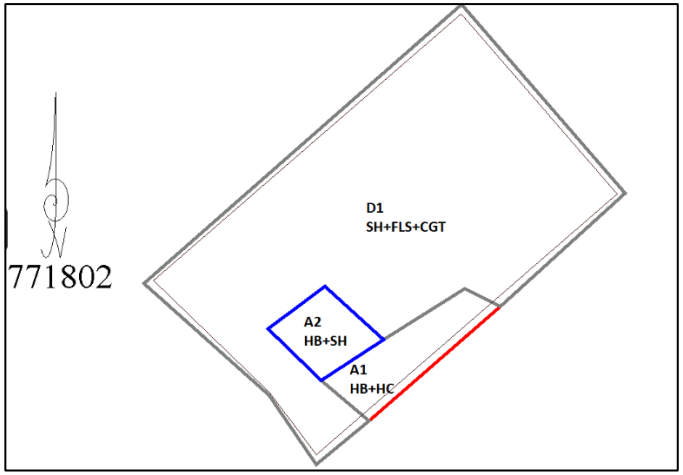

C:\Users\MMOABELO5\OneDrive - Anglo American\Desktop\MSc report\Data\Timing\Ore\1042106 Tagged and timed.vs3 Drilled
Set Chevron Timing
Chevron time ms/m
18.00
First Delay:
0
Target Deck:
All Decks
Calculation Method
Bottom of Deck
Show construction
Show affected area
Invert blast direction
Active edge time locked
Bisector/Nodes position locked
OK
Cancel

## Appendix F: Waste blocks geology

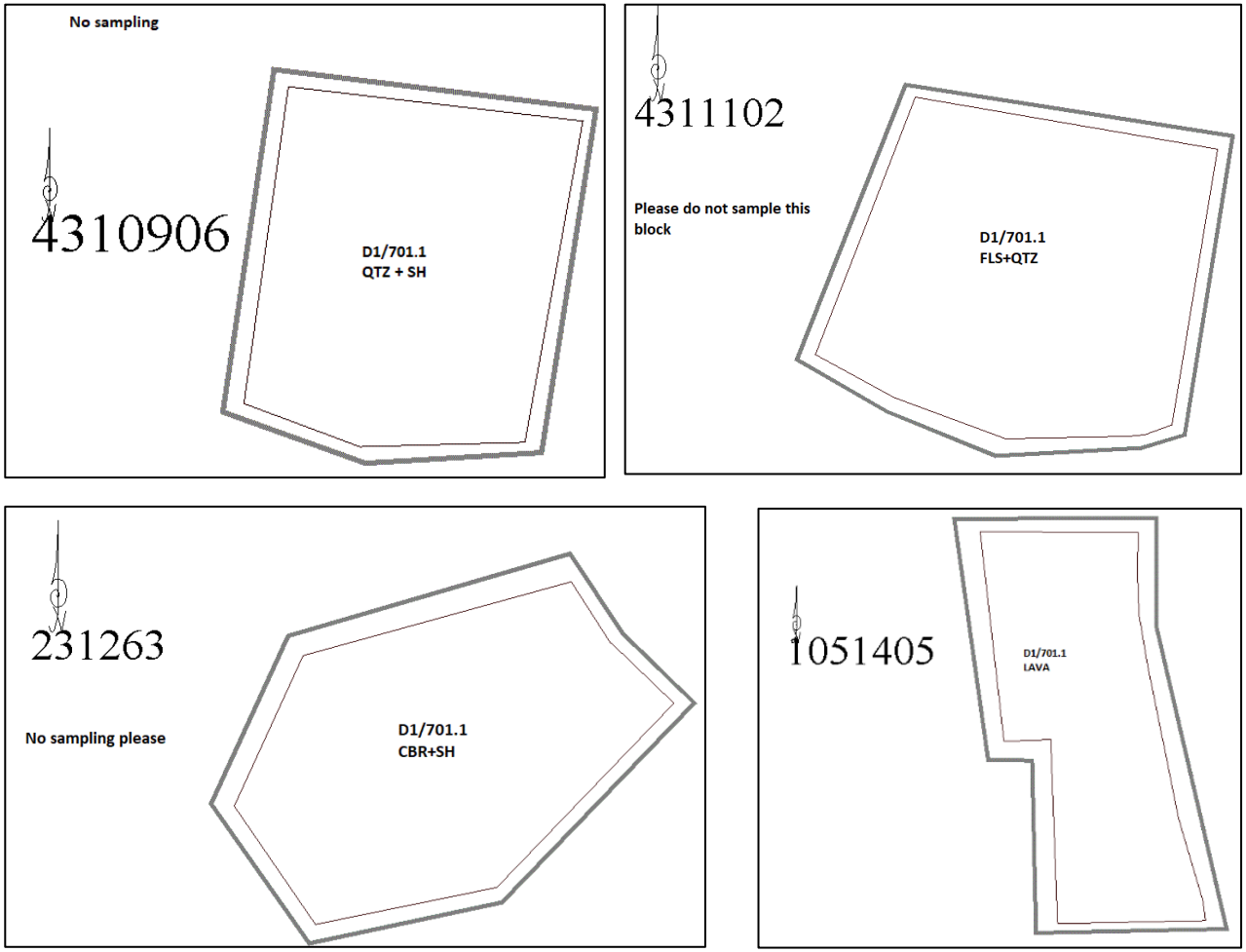
### Blocks charged using Powergel Eco 35



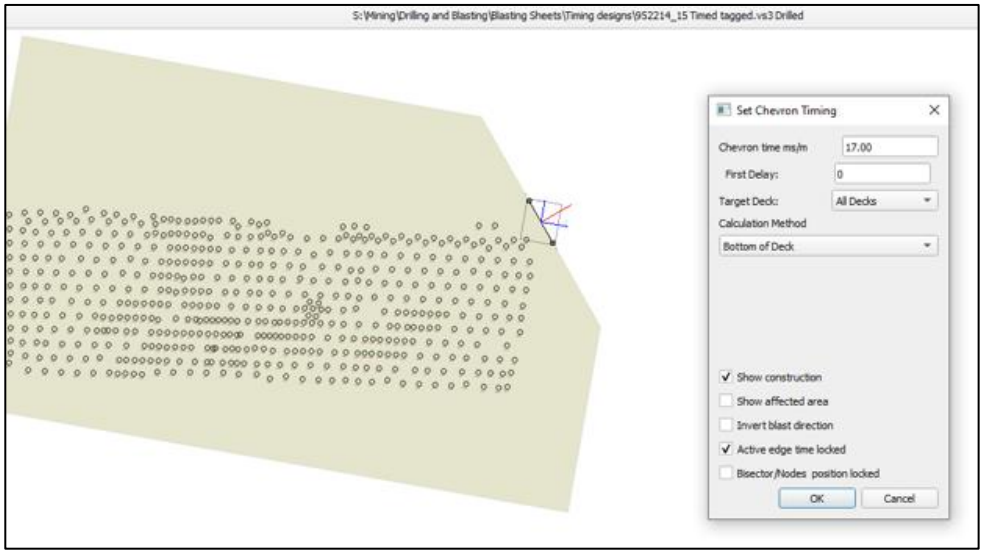
## Blocks charged using Innovex EGA

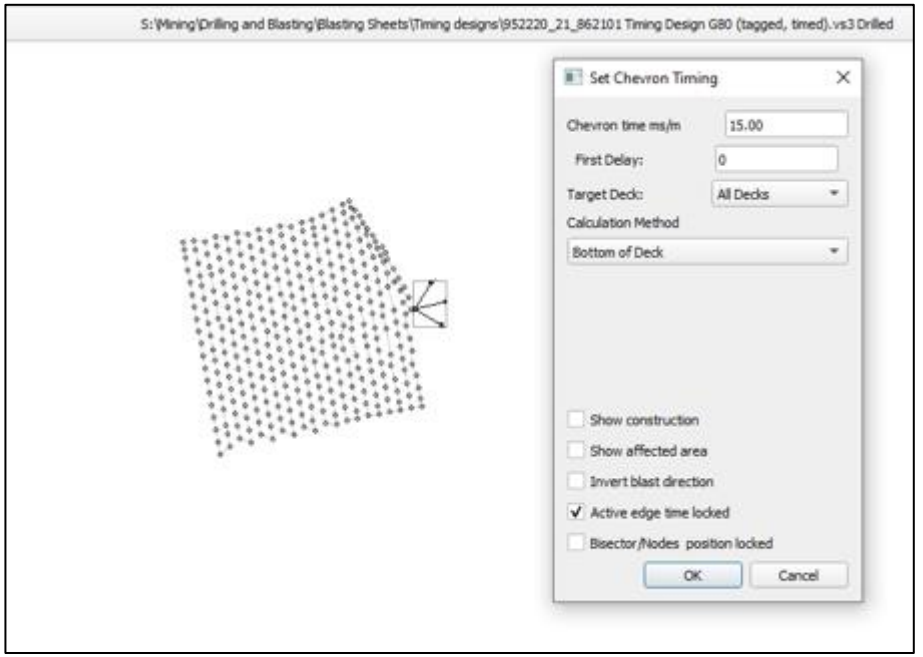


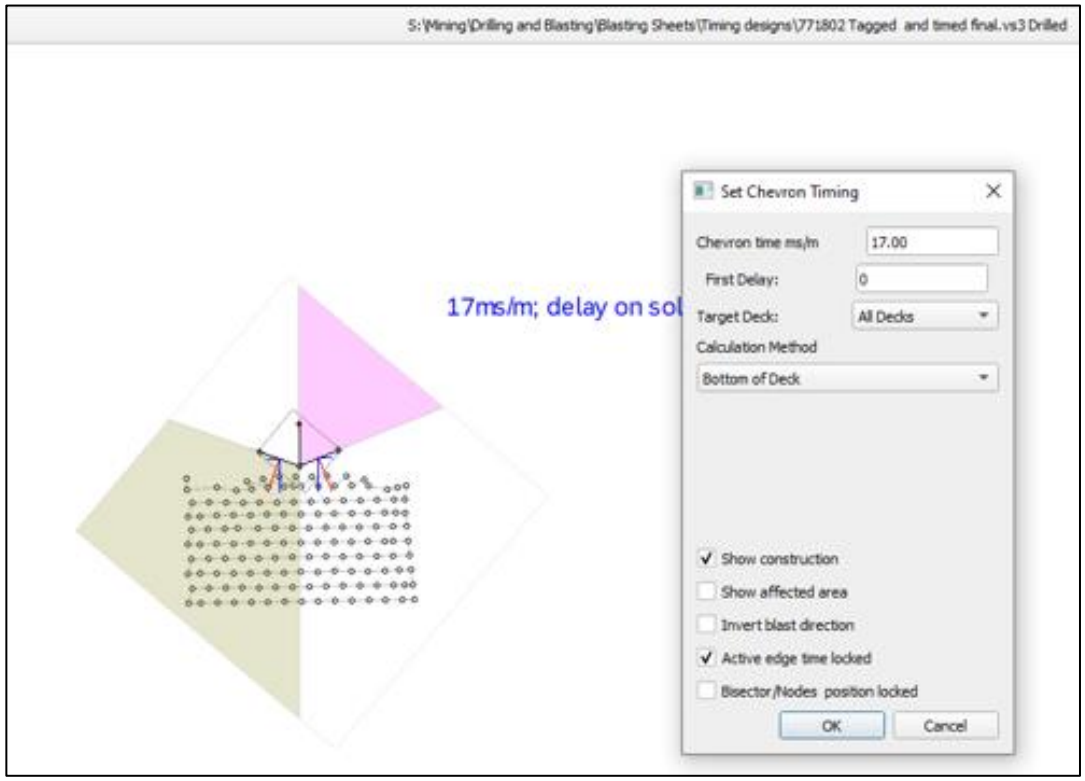

.

## Appendix G: Waste blocks timing plans

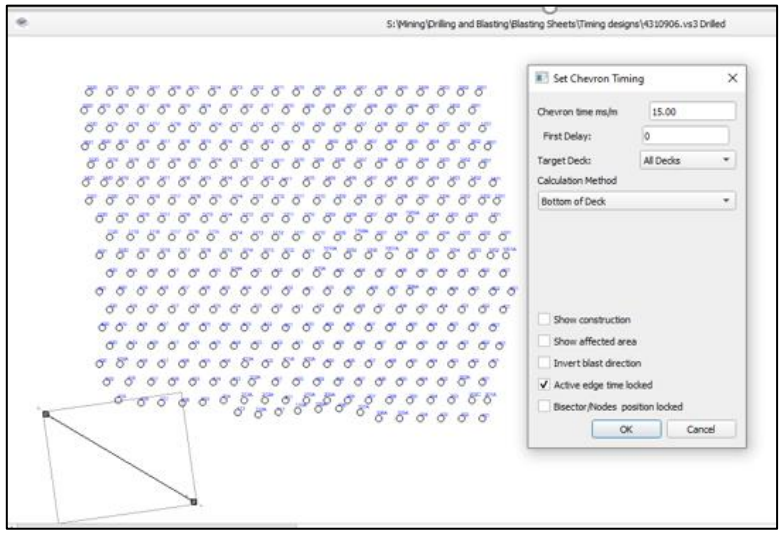
### Blocks charged using Powergel Eco 35

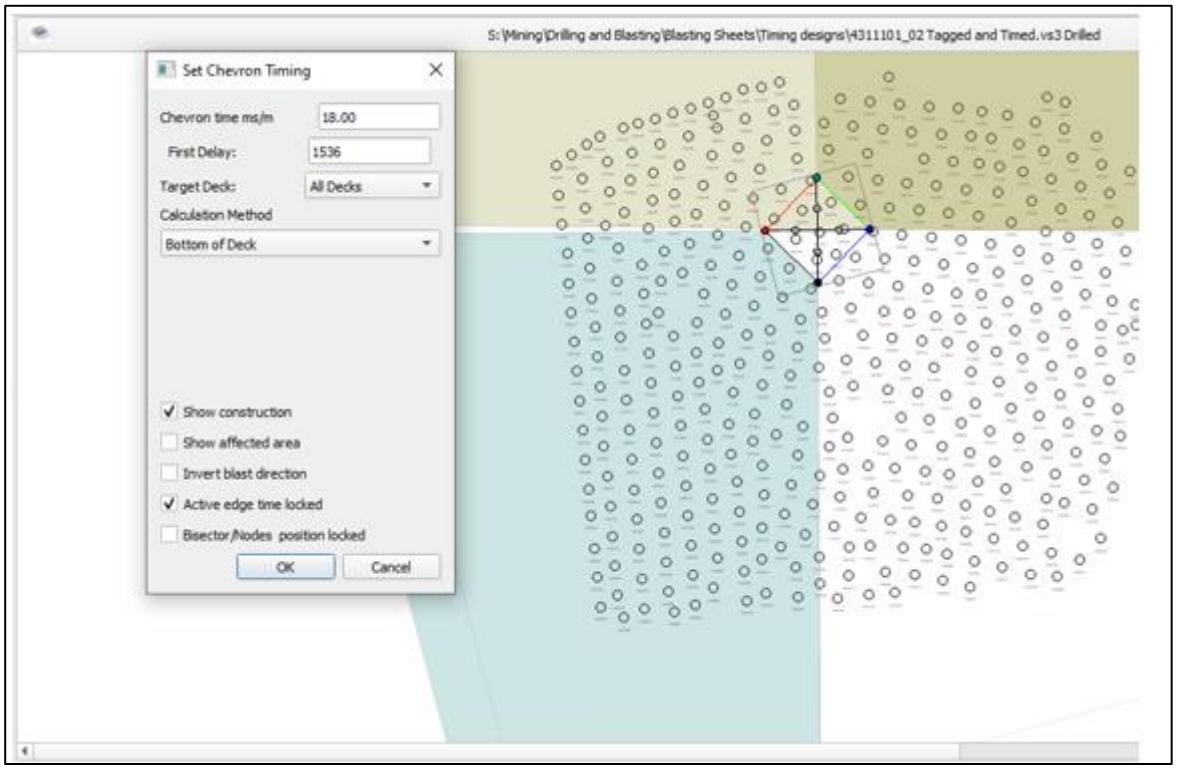


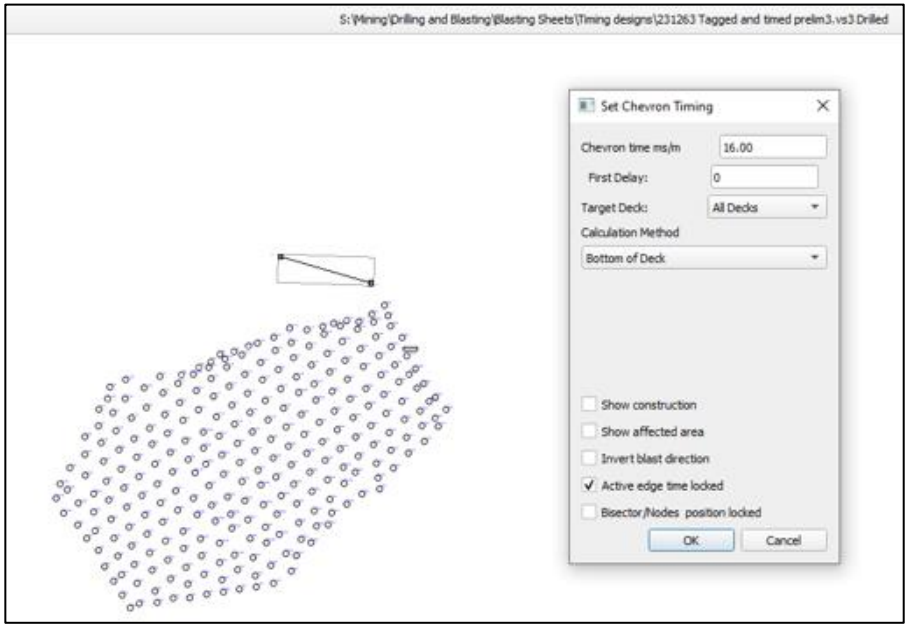



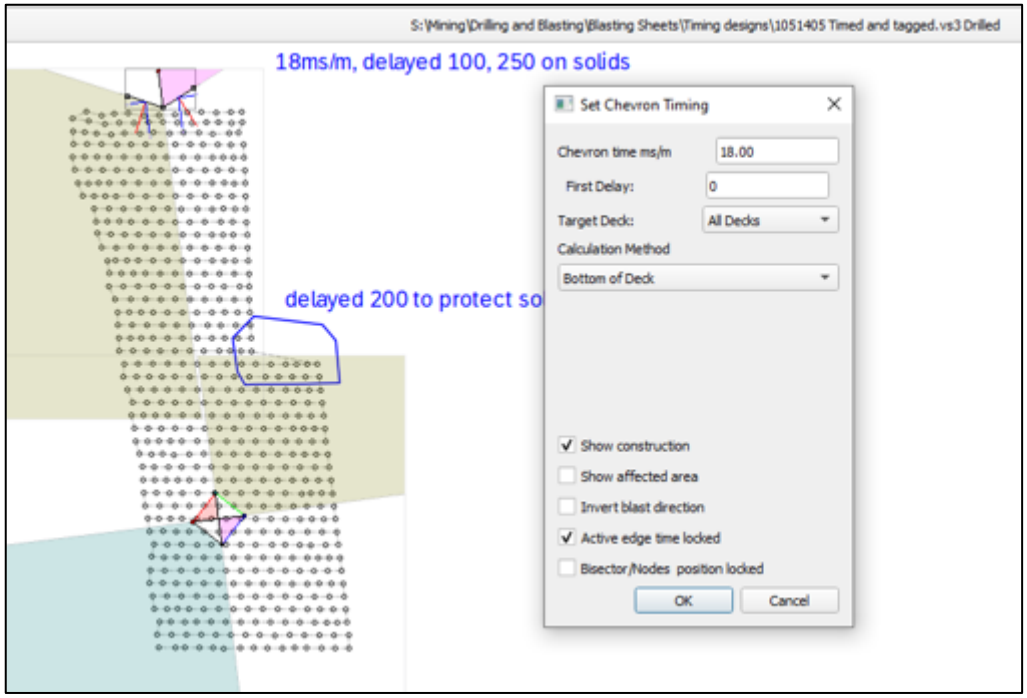

S:\Mining\Drilling and Blasting\Blasting Sheets\Timing designs\771802 Tagged and timed final.vs3 Drilled
17ms/m; delay on sol
Set Chevron Timing
Chevron time ms/m
17.00
First Delay:
0
Target Deck:
All Decks
Calculation Method
Bottom of Deck
Show construction
Show affected area
Invert blast direction
Active edge time locked
Bisector/Nodes position locked
OK
Cancel

**Blocks charged using Innovex EGA**



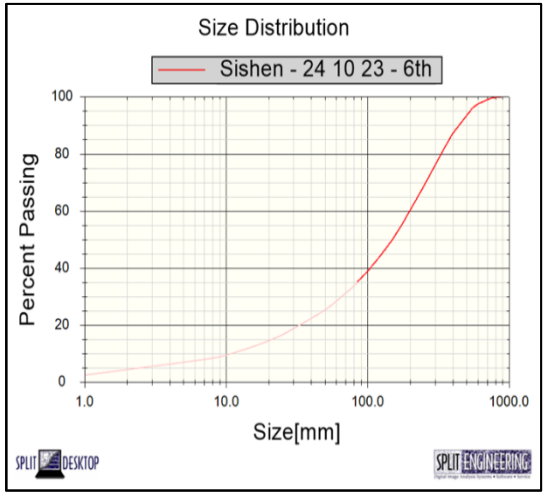

S:\Mining\Drilling and Blasting\Blasting Sheets\Timing designs\231263 Tagged and timed prelim3.vs3 Drilled
Set Chevron Timing
Chevron time ms/m
16.00
First Delay:
0
Target Deck:
All Decks
Calculation Method
Bottom of Deck
Show construction
Show affected area
Invert blast direction
Active edge time locked
Bisector/Nodes position locked
OK
Cancel


S:\Mining\Drilling and Blasting\Blasting Sheets\Timing designs\1051405 Timed and tagged.vs3 Drilled
18ms/m, delayed 100, 250 on solids
delayed 200 to protect so
Set Chevron Timing
Chevron time ms/m
18.00
First Delay:
0
Target Deck:
All Decks
Calculation Method
Bottom of Deck
Show construction
Show affected area
Invert blast direction
Active edge time locked
Bisector/Nodes position locked
OK
Cancel

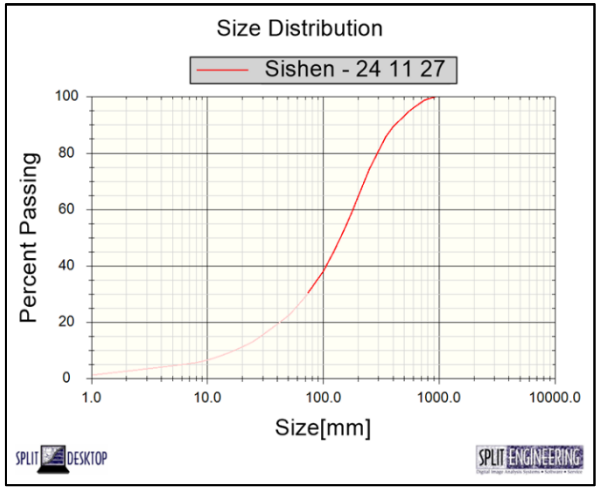
## Appendix H: Ore blocks fragmentation results

### Blocks blasted using Powergel Eco 35

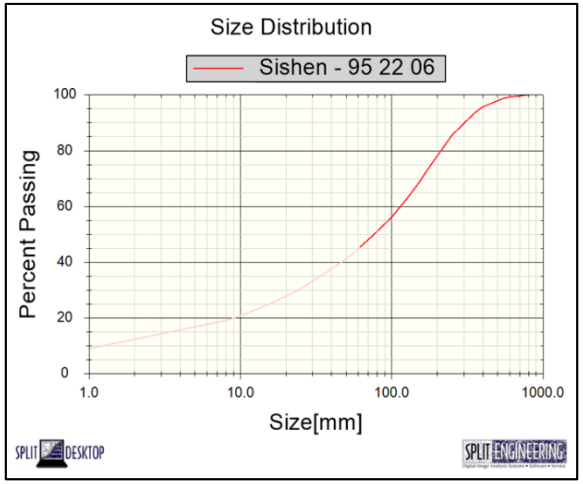
| Sishen - 24 10 23 | |
|---|---|
| **% Passing** | **Size (mm)** |
| F10 | 10.53 |
| F20 | 33.62 |
| F30 | 65.47 |
| F40 | 104.92 |
| F50 | 150.13 |
| F60 | 200.12 |
| F70 | 258.13 |
| F80 | 330.13 |
| F90 | 436.08 |
| Topsize (99.95%) | 874.97 |



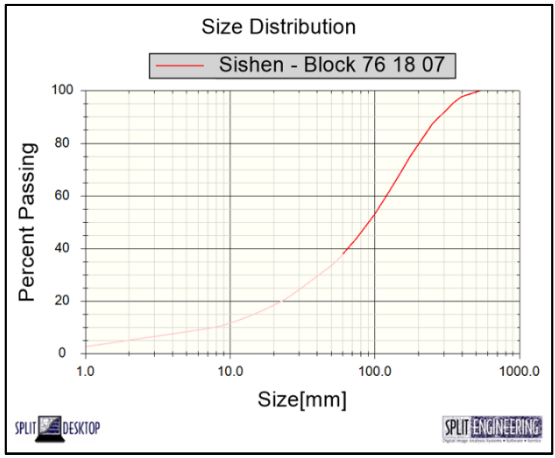

| Sishen - 24 11 27 | |
|---|---|
| **% Passing** | **Size[mm]** |
| F10 | 17.03 |
| F20 | 42.86 |
| F30 | 73.06 |
| F40 | 106.79 |
| F50 | 142.07 |
| F60 | 180.93 |
| F70 | 227.07 |
| F80 | 292.04 |
| F90 | 415.67 |
| Topsize (99.95%) | 926.78 |



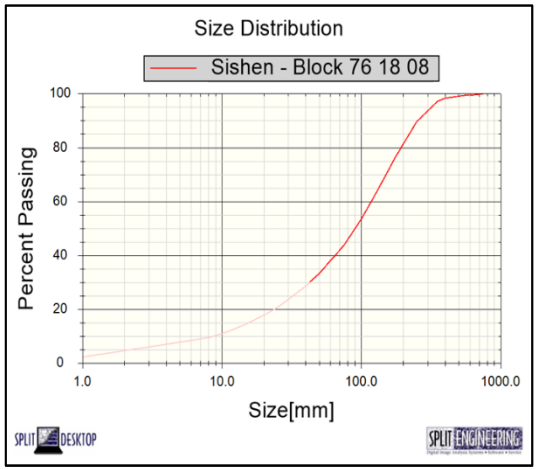
| Sishen - 95 22 06 | |
|---|---|
| % Passing | Size[mm] |
| F10 | 1.34 |
| F20 | 8.85 |
| F30 | 23.9 |
| F40 | 46.65 |
| F50 | 77.33 |
| F60 | 115.63 |
| F70 | 157.78 |
| F80 | 210.42 |
| F90 | 298.12 |
| Topsize (99.95%) | 813.7 |



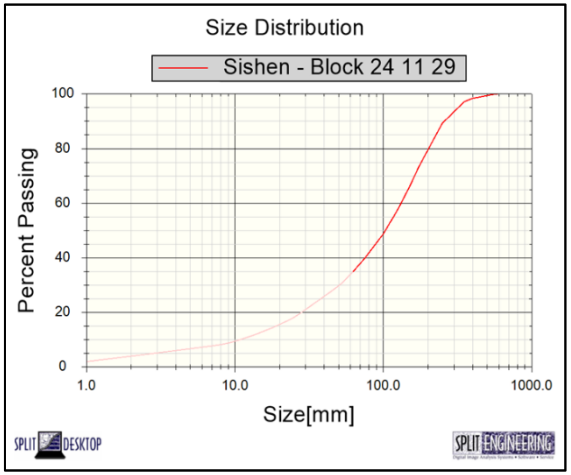

| Sishen - Block 76 18 07 | |
|---|---|
| % Passing | Size[mm] |
| F10 | 7.72 |
| F20 | 22.59 |
| F30 | 42.06 |
| F40 | 65.36 |
| F50 | 91.98 |
| F60 | 121.21 |
| F70 | 155.35 |
| F80 | 201.95 |
| F90 | 274.46 |
| Topsize (99.95%) | 538.33 |



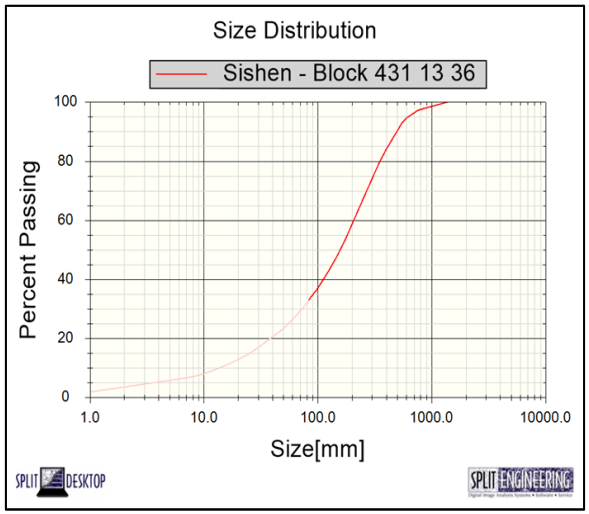

| Sishen - Block 76 18 08 | |
|---|---|
| % Passing | Size[mm] |
| F10 | 8.47 |
| F20 | 23.61 |
| F30 | 42.96 |
| F40 | 65.69 |
| F50 | 91.14 |
| F60 | 118.78 |
| F70 | 151.02 |
| F80 | 191.48 |
| F90 | 253.55 |
| Topsize (99.95%) | 755.46 |



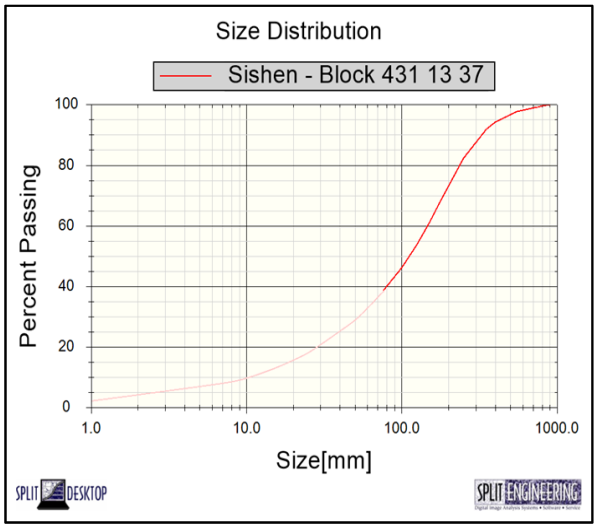

| Sishen - Block 24 11 29 | |
|---|---|
| % Passing | Size[mm] |
| F10 | 10.6 |
| F20 | 28.49 |
| F30 | 50.48 |
| F40 | 75.84 |
| F50 | 103.73 |
| F60 | 132.48 |
| F70 | 163.17 |
| F80 | 200.28 |
| F90 | 256.21 |
| Topsize (99.95%) | 587.99 |



| Sishen - Block 431 13 36 | |
|---|---|
| **% Passing** | **Size[mm]** |
| F10 | 13.47 |
| F20 | 39.07 |
| F30 | 72.42 |
| F40 | 112.7 |
| F50 | 158.49 |
| F60 | 208.18 |
| F70 | 269.82 |
| F80 | 354.63 |
| F90 | 490.12 |
| Topsize (99.95%) | 1370.52 |

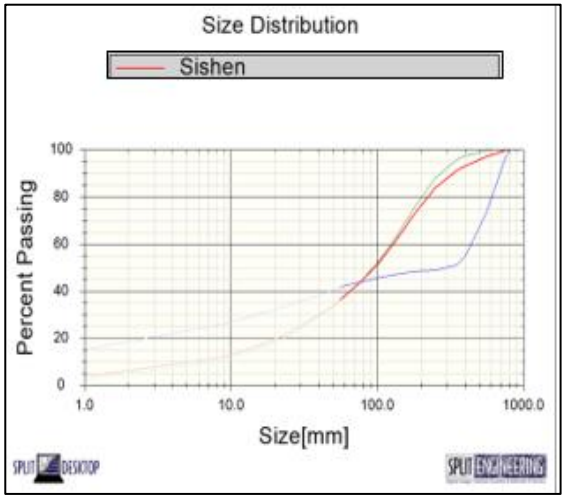



| Sishen - Block 431 13 37 | |
|---|---|
| **% Passing** | **Size[mm]** |
| F10 | 10.15 |
| F20 | 28.8 |
| F30 | 52.65 |
| F40 | 80.62 |
| F50 | 112.99 |
| F60 | 146.71 |
| F70 | 184.64 |
| F80 | 234.82 |
| F90 | 323.6 |
| Topsize (99.95%) | 896.58 |

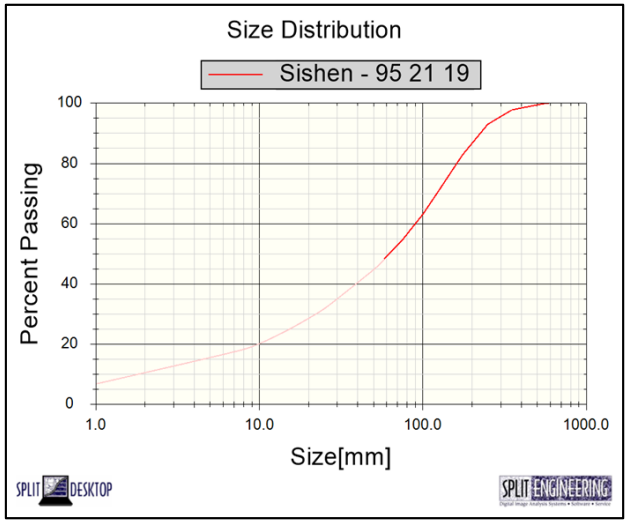


**Blocks blasted using Innovex EGA**

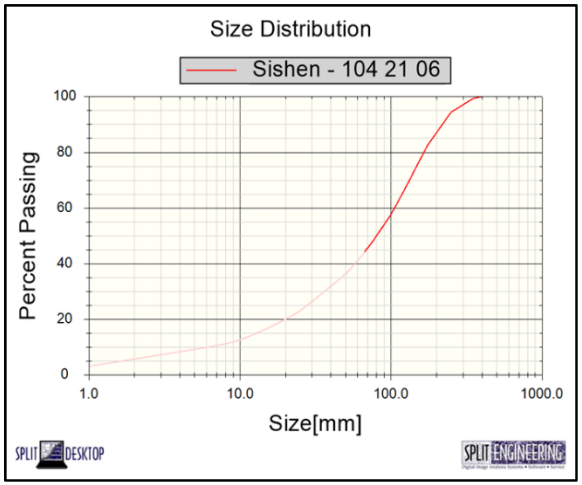
| Sishen - block 31 13 97 | |
|---|---|
| **% Passing** | **Size[mm]** |
| F10 | 6.09 |
| F20 | 20.5 |
| F30 | 40.68 |
| F40 | 65.79 |
| F50 | 96.26 |
| F60 | 129.41 |
| F70 | 167.13 |
| F80 | 220.24 |
| F90 | 323.74 |
| Topsize (99.95%) | 799.42 |




| Sishen - 95 21 19 | |
|---|---|
| **% Passing** | **Size[mm]** |
| F10 | 2.28 |
| F20 | 9.64 |
| F30 | 22.15 |
| F40 | 39.81 |
| F50 | 62.72 |
| F60 | 90.87 |
| F70 | 123.01 |
| F80 | 161.65 |
| F90 | 222.01 |
| Topsize (99.95%) | 590.58 |



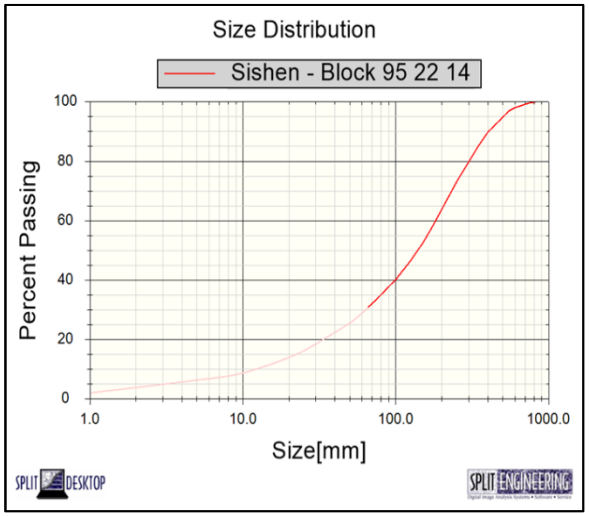
| Sishen - 104 21 06 | |
|---|---|
| % Passing | Size[mm] |
| F10 | 6.68 |
| F20 | 19.93 |
| F30 | 37.23 |
| F40 | 57.64 |
| F50 | 81.13 |
| F60 | 106.39 |
| F70 | 133.17 |
| F80 | 165.39 |
| F90 | 214.47 |
| Topsize (99.95%) | 418.07 |



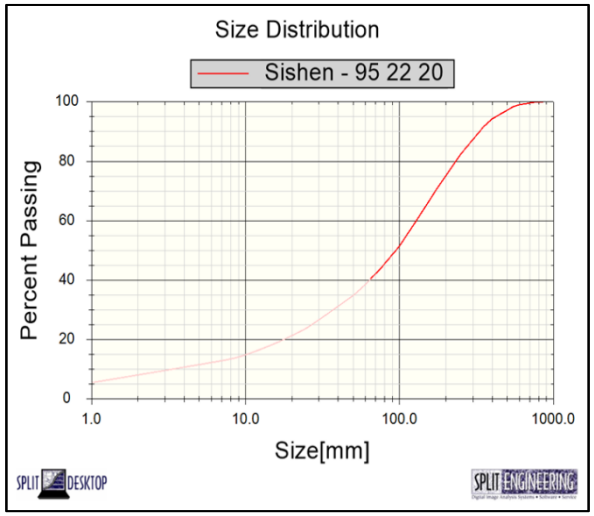
## Appendix I: Waste blocks fragmentation results

### Blocks blasted using Powergel Eco 35

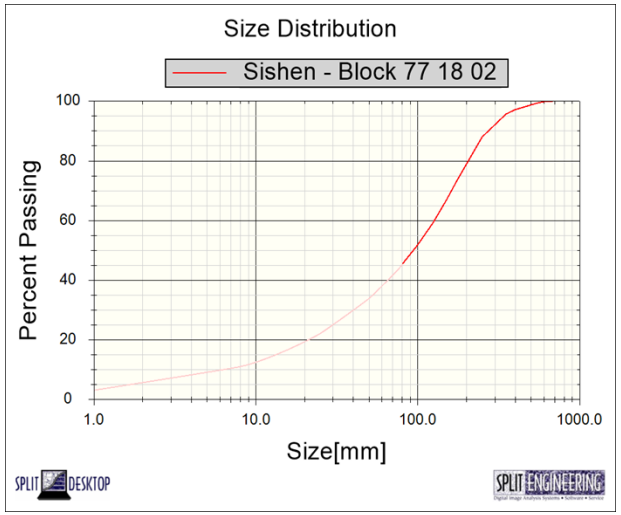
| Sishen - Block 95 22 14 | |
|---|---|
| **% Passing** | **Size[mm]** |
| F10 | 11.97 |
| F20 | 34.48 |
| F30 | 63.63 |
| F40 | 99.57 |
| F50 | 139.93 |
| F60 | 183.07 |
| F70 | 233.24 |
| F80 | 299.9 |
| F90 | 407.3 |
| Topsize (99.95%) | 822.28 |




| Sishen - 95 22 20 | |
|---|---|
| **% Passing** | **Size[mm]** |
| F10 | 4.22 |
| F20 | 17.68 |
| F30 | 38.01 |
| F40 | 63.9 |
| F50 | 95.34 |
| F60 | 129.54 |
| F70 | 171.53 |
| F80 | 231.8 |
| F90 | 329.85 |
| Topsize (99.95%) | 853.82 |

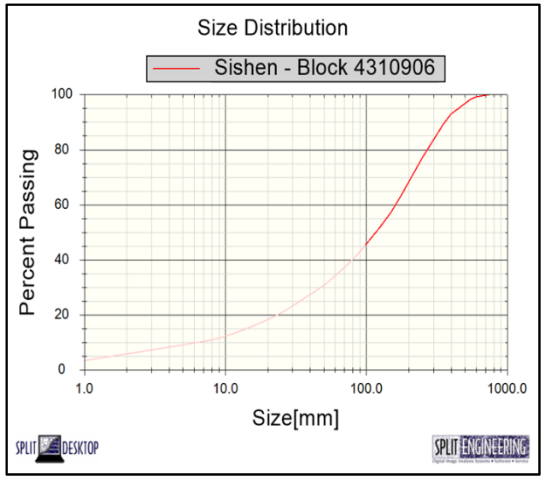


| Sishen - Block 77 18 02 | |
|---|---|
| **% Passing** | **Size[mm]** |
| F10 | 6.8 |
| F20 | 21.1 |
| F30 | 40.91 |
| F40 | 65.42 |
| F50 | 94.66 |
| F60 | 127.78 |
| F70 | 162.04 |
| F80 | 203.48 |
| F90 | 268.31 |
| Topsize (99.95%) | 682.55 |

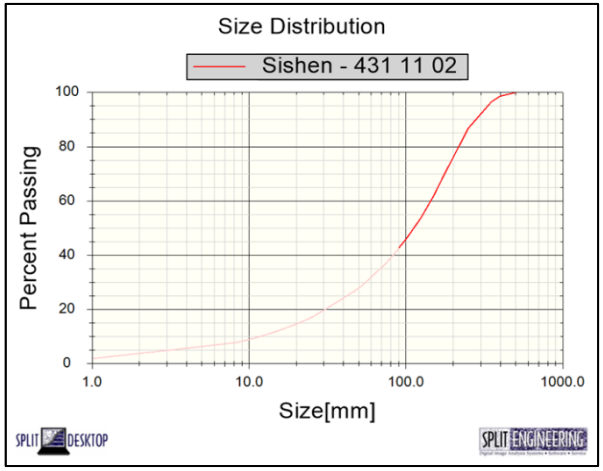


## Blocks blasted using Innovex EGA

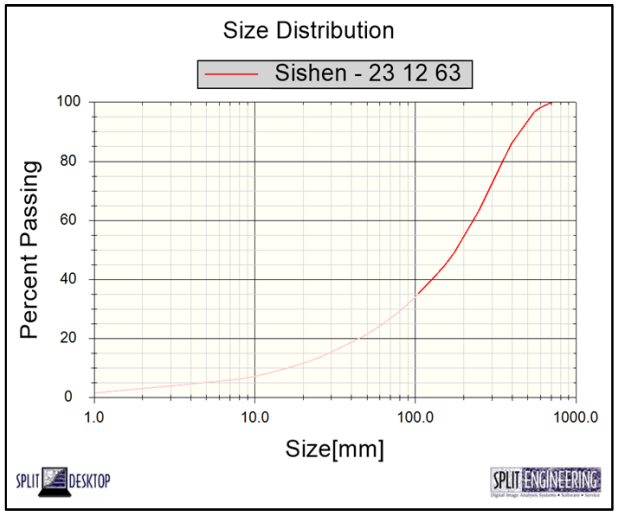
| Sishen - Block 4310906 | |
|---|---|
| **% Passing** | **Size (mm)** |
| F10 | 6.76 |
| F20 | 23.18 |
| F30 | 47.53 |
| F40 | 78.95 |
| F50 | 117.8 |
| F60 | 161.52 |
| F70 | 209.39 |
| F80 | 268.96 |
| F90 | 359.69 |
| Topsize (99.95%) | 739.85 |




| Sishen - 431 11 02 | |
|---|---|
| **% Passing** | **Size[mm]** |
| F10 | 11.55 |
| F20 | 31.23 |
| F30 | 55.36 |
| F40 | 82.76 |
| F50 | 113.78 |
| F60 | 144.94 |
| F70 | 177.28 |
| F80 | 215.36 |
| F90 | 274.06 |
| Topsize (99.95%) | 504.91 |



| Sishen - 23 12 63 | |
|---|---|
| **% Passing** | **Size[mm]** |
| F10 | 15.91 |
| F20 | 44.94 |
| F30 | 82.62 |
| F40 | 127.95 |
| F50 | 180.42 |
| F60 | 232.71 |
| F70 | 286.61 |
| F80 | 349.88 |
| F90 | 440.61 |
| Topsize (99.95%) | 712.51 |




| Sishen - Block 1051405 | |
|---|---|
| **% Passing** | **Size[mm]** |
| F10 | 8.81 |
| F20 | 27.36 |
| F30 | 52.46 |
| F40 | 82.78 |
| F50 | 119.62 |
| F60 | 156.84 |
| F70 | 196.58 |
| F80 | 245.31 |
| F90 | 319.3 |
| Topsize (99.95%) | 623.7 |

